THE UNIVERSITY OF CALGARY

Synthesis and Characterization of Mesoporous Sulfated Zirconia

and its use as a Solid Acid Catalyst

by

Debra Joy McIntosh

A THESIS

SUBMITTED TO THE FACULTY OF GRADUATE STUDIES

IN PARTIAL FULFILMENT OF THE REQUIREMENTS FOR THE

DEGREE OF MASTER OF SCIENCE

DEPARTMENT OF CHEMISTRY

CALGARY, ALBERTA

AUGUST, 1999

0-612-48026-7

Abstract

Mesoporous sulfated zirconia can be synthesized by the surfactant templating route which was first demonstrated for silica. However, the factors which determine the sizes of the pores in zirconia are many, and they interact with each other, making the synthesis of zirconia with a specific, narrow pore size distribution a complex problem. In this work, many of the factors were studied in an attempt to prepare samples with a range of non - overlapping pore sizes which could be tested for "shape - selectivity" in an alkylation reaction.

Attempts were made to synthesize mesoporous sulfated zirconia by many different methods, including various ionic routes and the neutral templating route. The ionic routes were found to be unsuccessful, resulting in material with only micropores, material with very large, broad pores or thermally unstable material. However, mesoporous sulfated zirconia synthesized by the neutral templating route was thermally stable up to 650°C, the temperature required to form the tetragonal, catalytically active phase of sulfated zirconia.

It was discovered that changing the alkyl chain length of the incorporated surfactant did not yield the expected result (the pore size did not increase with increasing alkyl chain length). However, the pore size of the material could be altered by other synthetic parameters, such as concentration of the surfactant. Cosolvents, such as ethanol and acetonitrile, could be used to adjust the pore sizes; also altering the order of the sulfation and extraction steps affected the porosity. The pore size could also be adjusted by varying the aging time and the aging temperature. By using all of these factors, mesoporous material that had pore size distributions with maxima that ranged from 2.0 nm to 4.0 nm was synthesized.

The alkylation of p-xylene with cyclohexene was used for the catalytic testing of mes-

oporous sulfated zirconia, and the results revealed that the pore diameter did affect the catalytic activity. As the pore diameter increased, the catalytic activity of the catalyst also increased. Microporous sulfated zirconia had almost no activity for this reaction, which indicated that mesopores were vital for catalytic activity. It was also discovered that catalysts from which the surfactant had been extracted prior to sulfation were more active than those in which the order of sulfation and extraction were reversed, possibly due to the amount and type of sulfate groups on the catalyst surface. Some catalysts were loaded with platinum in order to decrease the rate of deactivation of the catalysts. However, it was discovered that if the amount of platinum was high enough to decrease deactivation, that hydrogenation of the reactants also occurred rather than the desired alkylation.

Acknowledgements

I would like to thank the following individuals and groups for all of the help that they have provided:

Dr. Ron Kydd, my research supervisor, for all his support and encouragement throughout the course of this work.

Dr. Laurier Schramm for being on my committee and for useful suggestions dealing with the surfactants.

Dr. Mark Weir for his help with the infrared spectroscopy, nitrogen adsorption and x-ray diffraction measurements.

Dr. Steven Song for his help with the catalytic work.

Dr. Andy Kirk for his help with the mesopore size distributions and the model calculations.

Dorothy Fox for her help with the GC-MS work and for obtaining all of the carbon analyses.

Deb Glatiotis for help with the x-ray diffraction and for running the SEM pictures.

Norm Dowling, Greg Butlin and other staff members at ASR for running the SO_2 sulfation and analysing the sulfate content of my samples.

Dr. Scott Hinman for his help in running the ICP-AES measurements.

In addition, I would like to thank the following agencies for financial support:

- the Natural Sciences and Engineering Research Council (NSERC) of Canada for support in the form of a post graduate scholarship.
- the Province of Alberta for support in the form of a government scholarship.

- the Department of Chemistry for Graduate Teaching Assistantships.

- Research Services at the University of Calgary for a Graduate Conference Travel Grant.

To Dave

Table of Contents

List of Tables

List of Figures

Symbols and Abbreviations

Å	Angstrom (10^{-10} m)
BET	Adsorption isotherm model proposed by Brunauer, Emmett and Teller
BJH	Adsorption isotherm model proposed by Barrett, Joyner and Halenda
C_{16}TMAB	Hexadecyltrimethyl ammonium bromide
C16 - C8	Number of carbon atoms in the alkyl chain of the surfactant
CH	Cyclohexene
CMC	Critical micelle concentration
cm^{-1}	Reciprocal centimeters - units of wavenumber
d_{100}	Distance between crystallographic 100 planes
ES	Extracted and then sulfated
GC	Gas chromatography
GC-MS	Gas chromatography - Mass spectroscopy
H-K	Adsorption isotherm model proposed by Horvath and Kawazoe
I	Inorganic component in liquid crystal templating (can be +,- or neutral)
IC	Ion chromatography
ICP-AES	Inductively coupled plasma - Atomic Emission Spectroscopy
IR	Infrared
λ	Wavelength
LCT	Liquid crystal templating

M^+	Counter cation used in liquid crystal templating
MCM	Mobil Corporation Material (mesoporous silicates)
μm	micrometre (10^{-6} m)
mol %	Mole percent
MTBE	Methyl tertiary butyl ether
nm	nanometre (10^{-9} m)
P12	$C_{12}H_{25}OP(OH)_2$
P/P_0	Relative pressure, i.e. actual pressure (P) divided by the vapor pressure at the temperature of the experiment
Pt/ES	Extracted, sulfated material loaded with platinum
Pt/SE	Sulfated, extracted material loaded with platinum
Pt/SZ	Conventional sulfated zirconia loaded with platinum
rf	Response Factor
S12	$C_{12}H_{25}OSO_3Na$
S	Surfactant component in liquid crystal templating (can be +,- or neutral)
SE	Sulfated and then extracted
SEM	Scanning electron microscopy
SES	Sulfated before and after extraction
SZ	Conventional sulfated zirconia
TCD	Thermal conductivity detector
TEM	Tunnelling electron microscopy

WHH	Width at half - height
wt%	weight percent
X^-	Counter - anion in liquid crystal templating
XRD	X-ray diffraction

Chapter 1

Introduction

1.1 Solid Acid Catalysts

Catalysts are chemical compounds that increase the rates of chemical reactions which are thermodynamically feasible, yet the catalysts are not themselves altered in any way by these reactions. Homogeneous catalysis refers to a reaction in which the catalyst itself is soluble in the reaction medium. Heterogeneous catalysis refers to reactions in which the catalyst is of a different phase than the medium in which the reactants are dispersed. Industrially, heterogeneous catalysts are indispensable agents in the processing of virtually all types of chemicals, and are particularly important in the petrochemical field, with uses ranging from the first steps of crude oil refining to the final stages of preparing the desired chemical products.[1] Solid acid catalysts such as zeolites and clays are important industrial heterogeneous catalysts. They are used in many processes such as hydrocarbon cracking, alkylation reactions and in the synthesis of methyl tertiary butyl ether (MTBE), an anti-knocking agent.

Currently, many of our industrial processes (e.g. the alkylation or isomerization of hydrocarbons) use highly toxic and corrosive acids as catalysts; there is growing environmental concern about the use of these corrosive liquid acids (such as hydrofluoric acid and 96 percent sulphuric acid). In addition it becomes very difficult to remove the products from the acid they were mixed in. Selective and active solid acids are therefore attractive as replacements. Because many of these solids hold their acidity internally, they are easy to handle - they can even be held safely in the palm of one's hand. They are also very effective; some of them exceed the acidity of concentrated sulphuric acid by a factor of more than 10 million.[2] The evergrowing family of molecular-sieve catalysts, with strong proton-donating sites distributed uniformly within the pores and cavities, offers a promising range of viable alternatives.[3]

Among the first kinds of solid acid catalysts to be used industrially were silica-alumina gels, which catalyse the cracking of hydrocarbons.[2] Silica-alumina gels have no defined internal structure and contain many micropores. Some characteristics of silica-alumina gels - especially their highly variable pore size and their amorphous quality - make them less ideal catalysts. Since the gels have no regular structure, their protons are unevenly distributed and it is therefore difficult to control catalysis precisely.

In the 1960s zeolites replaced most of the silica-alumina gels.[2] Zeolites are natural and synthetic highly porous silicate-aluminate crystals laced with minute channels that typically range in diameter from 0.3 nm to 1.4 nm (Figure 1.1).

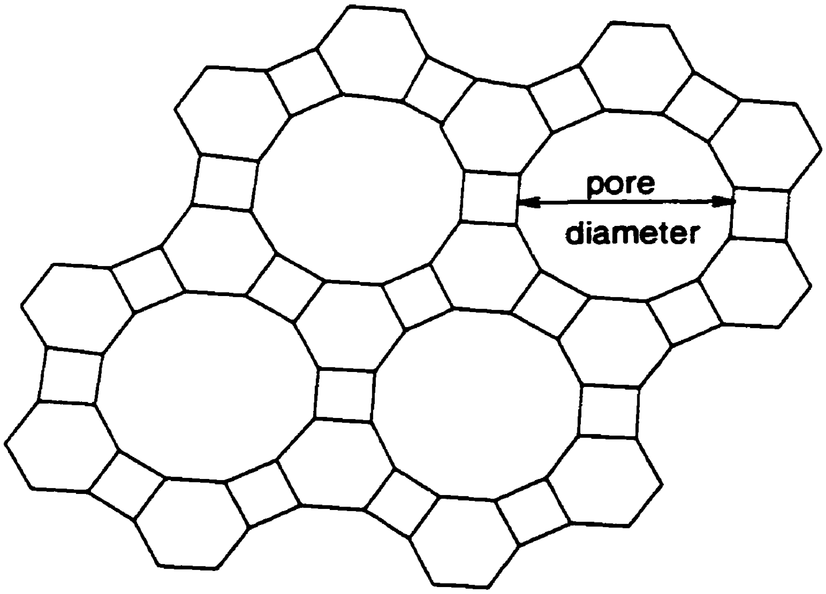

Figure 1.1: Two Dimensional Schematic of a Zeolite MTW Structure (The vertices represent Si or Al atoms and the lines represent bent M-O-M bonds, where M = Si, Al)

Zeolites have large surface areas and a well-defined, regular microstructure. Therefore, the active sites are evenly distributed through the entire structure and these acidic sites are accessible, at least to small molecules since these materials are typically microporous (< 2.0 nm in diameter). One of the most important qualities of zeolites is their ability to exhibit shape selective catalysis. When reactions take place within the tiny pores of a particular zeolite, only those product molecules that readily fit into and migrate along the channels will emerge. In other words, the shape of the cavities can control the size and shape of the final product generated by the catalysed reaction.[2] Today, zeolites are used in many commercial applications. Zeolite Y is the most important component of cracking catalysts and is produced on a scale of several hundred thousand tons per year worldwide.

Because heterogeneous catalysts play such a pivotal role in the petrochemical and other industries, chemists are forever searching for novel catalysts and seeking to improve those already in use. The desire to crack molecules that are too large to fit in the small pores of zeolites or to create products that are too large to emerge from their pores has led to a demand for new types of solid acid catalysts. Several new types of such solids have been developed. They include pillared clays,[4] larger pore zeolites and zeolite - like structures incorporating other transition metal oxides such as zirconium oxide.[5]

1.2 Catalytic Reactions

In solid acid catalysis, reactions frequently proceed through a carbocation intermediate. These types of reactions are very common in the petrochemical field and include catalytic cracking and reforming reactions, isomerizations and polymerizations. For all of these reactions, the presence of an acid site is required to form a carbocation intermediate which can be formed in several ways:[6]

i) The addition of a proton from a Bronsted acid to an olefin

ii) The removal of a halide from an aliphatic halide by a Lewis acid

iii) The oxidation of tertiary alkanes

iv) The addition of acids to alcohols

Carbocations are very reactive intermediates and often carbocations will rearrange to form a more stable carbocation. The order of stability for carbocations follows the trend:

tertiary > secondary> primary

allyl > alkyl

Intermediates can rearrange through hydride ion shifts or through R group migration. The carbocations may also react with other molecules present such as olefins or arenes. The carbocation may also lose a proton from an adjacent carbon to create an olefin.

Therefore, when strong solid acids react with organic compounds many different products can be created. To produce the desired product, in the highest possible yield, a catalyst's properties need to be tuned for a specific reaction.

A frequent problem with solid acid catalysts is deactivation of the catalyst by 'coking'. Coking occurs when a carbon rich deposit is formed on the surface of the catalyst. Often the catalyst can be regenerated by burning off the carbon deposits. This regeneration requires a high temperature and the catalyst must be able to withstand these thermal conditions without decomposing.

1.3 Conventional Sulfated Zirconia

In 1962, it was reported that zirconia, modified in the presence of sulfate groups and platinum crystallites, exhibited strong acidity.[7] Almost twenty years later, detailed studies were done and it was discovered that sulfated zirconia (SZ) catalysts possessed acid sites that were stronger than those present in zeolites and stronger than 100% sulfuric acid, due to which these systems have frequently been defined as solid superacids.[8] Using the Hammett-indicator method Arata and coworkers found that SZ had an acid strength 10^4 times higher than that of 100% sulfuric acid. The activity of sulfated zirconia in catalysing certain reactions (e. g., the low temperature isomerization of n-butane) is unequalled by most strong solid-acid systems including zeolites.[9] The conventional preparations of this catalyst lead to microporous material in which the pores are too small to exhibit high catalytic activity except for small molecules in the vapour phase. Conventional zirconia is prepared by hydrolysing a zirconium salt, such as $ZrOCl_2$ or $ZrO(NO_3)_2$, with aqueous ammonia to produce zirconium hydroxide and then the zirconium hydroxide is sulfated by stirring it in a dilute solution of sulfuric acid or ammonium sulfate. The resultant sulfated zirconium hydroxide must be calcined in air at 550°- 650°C to generate strong acidity. The surface areas obtained by these methods are typically in the 80-140 m^2/g range after calcination in flowing air.[9]

The active crystalline phase of sulfated zirconia is thought to be the tetragonal phase, which forms when the material is calcined at temperatures between 550°C and 700°C.[9] At 800°C the monoclinic phase starts to form. The optimal crystalization temperature is dependent on the concentration of sulfuric acid, since sulfate groups appear to inhibit the tetragonal-to-monoclinic phase transformation.

The nature of the acid sites is still being studied, but a dual Bronsted/Lewis site model has been proposed (Figure 1.2).[9]

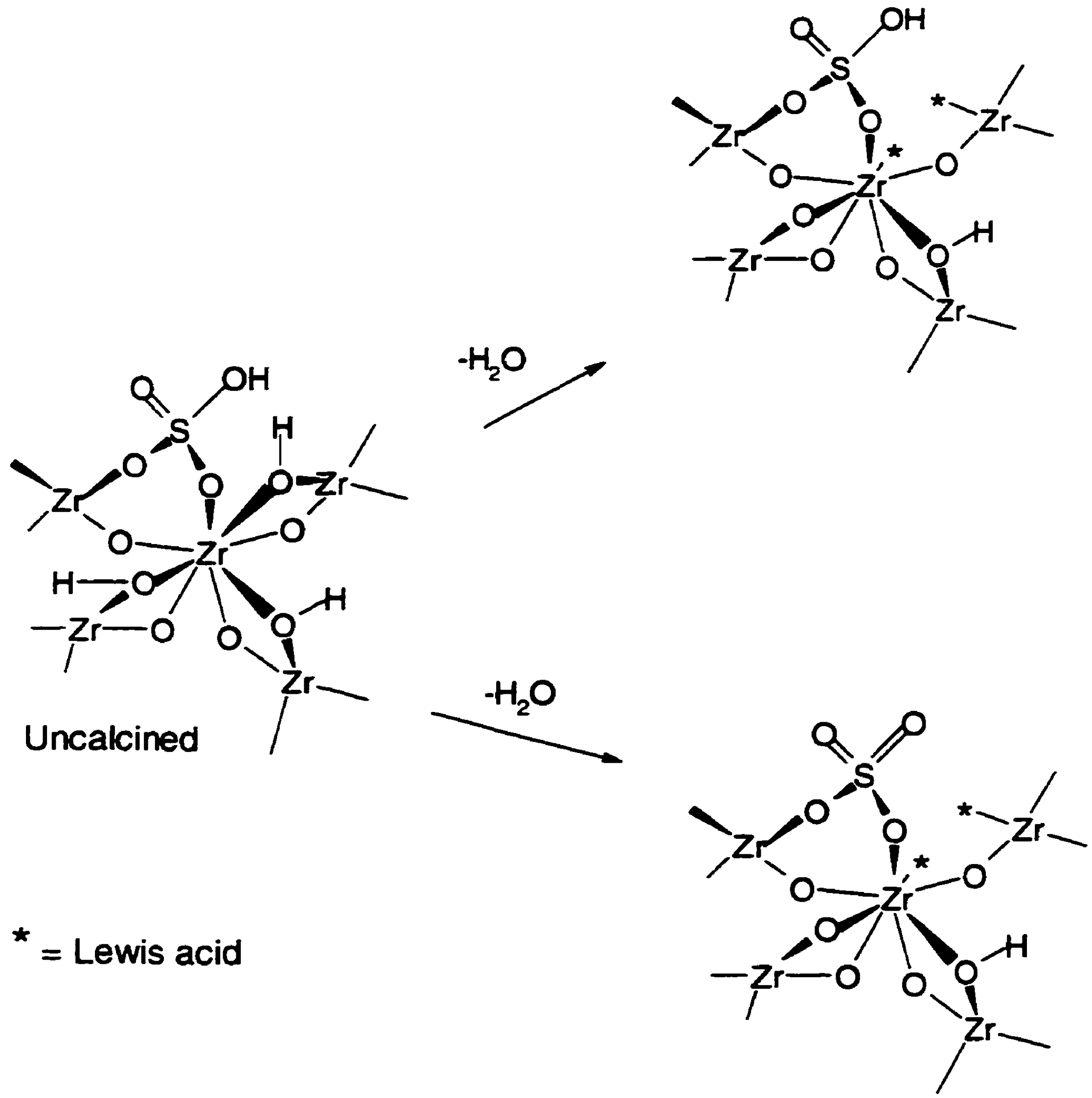

Figure 1.2: Postulated Structure of Acid Sites in Sulfated Zirconia (adapted from X. Song and A. Sayari, Catal. Rev.-Sci. Eng., **383**(3), 329 (1996))

In this model the uncalcined catalyst contains protons as bisulfate and as hydroxyl groups bridging two zirconium ions. During calcination, water is lost to form the two proposed structures shown. In both structures, Lewis acid sites are formed as indicated by asterisks, but in the top structure the bisulfate remains intact, which results in a Lewis acid site adjacent to an S-O-H group. These bisulfate groups act as highly acidic Bronsted sites because the neighbouring Lewis acid sites tend to withdraw electrons from the bisulfate group, thus weakening the SO-H bond. It is inferred that the combination of the bisulfate group with adjacent Lewis acid sites is responsible for the strong acidity.[9] Many other models have been proposed for the structure of the acid sites including tridentate sulfate groups and disulfate groups (S_2O_7). The location of the hydroxyl groups has also been debated. Various models have the hydroxyl groups as part of the sulfate structure (as in Figure 1.2) while other models attach the hydroxyl groups to the zirconia surface, placing them adjacent to the sulfate groups.[9-15]

Since the discovery of its strong acidity, sulfated zirconia has found a number of potential applications as a process catalyst. Hydroisomerization and hydrocracking of straight chain hydrocarbons to produce branched ones are among the most promising catalytic applications.[9] The more active sulfated zirconia catalysts allow the use of low temperatures which could lead to higher selectivity towards branched hydrocarbons. By adding small amounts of platinum to SZ and using the catalyst in an hydrogen atmosphere, deactivation by coking can be delayed. It has been reported that 0.5 wt% Pt/SZ maintained its initial activity for the isomerization of light normal paraffins for several days on stream, and could achieve equilibrium conversion at 140°C.[9]

Since uncalcined sulfated zirconia formed in the conventional manner does not have mesopores, it is less suited for reactions of larger molecules in the liquid phase. Conventional zirconia is known to be microporous; however, with increasing calcination temperature, the micropores collapse and larger pores are formed with wider pore size distributions.[16] Therefore, mesopores can be formed in conventional sulfated zirconia upon calcination at high temperatures, but the pores formed are wide, and also have a very broad range of sizes. To form a catalyst that has shape selectivity for larger molecules, in the same way that zeolites do for smaller molecules, narrow pore size distributions need to be created. If a method could be found that would form mesoporous sulfated zirconia with narrow pore size distributions and a regular well-defined structure, it could be used in the selective reactions of larger molecules.

1.4 Mesoporous Silicate Materials

Designing the structures of mesoporous metal oxides is a current challenge in solid-state chemistry. The methods used to make these materials are based on the synthesis of zeolite-type solids, in which small organic molecules are used as templates. The templates are occluded by crystalizing an inorganic framework around them during hydrothermal synthesis and upon removal of the template, a cavity is created that has morphological and/or stereochemical features related to those of the template.[17] The utility of the final material is determined, in part, by its microstructure. This microstructure allows molecules access to large internal surface areas and cavities that enhance catalytic activity and adsorptive capacity.[18] Zeolites are well-known for their regular microstructure, while pores in mesoporous materials are generally irregularly spaced and broadly distributed in size.[18]

In the early 1990s aggregates of surfactant molecules were first used as templates.[18] Surfactants are bifunctional molecules that contain a solvent-loving (lyophilic) head group and a solvent-hating (lyophobic) tail. As a result of their bifunctional structure, surfactants can associate into supramolecular arrays called liquid crystals. When a surfactant dissolves in water it will form micelles (Figure 1.3).

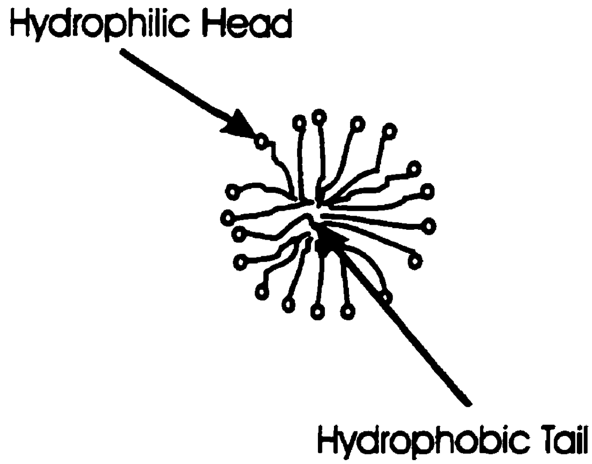

Figure 1.3: Structure of a Micelle

In the micelle, the hydrophilic head groups form the outer surface and the hydrophobic tails point toward the center. The extent of micellization, the shape of the micelles and the aggregation of the micelles into liquid crystals depends on the surfactant concentration and the temperature (Figure 1.4).

Figure 1.4 is a typical phase diagram for a surfactant. The actual concentrations at which the different phases form will vary depending on the type of surfactant. The concentration at which individual surfactant molecules start to form spherical aggregates (micelles) is the critical micelle concentration (CMC).[19] At higher concentrations, the micelles form elongated cylindrical micelles and eventually these cylindrical micelles associate to form liquid crystals. There are three types of liquid crystals: hexagonal, lamellar and cubic. In a hexagonal liquid crystal, the rod - like cylindrical micelles aggregate and form an hexagonal array with water occupying the spaces between the rods. In a lamellar liquid crystal, the individual surfactant molecules form layers in solution and the cubic liquid crystal has the cylindrical micelles branching in different directions forming two intertwined networks.

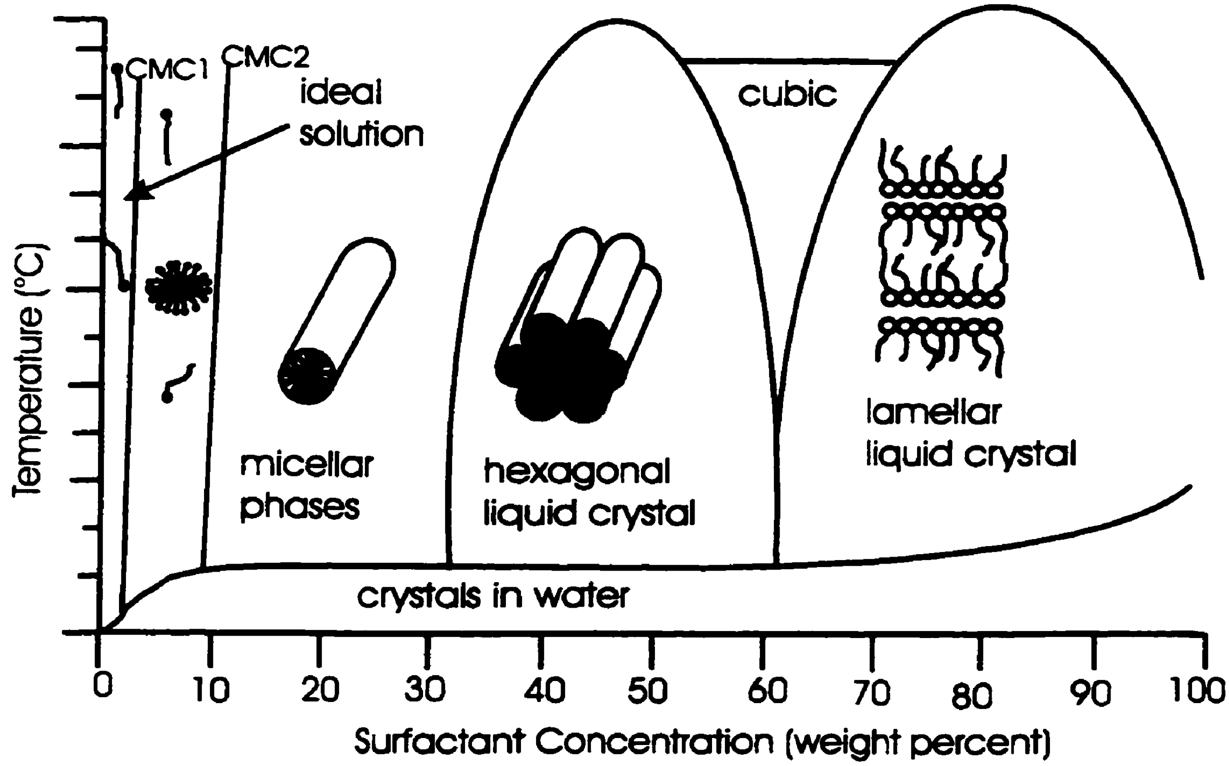

Figure 1.4: Typical Phase Diagram for A Surfactant

A hexagonal liquid crystal was used as the template to form the recently discovered MCM-41 (Mobil Corporation Material) materials.[18] Since liquid crystals were used as templates, this method was called liquid-crystal templating (LCT). Two possible pathways for these syntheses have been proposed (Figure 1.5)

In the first pathway, a surfactant liquid crystal phase exists in solution and serves as the template. Silicate species are deposited between the surfactant rods and then condense to form the inorganic network. Encapsulation occurs because the anionic inorganic species enters the solvent region (H_2O) to balance the charge on the cationic hydrophilic surfaces of the micelles. In the second model, the interaction of silicate species with the surfactant mediates the hexagonal ordering. Once formed, calcination at elevated temperatures burns off the or-

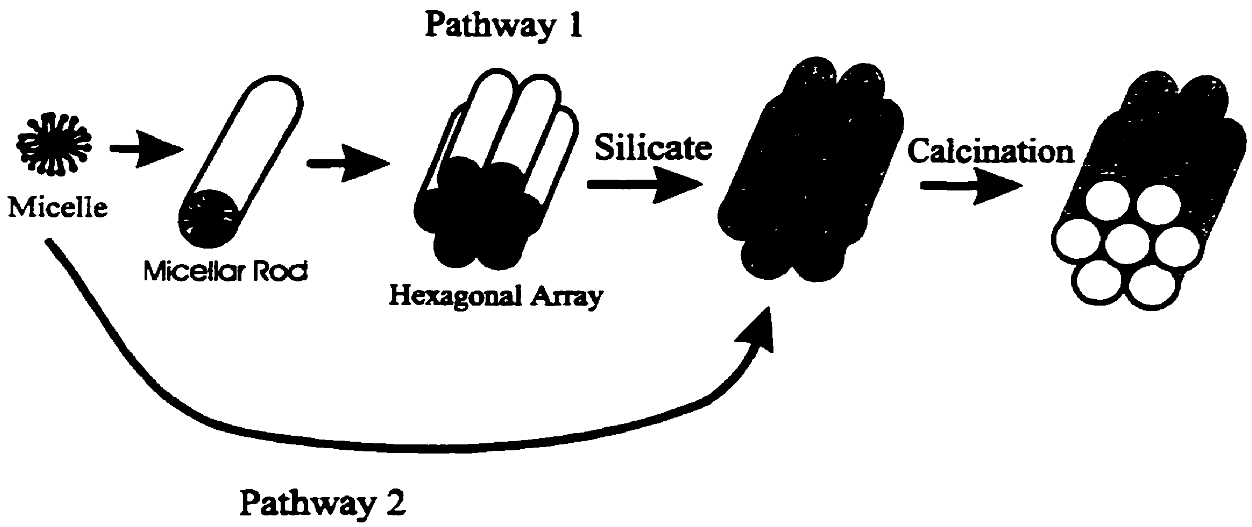

Figure 1.5: Liquid Crystal Templating (adapted from J. S. Beck et al., J. Amer. Chem. Soc., **114**, 10834 (1992))

ganic template to yield the mesoporous material with an array of uniform pores. Mesoporous materials are defined as materials that have pores with diameters between 2 and 50 nm. The MCM-41 material can be made with pore diameters ranging from 1.5 nm to 10 nm and with surface areas approaching 1400 m^2/g.[18] The pore size distribution of this material is quite narrow, with a typical width at half-height (WHH) of 0.5 nm. No micropores are thought to be present, from the shape of the nitrogen adsorption isotherm. The pore size of the material was adjusted by changing the alkyl chain length of the surfactant. The longer the alkyl chain is, the larger is the diameter of the surfactant rods forming the hexagonal array, and the larger the pores left after burning out the surfactant. However, the maximum pore sizes obtained by just using surfactants with longer alkyl chain lengths was around 4.5 nm. If larger pores are desired, an organic additive has to be used. This additive expands the micellar structure by entering into the hydrophobic parts of the micelle and causing it to swell. Using 1,3,5-trimethyl benzene as an additive, pore sizes up to 10 nm have been reported.[20] These materials also have high thermal stability and are stable up to temperatures of 1000°C.

The discovery of the synthesis pathway leading to the MCM family was thus considered a major breakthrough, since it opened the range of pore sizes between approximately 2 and 10 nm. The only drawback to these catalysts was their relatively low acid site concentration and acid site strength.[20] Also the materials only had amorphous wall structures; this lack of regular wall structure decreased the number and strength of acid sites. To improve the acidity of the material, other atoms such as aluminium and boron have been used to substitute for the silicon. This substitution broadened the pores and, in addition, studies have concluded that the acidity of Al-containing MCM-41 is comparable to that of amorphous silica-alumina and is much lower than the acidity of zeolites.[21]

The catalytic activity of MCM-41 has been tested in certain applications. Armengo et al. used the acid form of mesoporous aluminosilicate MCM-41 molecular sieve to carry out alkylation reactions of bulky aromatic compounds such as 2,4-di-tert-butylphenol with a bulky alcohol (cinnamyl alcohol).[22] This reaction did not take place in the presence of large-pore HY zeolite (pore diameter = 0.74 nm), indicating the importance of the mesoporous structure of the H-MCM-41 catalyst and the advantage of having accessible active sites.[21, 22] Many other examples have been given.[21] Due to the low acidity of the MCM material, it has been proposed that the best prospective use of this material is as a catalyst support.[20] For example NiMo impregnated on Al-MCM-41 was shown to have higher hydrodesulfurization activity and higher hydrodenitrogenation activity that NiMo loaded on USY (a commercial zeolite).[23] The higher activity was attributed to the higher surface area and the presence of mesopores in the MCM support which makes active sites readily accessible and causes there to be a high dispersion of active ingredients.[21, 23]

Since the LCT synthesis was discovered, it has been applied to other metal oxides. If a material more acidic than MCM-41, but with the same pore structure could be made it would have many potential applications. Following the guidelines of MCM synthesis, many groups have attempted to make mesoporous metal oxides, including niobia,[24] titania[25] and alumina.[26] One of the transitions metal oxides with potential is zirconia due to its superacidity and high catalytic activity.

1.5 Mesoporous Sulfated Zirconia

Binary metal oxides typically possess only one or a few thermodynamically stable modifications, providing a limited range for design. If, however, the formation of solid oxides is carried out at low temperatures and thus under kinetic control, it is possible to prepare metastable modifications and to influence the reaction process.[5] Using low temperatures and various surfactants, different modifications such as tetragonal and monoclinic, and different mesostructures such as hexagonal, lamellar and cubic can be formed. Using lower temperatures also allows hydrolysis to take place slowly and ordering to develop over time.

For construction of regular mesostructures it is important to adapt the headgroup chemistry of the surfactants (S) to that of the inorganic species (I). In aqueous solution, the inorganic species form oligomeric cations or anions that are able to undergo further condensation. Using ionic surfactants, four different combinations are possible for making mesoporous metal oxides (Figure 1.6).[5]

In this figure, the charge on the surfactant (S) is shown in the headgroup, while the charge on the inorganic species (I) is given in the box. The different methods include using

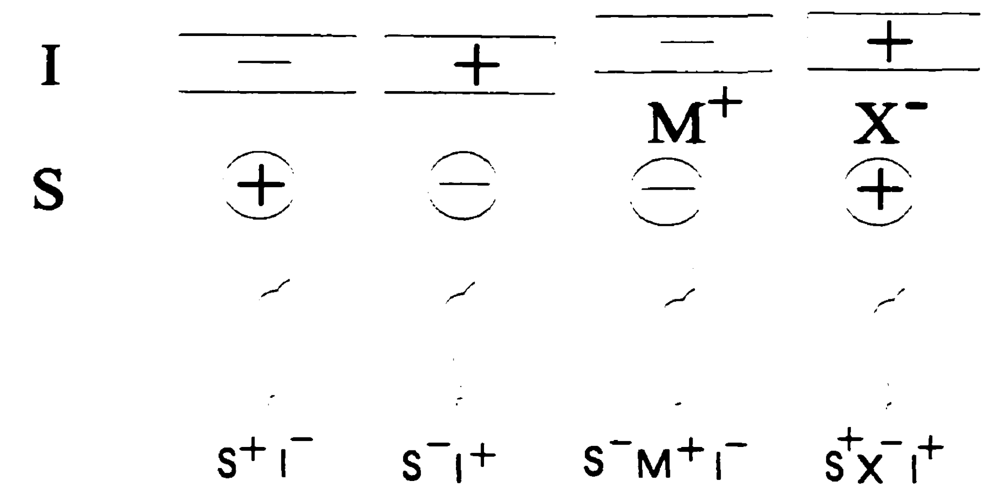

Figure 1.6: Ionic Combinations used for making Mesoporous Transition Metal Oxides

cationic surfactants and anionic inorganic species as in the MCM-41 synthesis. Also possible is the use of anionic surfactants and a cationic inorganic species. Organic-inorganic combinations with identically charged partners are possible, but then the formation of the mesostructure is mediated by counter-charged ions which must be present in stoichiometric amounts: $S^+X^-I^+$ or $S^-M^+I^-$ mesostructures. Examples of both cationic and anionic routes have been tried in the synthesis of mesoporous zirconia.

Hudson and Knowles prepared high surface area zirconium (IV) oxide by incorporation of cationic quaternary ammonium surfactants in the hydrous oxide.[27] The surfactants were incorporated by cation exchange under basic conditions. Under highly basic conditions, there is a degree of dissolution and reprecipitation of hydrous zirconium (IV) oxide allowing a degree of ordering to develop over time. The materials formed had high surfaces areas, around 300 m^2/g when calcined at 450°C. The materials were definitely mesoporous (pores between 3.0 and 5.0 nm in diameter), but their distributions were very broad. The width at half height of these distributions was greater than 2.0 nm. When the material was calcined at 650°C, the surface area decreased to 160 m^2/g. At 450°C, the material is amorphous and crystalization to the tetragonal form, which is essential for catalytic activity, does not start until 600°C and is complete at 800°C. However, the pore size distribution of the material was not measured after calcination at any temperature greater than 450°C. Also this material was not sulfated and sulfate groups are needed for acidity. The addition of sulfate groups would change the internal structure of the material. It is also not known if the high surface areas are due to the presence of some micropores as well as mesopores, but the nitrogen adsorption isotherm obtained indicates that the material has a structure similar to calcined zirconium (IV) oxide aerogels, which have very large pores (typically pore diameters between 60 and 200 nm).[28]

Larsen et al. used the anionic surfactant/cationic precursor route to make mesoporous zirconia.[29] Upon calcination at 575°C, the surface area is around 215 m^2/g and the pore size is around 2.5 nm, but again the distribution is very broad. This material was also not sulfated so its acidity was not studied. Fripiat et al. also tried using an anionic template.[30] Two different templates were tested, $C_{12}H_{25}OP(OH)_2$ and $C_{12}H_{25}OSO_3Na$, abbreviated P12 and S12 respectively. With S12, the structure collapsed at 500°C and the mesostructure completely disappeared. When P12 is calcined at 500°C over 50% of the mesoporosity is lost and the rest is left in pores with diameters between 1.0 and 10.0 nm. The distribution is centered around 8.0 nm and is very broad. When Sachtler and Huang used anionic surfactants, only lamellar zirconia was obtained.[31] The mesostructure was lost even when the template was removed by extraction instead of calcination and only amorphous zirconia was obtained.

Schuth et al. synthesized a porous zirconium oxo-phosphate by a surfactant-assisted synthesis.[32] Two different methods were tried. The syntheses were carried out in aqueous solution using hexadecyltrimethyl ammonium bromide as the template. When zirconium sulfate was used as the zirconium source the samples collapsed upon calcination at 500°C. To stabilize the structure, the samples were treated with phosphoric acid; the resulting material was stable at 500°C and had a surface area of 230 m^2/g. However, the nitrogen isotherms indicated the presence of micropores. When zirconium propoxide was used as the zirconium source and ammonium sulfate as the sulfating agent, the material was also stable at 500°C, and once again, the material possessed a nitrogen adsorption isotherm typical of a microporous material (surface area is 280 m^2/g). Some ordering in the structure was known to exist, as small angle peaks in the XRD pattern could be observed. When the zirconia catalyst was calcined at a temperature high enough to create the tetragonal phase, the catalyst no longer exhibited any hexagonal pore structure.[33]

Sayari and Reddy made both hexagonal and lamellar phases of zirconium oxide using the supramolecular templating approach.[34] The hexagonal zirconia was made using a cationic surfactant while the lamellar zirconia was made using a neutral amine. Different gel compositions as well as different crystalization temperatures and times were tested. All of the materials, both hexagonal and lamellar, collapsed when calcined at 500°C for 6 hours. Some of the material was made using zirconium sulfate or sulfuric acid but no additional sulfating was done to stabilize the material.

Later another route was discovered that would form mesoporous materials, the neutral templating route. This route has been used by Pinnavaia to form a mesoporous silica and a titanium substituted analogue.[35] This approach was based on hydrogen bonding and self-assembly between neutral primary amine micelles (S^0) and neutral inorganic precursors (I^0).

The route allows for simple solvent extraction of the template with ethanol due to the weaker interactions between the surfactant and the inorganic framework, but thicker pore walls are formed. These thicker walls improve the thermal and hydrothermal stability of the material. Removal of the template by solvent extraction tended to preserve the crystallinity of the product, whereas local heating by calcination caused some degradation of the mesoporous framework. The material was calcined at 450°C for 7 hours and still retained a peak in the low angle X-ray diffraction pattern (4.1 nm d-spacing) and a pore size distribution centered around 2.4 nm. The material also had a very high surface area around 1000 m^2/g, similar to that of the silicates made using the LCT route. The calcined material had a smaller pore size than material that was simply extracted without calcining indicating the partial collapse of the mesoporous framework on calcination. Pinnavaia has noted that the use of nonionic surfactants results in a 'wormhole motif' or a lack of regular channel packing.[35, 36] These wormlike channels, though more or less regular in diameter, have no discernible long-range order.

The nonionic surfactant route has also been applied to zirconia with success by Sachtler et al.when using zirconium propoxide as the precursor and hexadecylamine as the template.[37] Metal alkoxides are often used as precursors since their hydrolysis can be controlled by adjusting the pH and concentration of the aqueous solution. To slow down the hydrolysis process, acetylacetone is used as a stabilizing agent. This forms zirconium (acetylacetonate) trisisopropoxide which hydrolyses slower than the alkoxide. Sachtler et al. also reported that sulfate deposition was crucial for transformation of mesoporous zirconia with amorphous pore walls into a material with crystalline pore walls, while maintaining mesoporous morphology with narrow pore size distributions.[37] The transformation to the tetragonal modification started at 600°C and was complete at 650°C. At 700°C, the monoclinic modification started to form. Therefore, after calcination at 650°C sulfated zirconia which showed both maintenance of mesoporosity and tetragonal crystallinity was formed. This mesoporosity was completely lost when the tetragonal zirconia was transformed to the monoclinic modification. The surface area of this tetragonal material was about 95 m^2/g and it has a very narrow pore size distribution (0.30 nm) centered around 3.6 nm. A chaotic arrangement of pores was revealed by tunnelling electron microscopy (TEM).

This new mesoporous material was tested in catalytic reactions and compared to conventional microporous sulfated zirconia.[37] When these materials were used as catalysts for n-butane isomerization, both materials showed almost identical activity. Both samples also deactivated rapidly. To test the effects of mesoporosity, a conversion of large molecules in the liquid phase was also tested. Here, the mesoporous material had a faster conversion rate and a different selectivity. The advantage of wider pores was demonstrated by the superior catalytic performance of the mesoporous material in the liquid phase alkylation of large molecules.

However only one size of mesopores was investigated by Sachtler. In light of Sachtler's success with this method, it was thought that if material with different pore sizes could be made, the pore size of the material could be tailored for a specific reaction. Different pore sizes should show different conversion rates and different selectivity when tested on the same reaction. Changing the pore sizes of mesoporous zirconia (via the nonionic route) has not been studied and it is this problem that will be addressed in this thesis.

1.6 Thesis Objectives

The objective of this work is to investigate the various factors which affect the pore size, surface area and thermal stability of the material synthesized via the LCT method. The purpose of this work is to use the LCT method to synthesize mesoporous sulfated zirconia with a range of pore diameters. The pore sizes of mesoporous sulfated zirconia will be adjusted by varying synthetic parameters in an attempt to create a range of (nonoverlapping) narrow pore sizes. Preliminary catalytic studies of a reaction for which mesoporous sulfated zirconia is suited will be carried out, and the selectivity of the samples with different pore diameters will be tested. The results of these studies are presented and discussed in this thesis.

Chapter 2

Experimental

2.1 Synthesis of Mesoporous Sulfated Zirconia

Zirconia and other metal oxides can be made by using the sol-gel method.[38] In this method an inorganic compound, usually an alkoxide, is reacted with water. Alkoxides react readily with water in hydrolysis reactions to form an inorganic network. Depending on the water concentration different amounts of branching and condensation will occur. After the initial gelation has occurred, the sol-gel is aged. Aging may involve further condensation, dissolution and reprecipitation or phase transformations. Once the sol-gel has been made and aged, it is dried. This process removes the excess water and leaves behind the inorganic polymeric material, referred to as a xerogel.

In the synthesis of mesoporous sulfated zirconia the sol-gel method is used to form an inorganic framework around a template, following the LCT route used in making mesoporous silicates. When using this method it is important to match the headgroup chemistry of the surfactant with the inorganic component. Many different synthetic methods have been described in the literature.[27, 29-37] Typically, anionic zirconia species are used in combination with cationic surfactants, such as cetyltrimethylammonium bromide (C_{16}TMAB). No matter which ionic combination was used, the method always involved making a surfactant solution and then adding the inorganic component. Hydrolysis was initiated by the addition of acid or base to form a gel which was then aged and dried to give an inorganic solid. To make mesoporous sulfated zirconia this inorganic solid would then be sulfated (by stirring in dilute sulfuric acid) and calcined to remove the template. In order to determine which combination of surfactant and inorganic species was best, various combinations were tested. The different ionic combinations and methods used will be described in this chapter, along with the techniques used to characterize the final material. These methods are identified by a characteristic feature of their synthesis, e.g. "Ambient Temperature Synthesis".

2.1.1 Ambient Temperature Synthesis[39]

Hexadecyltrimethyl ammonium bromide (2.5g, 6.86 mmol) was dissolved in 85.00 mL of distilled water. Zirconium oxychloride (4.0g, 12.4 mmol) was also dissolved in water (20.00 mL) to form a clear solution which was added to the surfactant solution while stirring. The pH of the resulting mixture was adjusted to 11.7 with 1M sodium hydroxide and the solution was then stirred for 10 minutes. Then 1.0M H_2SO_4 solution was added until the pH of the slurry was approximately 10, and stirring continued for 30 minutes. The resulting gel was tightly sealed and kept sitting statically at ambient temperature for 30 days. The solid products, recovered by filtration, were washed with distilled water and dried at ambient temperature.

2.1.2 Zirconium Sulfate Synthesis[32]

Hexadecyltrimethylammonium bromide (2.5g, 6.87 mmol) was dissolved in H_2O (85 mL) and $Zr(SO_4)_2{\cdot}4H_2O$ (4.55 g, 0.0128 mol) dissolved in H_2O (15 mL) was added. This led to a white solid precipitate. The mixture was stirred for two hours at room temperature and then heated at 100°C for 2 days in a sealed container. The precipitate was filtered and dried at 100°C. The dried solid was stirred in a sulfuric acid solution (1.0 M, 50 mL) for 2 hours, then filtered, and dried again at 100°C.

Different aging times of 1 to 4 days were also tested with this method. Various treatments of the dried precipitate were conducted, instead of using 1M H_2SO_4. These included treating with 1M H_3PO_4, 0.08M H_2SO_4, 1M Na_2SO_4 or 1M $(NH_4)_2SO_4$.

2.1.3 Propanol Solvent Method[24]

A solution of zirconium (IV) propoxide (5.10 g, 15.6 mmol) in n-propanol (7.0 mL) was treated with hexadecyltrimethyl ammonium bromide (2.86g, 7.8 mmol). This mixture was stirred until homogenous and then more n-propanol was added (5.00 mL). When this solution was further treated with water (15 mL), a rapid reaction ensued, giving a white gelantinous precipitate. This gel was stirred for 10 minutes and left overnight at ambient temperature. The mixture was then transferred to an autoclave and aged at 180°C overnight. The solids were separated by centrifuging and dried at 100°C.

2.1.4 Delayed Low pH Synthesis[40]

$ZrOCl_2{\cdot}8H_2O$ (2.70g, 8.38 mmol) was dissolved in 10 mL of H_2O. To this solution, 0.82 g (2.25 mmol) of hexadecyltrimethyl ammonium bromide in 8.00 mL of water was added followed by a solution of $(NH_4)_2SO_4$ (4.4 g, 33.3 mmol) dissolved in water (24 mL). After stirring for 10 minutes, the pH of the mixture was adjusted to 2.1 using 1M H_2SO_4. The gel was then stirred for 30 minutes before being transferred to a polypropylene bottle, sealed and heated for 24 hours at 100°C. The solids were recovered by filtration, washed with large amounts of distilled H_2O, and dried at ambient temperature.

2.1.5 High pH Synthesis[27]

To an aqueous solution of $ZrOCl_2{\cdot}8H_2O$ (3.23 g, 10.0 mmol in 100 mL H_2O) was added an aqueous solution of hexadecyltrimethylammonium bromide (3.13g, 86.00 mL). The combined solution was stirred for 15 minutes. Concentrated aqueous ammonia was slowly added with continuous stirring until the pH was 11.5. Hydrous Zr (IV) oxide precipitated as a gelatinous solid a few moments after addition of the base. The resulting gel was stirred for 1 hour at ambient temperature and then heated to 70°C. Once the reaction mixture had reached thermal equilibrium, the reaction flask was sealed and continually stirred for 90 hours. The pH was readjusted back to 11.5 every 24 hours using concentrated aqueous ammonia. After the mixture had cooled, the solids were filtered off and washed with water and acetone. The white powder was dried at 60°C for 20 hours. After drying, the solids were stirred for 10 minutes in 0.5M H_2SO_4 (15 mL/g) and then filtered and dried.

2.1.6 Initial Low pH Synthesis[32]

Hexadecyltrimethyl ammonium bromide (2.5 g, 6.87 mmol) was dissolved in a solution of water (115 mL) and HCl (21.0 mL, 37%). Once the surfactant was completely dissolved, $Zr(OPr)_4$ (5.80 mL of 70 wt% solution in n-propanol) was added slowly to the solution. After the hydrolysis products had dissolved, $(NH_4)_2(SO_4)$ (2.04 g, 0.0155 mol) in water (23 mL) was added and the mixture was stirred at room temperature for one hour. The initially clear solution was heated at 80-85°C for two days in a sealed container. The white precipitate was filtered, washed with water and dried at 90°C.

2.1.7 Neutral Templating Method[37]

Hexadecylamine (7.00 g, 0.030 mol) was dissolved in a mixture of 70.00 mL deionized water and 6 drops of 37% HCl under heating (below 80°C) and stirring to homogenize the mixture. Then 45.0 mL (0.10 mol) of $Zr(OPr)_4$ (70 wt-% solution in n-propanol) was mixed with 5 mL of acetylacetone (0.05 mol). This mixture was stirred for 5 minutes. A clear yellow solution was obtained. It was added dropwise to the surfactant solution under strong stirring.

Heating was stopped to cool down the surfactant mixture a few minutes before the solutions were mixed. A large amount of white precipitate formed upon mixing. Stirring was continued for another half hour and then the mixture was aged at ambient temperature for at least 120 hours. The solids were separated by centrifuging or filtering and drying at room temperature.

Different surfactants, as well as different surfactant concentrations, were used. Co-solvents, such as acetonitrile and ethanol, were sometimes added to the $Zr(OPr)_4$ solution. The final mixture was sometimes heated during the aging process.

2.1.8 Extraction and Sulfation Procedures

Solids were extracted twice by stirring them in 90% ethanol (50 mL/g) at 75°C for 10 minutes. The solids were then filtered, washed with 100% ethanol and dried at ambient temperature. The solids were sulfated by stirring them in 0.5M H_2SO_4 (15 mL/g) for 10 minutes. For some syntheses, the order of sulfation and extraction steps were reversed, and the sulfation was sometimes repeated (once before and once after the extractions). The sulfated and extracted solids were dried overnight at 100°C.

Since sulfation under aqueous conditions may affect the porosity, gas - phase sulfation was also used. Gas - phase sulfation was performed at Alberta Sulphur Research by the following procedure: 1 g of catalyst was divided into three quartz boats which were placed in a densified alumina catalyst reactor tube such that they occupied the middle of the "hot zone" of the furnace. The reactor was purged with 200 mL/min of nitrogen for 1 hour. The reactor was then heated to 200°C under a flow of nitrogen (100 mL/min) and allowed to equilibrate overnight. A 13.7% SO_2 and 86.3% air mixture was then flowed over the catalyst at the same rate with the outlet of the reactor attached to a KOH scrubber. After sulfation was completed, nitrogen was used to purge the reactor for 1 hour (200 mL/min) before the reactor was cooled back to ambient temperature under a flow of nitrogen (100 mL/min).

2.1.9 Calcination Procedures

Solids were heated to the desired temperature (usually 650°C) at a rate of 1°C/min, held at the desired temperature for 2 - 6 hours as appropriate and then cooled back to room temperature at 1°C/min. Calcination was done in static air unless otherwise stated.

2.2 Catalyst Characterization

2.2.1 Fourier Transform Infrared Spectroscopic Studies

Infrared (IR) spectra of the samples pressed in KBr pellets were obtained at a resolution of 2 cm^{-1} between 4000 and 350 cm^{-1}. Spectra were collected using a Mattson Instruments Genesis Series FT-IR spectrometer using 32 samples scans and 32 background scans. In each case, the sample was referenced against a blank KBr pellet.

2.2.2 X-ray Diffraction Studies

Powder X-ray diffraction patterns were obtained with a Scintag XDS 2000™ diffractometer using Cu Kα radiation (λ = 1.540562 Å). Samples were step-scanned from 1 to 40° in 0.03° steps with a stepping time of 1 second. Random powder mounts were prepared for all zirconium oxide samples by grinding the calcined material and transferring to an aluminium sample holder prior to measuring the diffraction pattern at room temperature.

2.2.3 Surface Area Measurements

Surface area measurements were made by nitrogen adsorption using the BET method[41] on an ASDI RXM 100 instrument at an adsorption temperature of 77 K, after pretreating the sample under high vacuum at 250°C for one hour. Four data points were collected using initial pressures of nitrogen that were chosen in order to yield final P/P_0 values of 0.02, 0.04, 0.08 and 0.16, which are approximately evenly spaced along the linear portion of the BET adsorption isotherm.[41] The dry weight of the sample, as measured after the adsorption experiment, was used to obtain the final value of the specific surface area.

2.2.4 Elemental Analysis

Analysis for carbon was performed in the Department Instrumentation Facility using a Control Equipment Corporation 440 Elemental Analyser using approximately 2 mg of sample. The instrument has an absolute precision of 0.3%.

Analysis for sulfate was performed at Alberta Sulphur Research using Ion Chromatography (IC). The solid samples were ground and then stirred in 0.1 M NaOH (15 mL/g) for 1 hour at room temperature to extract the sulfate groups. The mixture was then filtered and the filtrate (after dilution) was analysed by IC. The concentration of sulfate in the filtrate was obtained by comparing the results to data obtained from solutions of known sulfate concentration (prepared from Na_2SO_4).

Analysis for platinum was performed using a Thermo Jarrell Ash Atom Scan 16 Inductively Coupled Plasma - Atomic Emission Spectrometer (ICP - AES). The platinum was extracted from the samples by stirring them in aqua regia (approximately 0.50 g catalyst in 25 mL of acid), filtering the mixture and then diluting the filtrate before analysis (1 mL aqua regia solution in 10 mL total deionized water). The wavelengths used for analysis were 214.4 nm and 265.9 nm. The concentration was obtained from calibration curves that were prepared using commercially available standard solutions and the reagent blank.

2.2.5 Mesopore Size Distribution

Mesopore size distributions were derived from nitrogen adsorption isotherms obtained at 77 K, after pretreating the sample at 250°C for one hour under high vacuum. The software used to analyse the adsorption data uses the method of Barrett, Joynner and Halenda (BJH) and the Halsey equation for nitrogen to calculate the thickness of the adsorbed film.[42, 43]

Many other models are available and are used for the calculation of pore size distributions from nitrogen (or argon) adsorption/desorption isotherms. These include the method by Horvath and Kawazoe (H- K) which was used by the researchers at Mobil Research to calculate the pore size distribution for their MCM (silicate) materials.[18, 44] This method is thought to be only applicable to slit - shaped micropores, but the pore diameters calculated using this method are very close to the values obtained by TEM.[18] However, since this method was intended for micropores (and not mesopores) and the pores are thought to be cylindrically shaped in these materials the BJH theory will be used in this report to calculate pore sizes. For ease of comparison, the pore sizes reported by other researchers (which were calculated using the H - K method) have been recalculated using the BJH theory. The adsorption isotherm (rather than desorption) has been used unless otherwise stated. It has been suggested that methods based on the Kelvin equation (e.g. the BJH method) lead to underestimation of the pore diameters and this must be kept in mind when studying the pore size distributions obtained.[45]

2.3 Catalytic Studies

2.3.1 Model Reaction: Alkylation of p-Xylene with Cyclohexene

The alkylation reaction of xylenes with cyclohexene has previously been used as a means of investigating the acid properties of the catalytic sites of solid acid surfaces.[46] The rate of formation of product (disappearance of cyclohexene) may be regarded as a measure of the acidity of the active sites. The rate and the selectivity of the reaction should be affected by the pore size of the catalyst. In this study p-xylene was used so only one product would be formed. Only a small amount of cyclohexene was used and the p-xylene was used in excess, so that dimers of cyclohexene would not form.

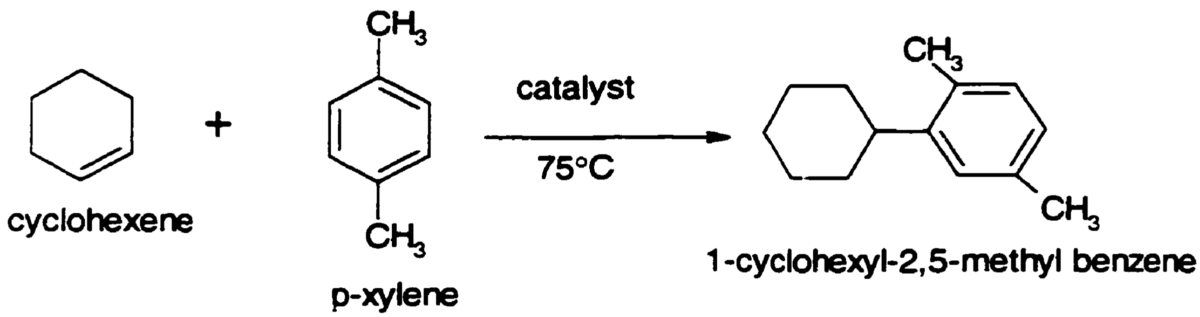

Figure 2.1: Reaction used for Catalytic Testing

2.3.2 Experimental Setup

A 3-neck, round-bottom flask equipped with a condenser, thermometer and septum was used to carry out the catalytic alkylation of p-xylene. For pretreatment, approximately 500 mg of the finely ground catalyst was placed in a quartz boat and placed at the center of a tube furnace. During pretreatment, nitrogen was passed over the catalyst. The catalyst was heated to 450°C and held at that temperature for 2 hours. The catalyst was then cooled to about 150°C before being quickly transferred to the r.b. flask. Immediately, the p-xylene (40.0 mL) was poured over the catalyst, the reaction flask was sealed, stirring was started and the mixture heated to 75°C. When the reaction mixture had reached 75°C, 1.00 mL (9.87 mmol) of cyclohexene was injected and the reaction started. Samples (ca. 0.1 mL) were taken out of the reaction mixture every few minutes and analysed by gas chromatography using a Hewlett Packard 5890 gas chromatograph equipped with a stainless steel column (1/8", 20m) packed with 10% Carbowax on Chromsorb W. The oven was held at a constant temperature of 90°C for two minutes and then ramping at a rate of 10°C/minute to 180°C was employed. Products were detected with a thermal conductivity detector (TCD) at 180°C. The retention times and response factors for each component are listed in Table 2.1.

2.3.3 Data Interpretation

To find the response factors for the reactants, solutions of known weight percent were analysed by GC. The response factor, rf, was found using Eq. (1).

$$\text{rf A} = \text{wt \% A/peak A area \%} \qquad (1)$$

To find the response factor for the product, a different method was used, since pure product could not be purchased. It was assumed for each mole of cyclohexene that disappeared, a mole of product was formed. Using the mole percents of cyclohexene during a catalytic run, the mole percent of product formed was calculated at various time. These were converted to wt% and then the peak area % was used to find the response factors at various times. The response factor was higher for the first few minutes, but the remaining response factors were constant (average = 1.300). The initial response factors are thought to be high due to adsorbed cyclohexene that has not yet reacted, causing the amount of unreacted cyclohexene detected to be low. Therefore, the calculated mole percent of product would be too high (since we assumed for each mole of cyclohexene that reacts, one mole of product forms) which, in turn, would cause a higher response factor to be obtained initially.

Table 2.1: Response Factors and Elution Time for the p-xylene Alkylation Reaction

Compound	Response Factor	Elution Time (min)
cyclohexene	0.930	0.33
p-xylene	1.01	0.89
1-cyclohexyl-2,5-methyl benzene	1.30	8.06

Once the response factors were calculated the raw intensity (area under the GC peak) for each compound was corrected by dividing by the response factor and the mol % of each compound was calculated using Eq. (2).

$$\text{mol \% A} = \frac{\text{Area A/rf A}}{\sum_i \frac{\text{Area i}}{\text{rf i}}} \times 100 \qquad (2)$$

The mole percent of cyclohexene was then converted to mmoles of cyclohexene unreacted at that time. These values were plotted versus time and the slope taken between one and ten minutes to find the rate of conversion during that time interval. To facilitate direct comparison, the rates were normalized on a unit area basis by dividing by the surface area of the catalyst after pretreatment (obtained from the specific surface area and the weight of catalyst used). In order to compare the amount of deactivation that occurred, the extent of reaction was calculated using Eq. (3). The extent of reaction between 1 and 180 minutes shows how much of the cyclohexene (CH) present at 1 minute has reacted by the end of the reaction (as a percentage of the amount present at 1 minute).

$$\text{Extent of Reaction} = \left(\frac{\text{moles CH (1 min) - moles CH (180 min)}}{\text{moles CH (1 min)}}\right) x 100 \qquad (3)$$

These calculations can be justified on the basis that the only product observed was 1-cyclohexyl-2,5-methyl benzene and that, according to the equation, for each mole of cyclohexene that disappears one mole of product is created.

The used catalysts were analysed for the amount of carbon deposited on the surface during the reaction. The used catalysts were treated under vacuum and the percent of carbon on the catalyst then measured; this procedure was designed to remove any adsorbed, unreacted reactants. The pore size distributions and surface areas were also measured for some of the used catalysts.

2.3.4 Loading of Platinum onto Catalysts

To load platinum onto the catalysts, an aqueous solution containing 0.10 g Pt was prepared by dissolving H_2PtCl_6 (0.210g) in 40 mL of distilled water. The catalyst was stirred (2 mL of catalyst/1 mL solution) in this solution for 5 minutes and then filtered and dried at 100°C overnight. The samples were then calcined using the procedure already mentioned. Catalytic reactions performed with catalysts loaded with platinum had hydrogen gas bubbled into the reaction mixture at a rate of 30 mL/min.

Chapter 3

Physico-Chemical Characterization of Catalysts

3.1 Synthetic Methods

The different synthetic methods tested can be divided into four categories: cationic, cationic/acidic, cationic/basic, and neutral, referring to the type of surfactant used and the pH used for the hydrolysis. The characteristics of the material obtained from each of these methods will be discussed. The materials obtained were characterized by X-ray diffraction (XRD) powder patterns, infrared (IR) spectroscopy and nitrogen adsorption measurements which yielded surface areas and pore size distributions.

3.1.1 Cationic Methods

In these methods hexadecyltrimethyl ammonium bromide (C_{16}TMAB) was used as the surfactant and no additional acid or base was used to initiate the hydrolysis. Two methods of this type were used (refer to sections 2.1.2 and 2.1.3).

When zirconium sulfate was used as the inorganic precursor (Section 2.1.2) peaks were observed in the low-angle X-ray diffraction pattern for the uncalcined samples (Figure 3.2). These peaks show that some long-range order is present and these reflections can be indexed as (100), (110) and (210), assuming a hexagonal unit cell and indexing the peaks in analogy to MCM-41.[18] The 'very' broad peak between 25° and 30° (2θ) is typical for amorphous material. The d-spacing of the 100 peak was 4.08 nm which is similar to that of the silicate materials made using the same surfactant. When using C_{16}TMAB the d-spacing will be approximately equal to 3.6 nm.[47] The d-spacing is the spacing between layers in a lattice and for these compounds is equal to twice the length of the surfactant plus the thickness of two walls (Figure 3.1).

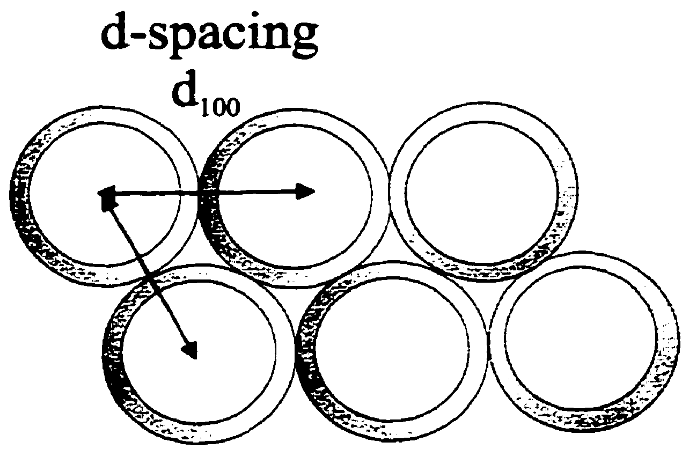

Figure 3.1: The d- spacing in Mesoporous Sulfated Zirconia

When the aging time was increased from 1 day to 2 days the intensity of the (100) reflection increased. After treating the material with 1M H_2SO_4 four reflections were clearly present in the diffraction pattern. Thermal treatment of these samples in air at 500°C lead to a collapse of the ordered pore structure, as shown by in the disappearance of the low angle reflections (Figure 3.2d)

It was thought that the 1 M acid may have destroyed the pore structure, so different methods of sulfating the material were attempted. Sulfation with a weaker H_2SO_4 solution (0.081M), with 1M Na_2SO_4 and 1M $(NH_4)_2SO_4$ were tested. All three treatments resulted in similar XRD patterns as seen previously for the uncalcined material. When these materials were calcined at 500°C the low angle reflections disappeared, but two weak reflections at 30° and 35° 2θ were formed. The peaks indicate that some crystalline phase of zirconia is starting to form; both the tetragonal and monoclinic forms of zirconia have XRD peaks in this area. The surface area of the material treated with 1M $(NH_4)_2SO_4$ and calcined at 500°C was found

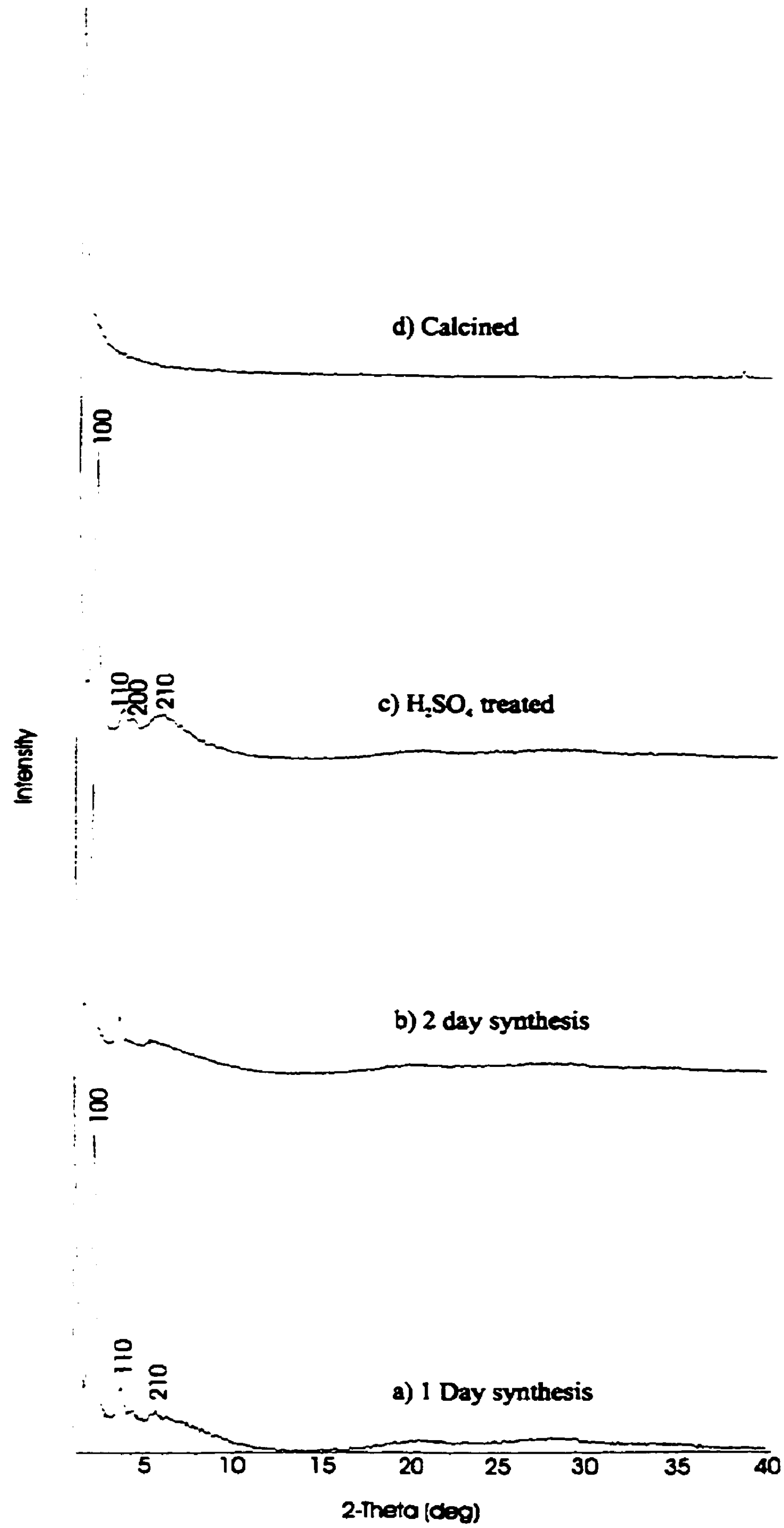

Figure 3.2: XRD Powder Patterns for Material made using the Zirconium Sulfate Synthesis (Note: Scale is not the same for all of the XRD patterns)

to be 32 m^2/g. Sulfate groups were present on the catalyst as evidenced by the sulfate peaks which were seen in the infrared spectra (1300-1000 cm^{-1}) (Figure 3.3). The pattern of peaks in this region will be discussed in a later chapter.

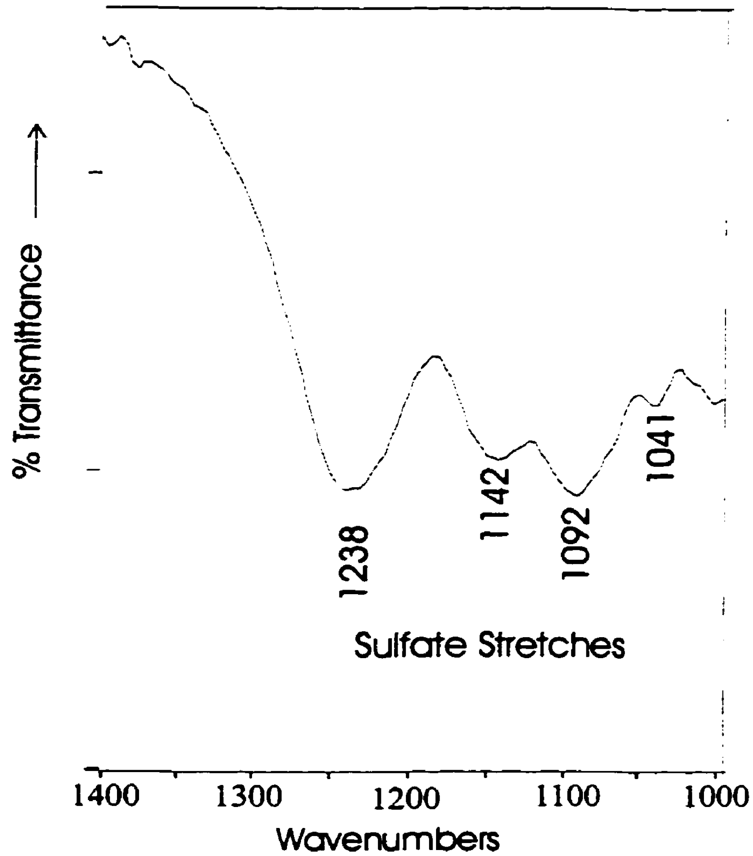

Figure 3.3: Infrared Spectra in the Sulfate - Stretching Region of Sulfated Zirconia made via the Zirconium Sulfate Synthesis

Treatment with 1M H_3PO_4, instead of H_2SO_4, was also used to stabilize the structure since this method had proved successful in earlier work.[32] After calcination of such a sample, one low angle reflection was present with a d-spacing of 2.83 nm (Figure 3.4) which can be compared to a d-spacing of 3.5 nm for calcined MCM-41. Before calcination the d-spacing of both materials was similar (around 4.0 nm). The smaller d-spacing for the zirconia after calcination implies that a larger contraction of the structure took place during calcination and therefore, the pores are smaller and the pore walls are thicker. The calcined phosphate - treated zirconia was very dark and the surface area was negligible which indicates that carbon, formed during the calcination of the material, has been deposited on the catalyst surface. During calcination, some of the surfactant is converted to a gaseous mixture of carbon dioxide, carbon monoxide and water, however, in this case, some of the surfactant was apparently left behind as carbon. The infrared spectra of the material after calcination at 500°C no longer had any alkyl peaks present around 2900 cm^{-1} which showed that the surfactant had partially been converted to gaseous products and the remaining surfactant was left behind, presumably as a highly polymerized carbonaceous deposit. The infrared spectra no longer had a group of peaks between 1300 and 1000 cm^{-1}(due to the sulfate groups), but one large broad peak centered at 1036 cm^{-1} was present, attributed to the phosphate ligand (Figure 3.5).

Various orders of treatment were tested, such as treating with phosphoric acid followed by sulfuric acid, but no material had any long range order or crystallinity after calcination.

Although Ciesla et al. has used phosphoric acid treatment to obtain material that would not collapse upon calcination, they did not obtain any long range order using this method either.[32] Only micropores were obtained (as indicated by their nitrogen adsorption isotherm) which seemed to be inconsistent with the d spacings obtained by XRD. The reason given for this inconsistency was the existence of thicker walls (compared to silicates) in the zirconia material. Based on the phosphorus content of the material their material was mostly zirconium phosphate and not sulfated zirconium oxide.

The second method of this type (Section 2.1.3) involved using zirconium propoxide

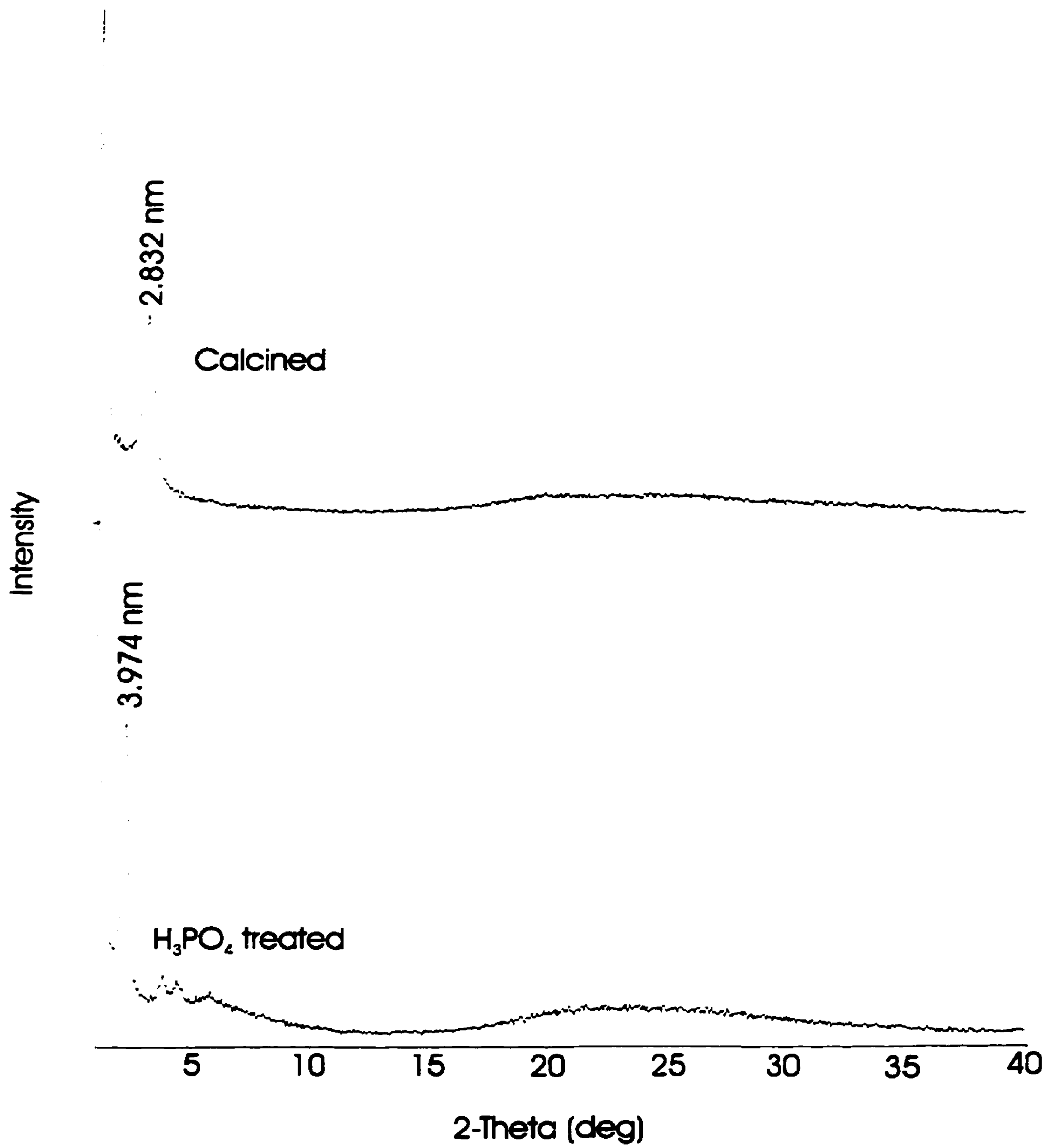

Figure 3.4: XRD Powder Patterns for Zirconia treated with H_3PO_4 (Synthesized via the Zirconium Sulfate Method)

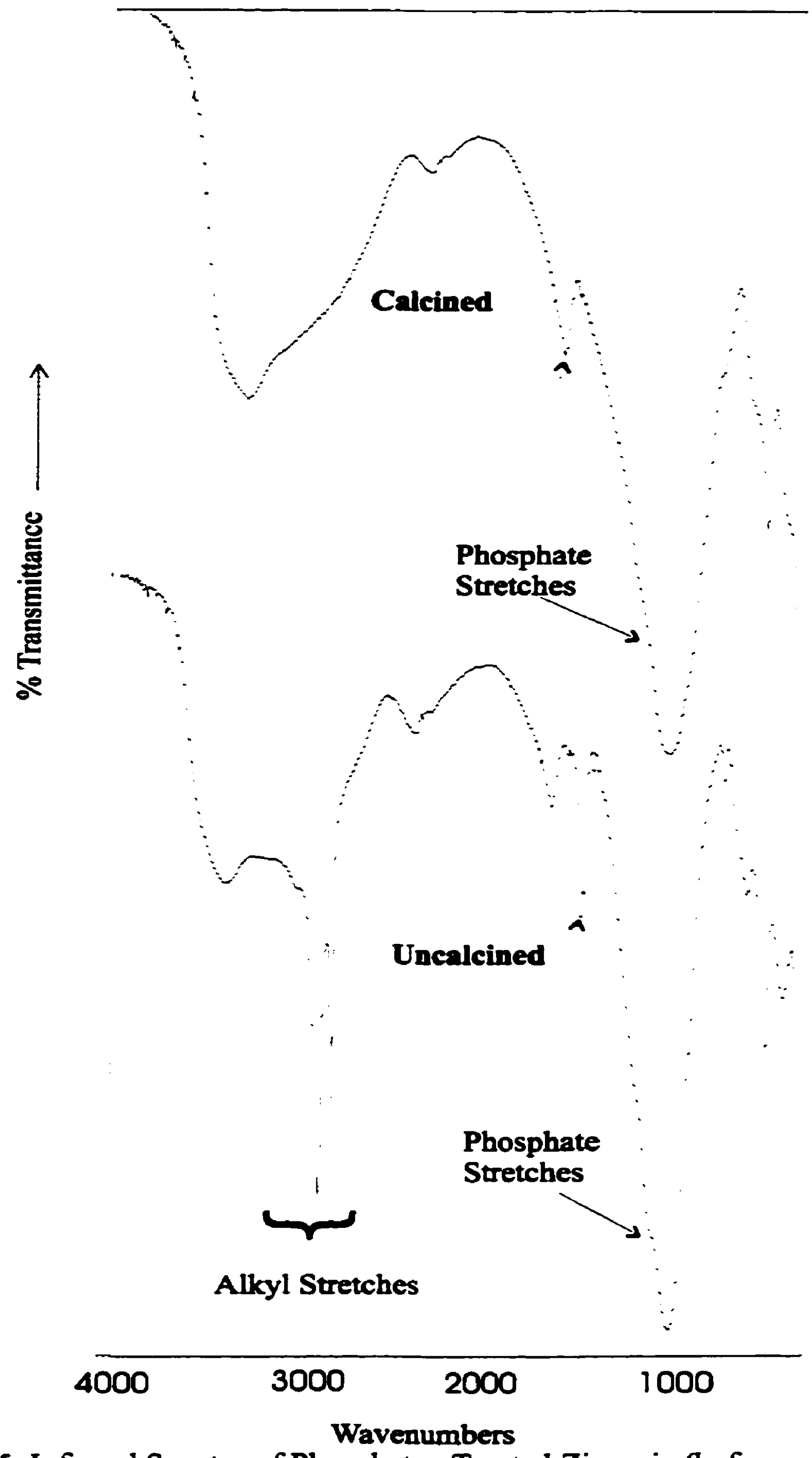

Figure 3.5: Infrared Spectra of Phosphate - Treated Zirconia (before and after calcination at 500°C)

rather than zirconium sulfate. This method was reported in the literature as a way to synthesize mesoporous niobium oxide with a surface area of 380 m^2/g and a pore size distribution centered around 2.6 nm after calcination at 400°C.[24] However when we attempted to use this method to synthesize mesoporous zirconia the XRD pattern had no reflections present indicating that no long range order was present even before calcination. In the literature procedure a neutral surfactant (tetradecylamine) and niobium (V) ethoxide were used which formed a amino(ethoxy) niobium complex with the surfactant covalently bonded to the metal atom. In our attempted synthesis of mesoporous zirconia a cationic surfactant was used, so the formation of the amino(propoxy) zirconium complex would not occur. The differences in the interactions between the surfactant and the inorganic phase would determine which route would be successful.

3.1.2 Cationic/Acidic Methods

In these methods hexadecyltrimethyl ammonium bromide was used as the template and acid was used to initiate the hydrolysis. Two different methods were tried that used this approach.

The first of these methods (Section 2.1.4) used $ZrOCl_2{\cdot}8H_2O$, and was adapted from a synthesis which was successful in preparing microporous hafnium oxide.[40] When this method was used to synthesize porous zirconia the XRD pattern of the uncalcined material had four reflections, indicating long-range order, and the (100) reflection had a d-spacing of 4.51 nm. After calcination at 500°C only one low-angle reflection remained with a d-spacing of 2.77 nm (Figure 3.6). Some long range order is still present, but contraction of the inorganic structure took place during removal of the surfactant at high temperature. The calcined material was medium brown (carbonaceous deposit) and the surface area was 0.43 m^2/g indicating that not all of the template had been removed during calcination. A higher temperature may have removed the template, but this would also cause a larger contraction of the porous structure and probably a microporous material would have been obtained (as with the hafnium).

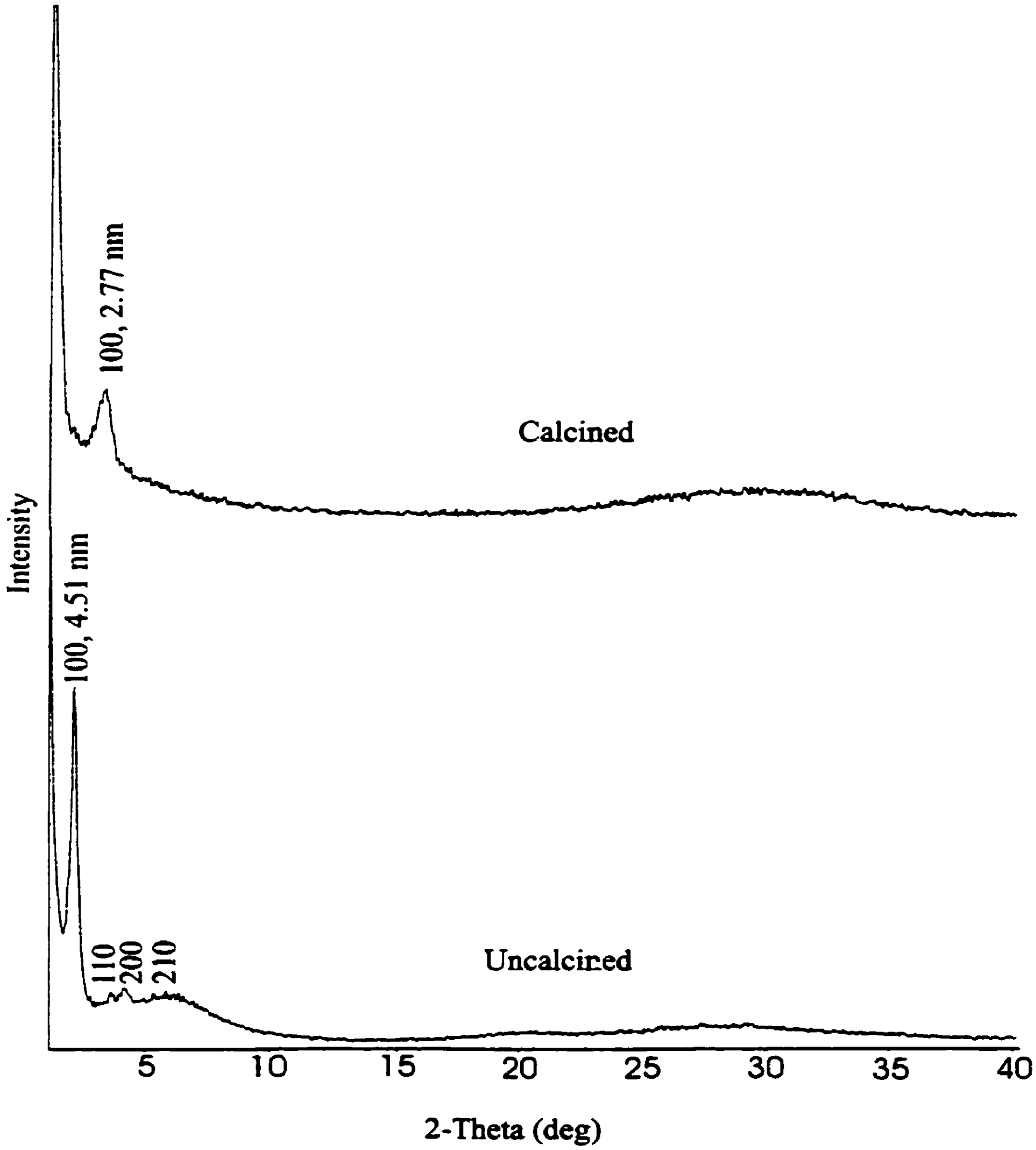

Figure 3.6: XRD Powder Patterns for the Low pH synthesis of Sulfated Zirconia (before and after calcination at 500°C)

The second of these methods (Section 2.1.6) used $Zr(OPr)_4$, and was slightly more successful. The uncalcined material gave a low angle reflection (100) with a d-spacing of 4.51 nm, and this reflection was retained after calcination at 500°C. The d-spacing after calcination was lower (3.50 nm), but equal to that of the analogous MCM-41 material. The calcined material was light brown and had a surface area of 188 m^2/g. However, the pore size distribution of the material was very broad, centered around a diameter of 6.35 nm and with a width at half height (WHH) of 3.38 nm. The adsorption isotherm obtained with this material most closely resembles a Type II isotherm in the Brunauer classification.[43] A Type II isotherm occurs when adsorption takes place on nonporous powders or on powders with pore diameters larger than mesopores. The calcined material is amorphous, not crystalline, suggesting that the calcination temperature used may not be high enough to get a transition to a crystal phase which is needed for catalytic activity.

Ciesla et al. also had some success with this method in the synthesis of porous zirconia. The XRD patterns obtained by them were similar, but their nitrogen adsorption isotherm was more typical of a Type I isotherm which is indicative of microporous material.[32] The surface area of their material after calcination at 500°C was 280 m^2/g.

3.1.3 Cationic/Basic Methods

In these methods hexadecyltrimethyl ammonium bromide was used as the template, and the hydrolysis was initiated by the addition of concentrated aqueous ammonia or sodium hydroxide. Two different methods were tried that used this approach.

The first of these methods (Section 2.1.1) used $ZrOCl_2{\cdot}8H_2O$ and 1 M NaOH, and was adapted from an ambient temperature synthesis of MCM-41.[39] When we used this method to synthesize zirconia only amorphous zirconia was formed before calcination as indicated by a broad peak around 30° (2θ). No other peaks were seen in the low or high angle XRD patterns. In order to test the synthetic method, we also made MCM (silicate) material using this method and this also turned out to be unsuccessful. The XRD pattern showed a multitude of low and high angle peaks. In the literature report the MCM material made by this method had both micropores and mesopores present.[39] Currently, this is the only report of an ambient temperature synthesis of MCM material and therefore, this work has not been reproduced by other researchers as well.

The second method (Section 2.1.5) used $ZrOCl_2{\cdot}8H_2O$ and concentrated aqueous ammonia, and was adapted from a method used to make mesoporous, high surface area zirconium (IV) oxide.[27] We synthesized both sulfated and unsulfated zirconia. Upon calcination at 500°C in static air the unsulfated material turned brown while the sulfated material turned black. The unsulfated calcined material had a surface area of 296 m^2/g and a broad pore size distribution (WHH = 3.13 nm) centered around a diameter of 3.45 nm. The adsorption isotherm did not indicate whether micropores or mesopores were present. The nitrogen adsorption isotherm of the sulfated material was not measured as the black colour indicated that a large amount of carbon was deposited on the surface and this would affect the measurements. Since no peaks were present in their XRD patterns, the materials were amorphous after calcination at 500°C.

Since the materials calcined in air were dark, calcination was attempted in an oxygen atmosphere to remove all of the surfactant. The unsulfated material came out light yellow, had a surface area of 246 m^2/g and a maximum in the pore size distribution at 2.08 nm (WHH

= 0.77 nm) (Figure 3.8). The pore size distribution had a large tail on the high relative pressure side. The nitrogen adsorption isotherm was fairly steep at low relative pressures and did not level off indicating a broad pore size distribution (Figure 3.7). The sulfated material came out a light cream colour, had a surface area of 247 m^2/g and a pore size distribution curve with a maximum at 1.96 nm (WHH = 0.75 nm) (Figure 3.8). However, the pore size determination by nitrogen adsorption measurements is not very precise in this region because no data points could be collected at low relative pressures for this sample. The first data point obtained in the pore size distribution (after analysis of the adsorption isotherm by BJH analysis) was near the maximum. The nitrogen adsorption isotherm for this sulfated, calcined (500°C) material was fairly steep at low relative pressures, but a bend and levelling off of the isotherm was observed at $P/P_0 = 0.4$ (Figure 3.7) which suggest that nitrogen adsorption is complete at this point. This suggests that a fairly narrow pore size distribution will be obtained.

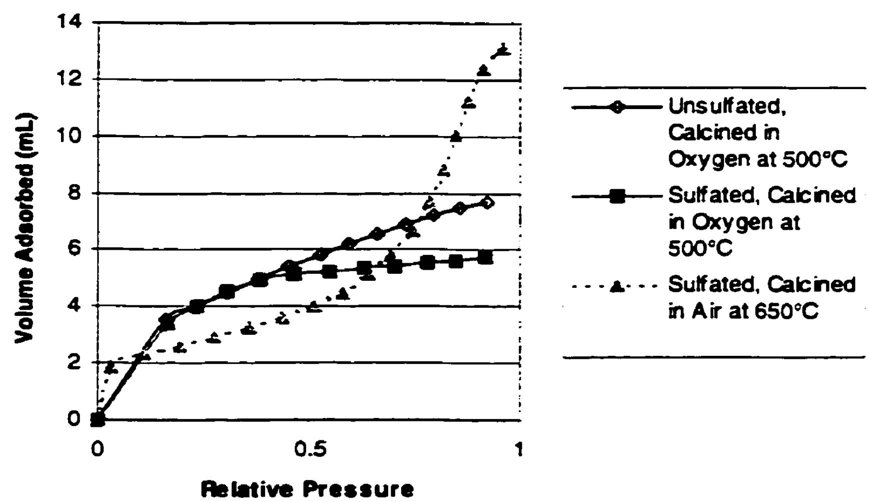

Figure 3.7: Nitrogen Adsorption Isotherms for Zirconia made via the Cationic/Basic Method

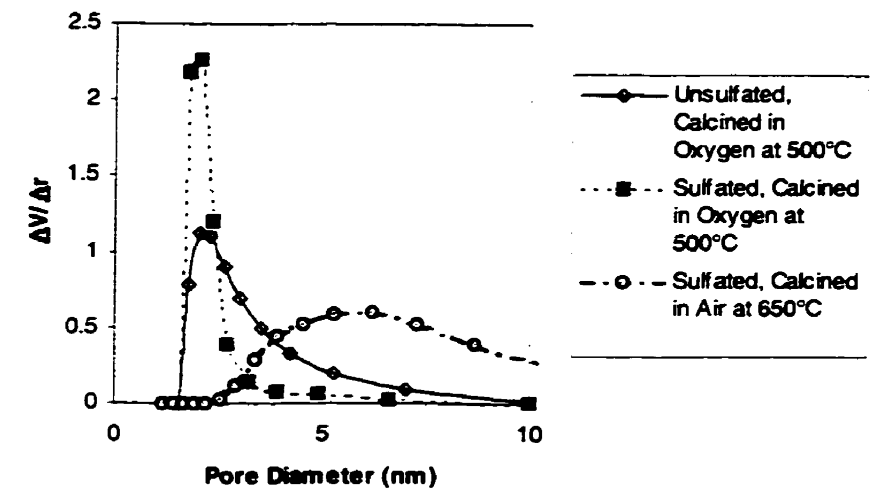

Figure 3.8: Pore Size Distributions for Zirconia made via the Cationic/Basic Method

To obtain crystalline material the calcination temperature typically has to be 650°C or greater. Therefore, the sulfated material was also calcined at 650°C. Upon calcination at this higher temperature the material came out white and had a surface area of 95.3 m^2/g. The pore size distribution was centered around a diameter of 6.16 nm and had a WHH of 2.7 nm (Figure 3.8). The nitrogen adsorption isotherm was unlike those of the templated silicates, with the absence of a sharp step indicating a very narrow pore size distribution (Figure 3.7). However, a step was observed between $P/P_0 = 0.05$ and $P/P_0 = 0.6$ which indicates that mesopores are present, but a broad pore size distribution will be obtained. This pore size is much larger than would be expected for material made using a surfactant with a chain length of sixteen carbons.

Hudson and Knowles also experienced difficulties with this method, although they only synthesized unsulfated zirconia.[27] They found that the adsorption isotherms for the unsulfated material had the shape mentioned above (absence of a sharp step). Their surface areas were also high (typically greater than 250 m^2/g) after calcination at 500°C. The maximum in the pore size distribution curve for their material was around 3.6 nm and the distribution was very broad (WHH = 2.0 nm). They used different chain length surfactants in an attempt to make material with different pore sizes, but found that this method did not show a consistent variation in pore size with chain length of incorporated alkyltrimethyl ammonium cation.

3.1.4 Neutral Templating Method

In this method neutral primary amines, such as hexadecylamine, with alkyl chain lengths ranging from 8 to 18 were used to make a template and no additional acid or base was needed to initiate the hydrolysis (Section 2.1.7). This method has been used successfully by Pinnavaia to synthesize a mesoporous silicate and a mesoporous titanium - substituted silicate[35] and by Sachtler to synthesize mesoporous sulfated zirconia.[37] In both instances, no long range order was present and a chaotic arrangement of pores was revealed in the zirconia by tunnelling electron microscopy (TEM).[37]

After extraction of the template and drying, only one peak was present in the XRD powder pattern which revealed that the materials we synthesized were all amorphous. The one XRD peak present was very broad and weak, indicating that very little long-range order exists. This pattern was to be expected, since TEM by Sachtler has revealed that a chaotic distribution of pores is created when using this method.[37] After calcination at 500°C amorphous zirconia is still present, but after calcination at 650°C tetragonal zirconia is formed (Figure 3.9). A small amount of monoclinic zirconia may be present as indicated by the small shoulder at 31.7° (2θ), but all the other peaks are due to tetragonal zirconia.

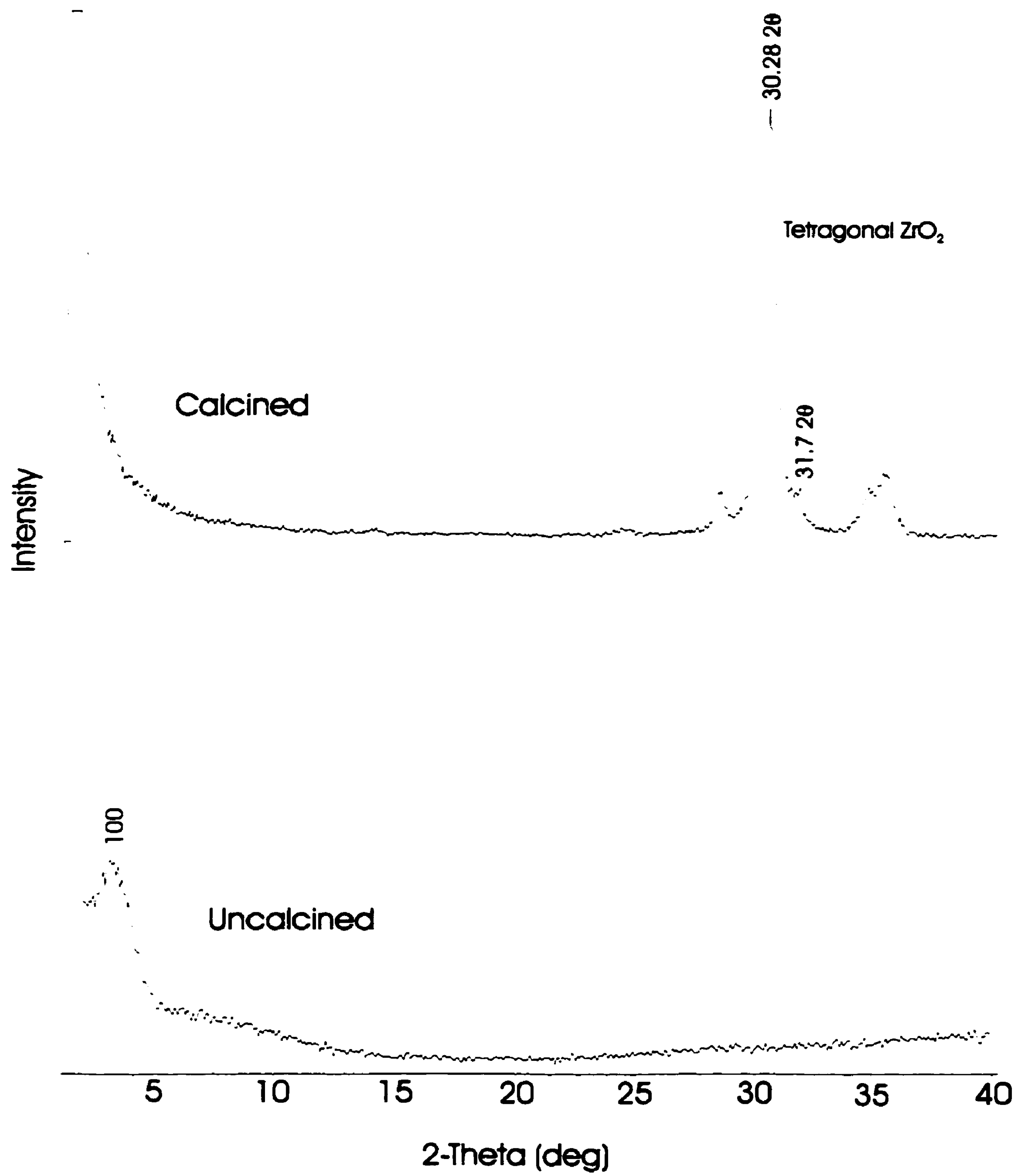

Figure 3.9: XRD Powder Patterns of Sulfated Zirconia made via the Neutral Templating Method (before and after calcination at 650°)

Infrared spectra, taken of the samples before and after extraction and sulfation, are collected in Figure 3.10. Before the template is extracted, the alkyl C-H stretches were clearly seen between 2900 and 2920 cm^{-1} (not shown in Figure). When the material was sulfated before extraction, the alkyl peaks decreased in intensity but were still present in the uncalcined material. A sample of the uncalcined, sulfated, extracted material was placed under high vacuum and the infrared spectra redone to ensure that the alkyl peaks seen were not due to the ethanol used to extract the template. The alkyl peaks were still present in the infrared spectrum of the vacuum treated sample, indicating that some of the template was still present. If the material was extracted first, the template was completely removed before calcination (Figure 3.10). After calcination at 650°C, no alkyl peaks were present in the infrared spectra implying that the template was completely removed. Sulfate stretches appeared in the 1300 to 1000 cm^{-1} range in all the materials and these peaks have a different pattern depending on the types of sulfate groups present.

Conventional sulfated zirconia, which is known to be catalytically active, has a pattern of four peaks in this region, consisting of three strong peaks at 1236, 1142 and 1038 cm^{-1}, and a weak shoulder at 997 cm^{-1} (Figure 3.11). When the material is extracted and then sulfated (ES) the pattern is very similar to that of conventional sulfated zirconia. However, if the material is sulfated and this is followed by extraction (SE) the pattern changes. Now the middle peak in the pattern (1142 cm^{-1}) is much weaker. From comparison of these spectra to spectra with known types of sulfate ligands[48] it was thought that two types of sulfate groups may be present. The pattern seen for conventional sulfated zirconia is the type of pattern seen for bridging bidentate sulfate groups. When the symmetry of the sulfate group is lowered to

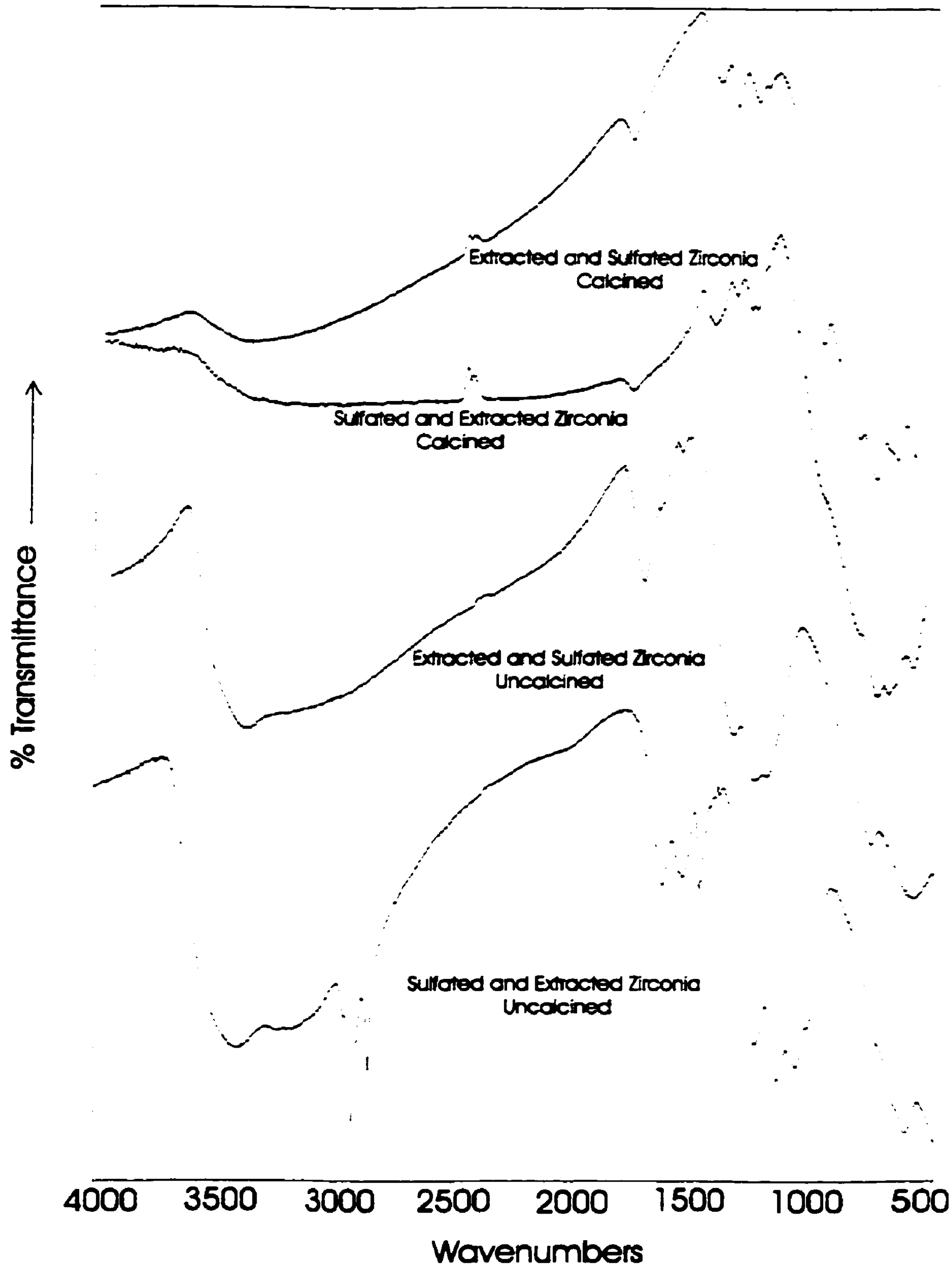

Figure 3.10: IR Spectra of Uncalcined and Calcined Zirconia made via the Neutral Templating Method

C_{2v}, the IR active fundamental in this region splits into three bands (the three strong peaks shown). Also, the fundamental in this region which is only Raman active in the tetrahedral

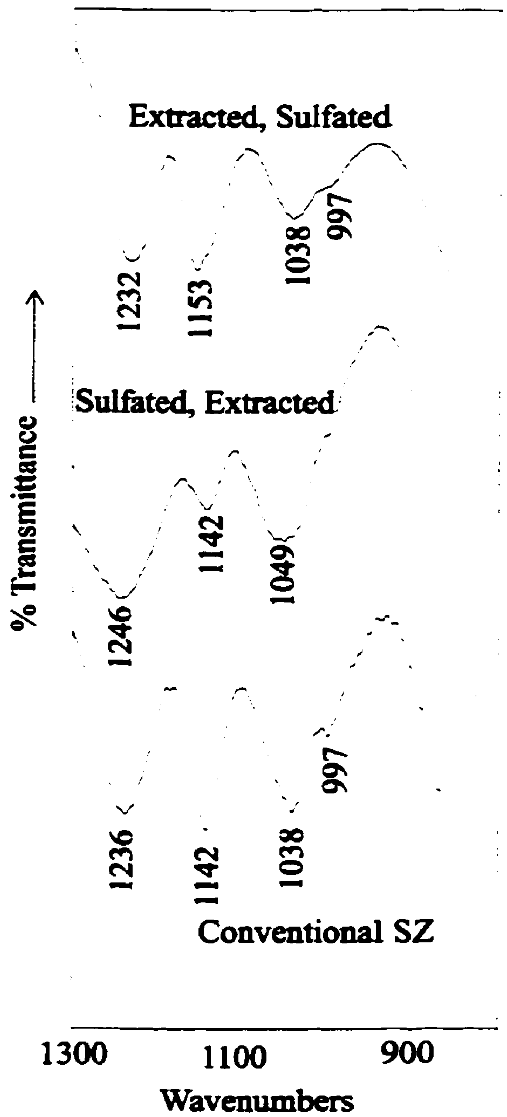

Figure 3.11: Infrared Spectra in the Sulfate Stretching Region of Conventional Sulfated Zirconia (SZ) and Mesoporous Sulfated Zirconia after calcination at 650°C

molecules becomes infrared active when the symmetry is reduced to C_{2v} and appears as a weak shoulder at 997 cm^{-1}. The bridging bisulfate group is thought to be a common sulfate group in sulfated zirconia (Figure 1.2). The other type of sulfate group that may be present is monodentate sulfate. In monodentate complex formation, the symmetry of the sulfate group is C_{3v} and therefore, the fundamental only splits into two bands (the two strong bands at 1246

cm^{-1} and 1049 cm^{-1} in the SE spectra). The other peaks present in the SE spectra are presumably due to a small amount of bridging bisulfate groups. Therefore, the material that was sulfated and then extracted appears to have both types of sulfate groups present. This combination of groups gives the pattern seen in the IR spectra, with the middle peak being weaker (due to bridging sulfate) and the lower wavenumber peak being stronger (due to monodentate sulfate). A very weak peak at approximately 1440 cm^{-1} was seen in all three spectra (not shown) which is thought to be due to the symmetric S=O stretch. A key to the activity of these catalysts is the number of Bronsted sites present which require a hydroxyl group. However, the specific IR bands ascribable to the bisulfate OH groups are difficult to detect due to their hydrogen bonding to the surface.[9]

To see how a difference in acid concentration would affect the number and type of sulfate groups on the surface, different concentrations of sulfuric acid were used to sulfate the zirconia and the infrared spectra of these materials were obtained (Figure 3.12). All of these materials were sulfated before and after extraction, so that any differences seen would be due to the concentration of the acid and not to the order of sulfation and extraction used. When the material was sulfated using 0.25 M or 0.375 M H_2SO_4, the pattern indicated that both types of sulfate groups (bridging bidentate and unidentate) were present, but the spectra indicated that the unidentate groups dominated since the intensity of the peak at 1144 cm^{-1} was fairly weak. However, when 0.5 M H_2SO_4 was used, the pattern indicated that only bridging bidentate sulfate groups were present. These spectra show that a certain concentration of sulfate groups may be needed to cause bridging bisulfate groups to predominate. When the material is extracted first, there is more surface exposed for the sulfate groups to adsorb on and

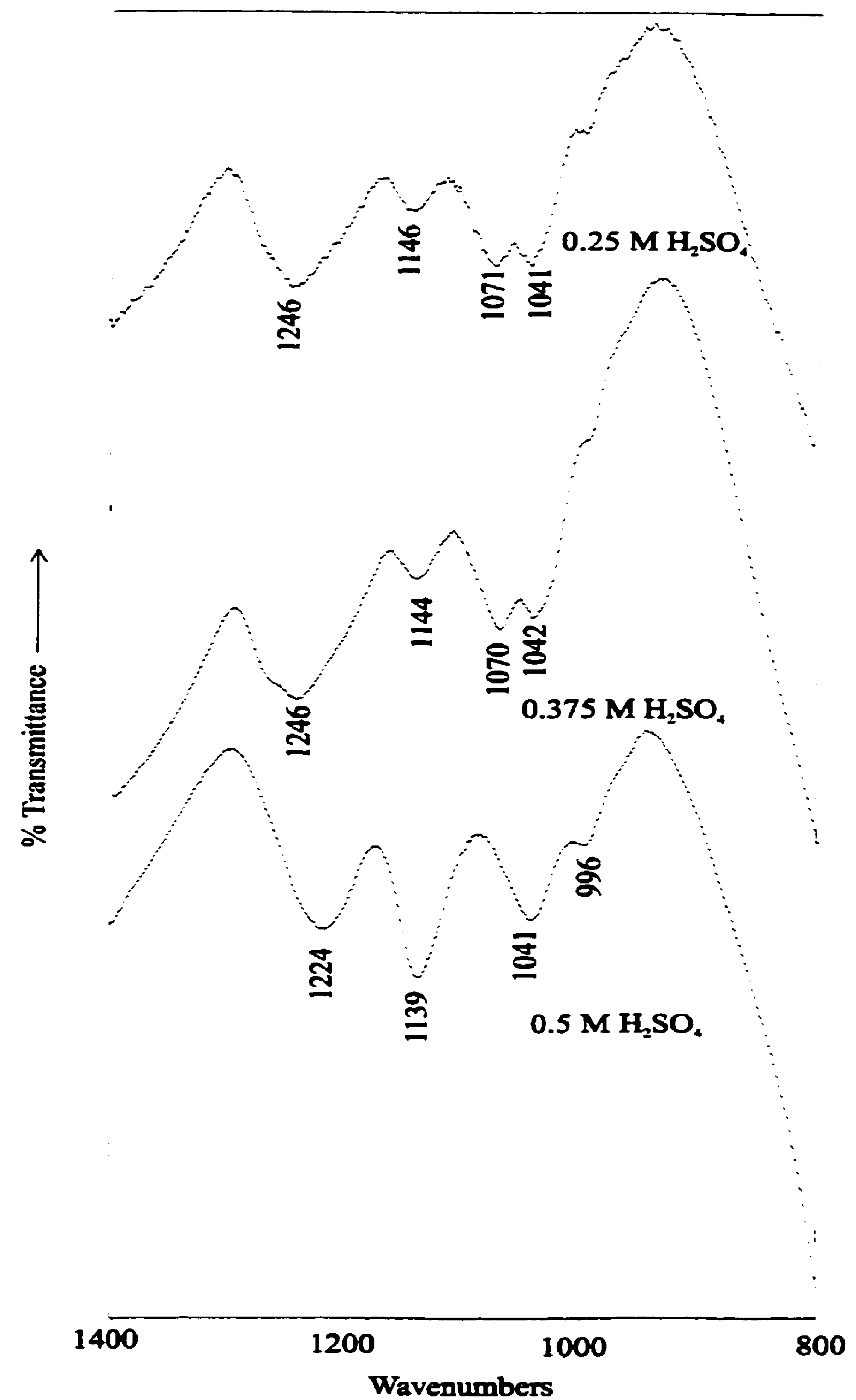

Figure 3.12: Infrared Spectra in the Sulfate Stretching Region for Sulfated Zirconia Sulfated with Different Concentrations of H_2SO_4

therefore, more sulfate groups may attach to the surface of the catalyst and form bridging bi-sulfate groups as are formed in conventional zirconia (Figure 3.11). It is also known that the formation of Bronsted acidity (needed for catalytic activity) is favoured at higher sulfate loadings which would occur when using more concentrated sulfuric acid solutions.[12]

In the nitrogen adsorption isotherms of these materials, a characteristic step between $P/P_0 = 0.1$ to $P/P_0 = 0.6$ can be seen which indicates that mesopores are present even after calcination at 650°C (Figure 3.13). The increase in the amount adsorbed at low relative pressures

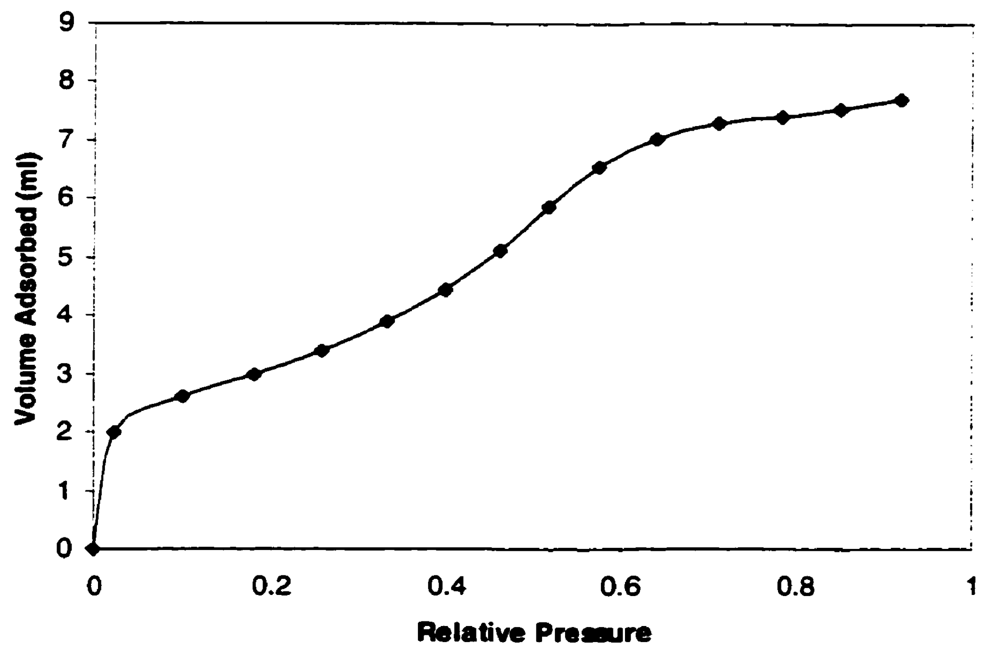

Figure 3.13: Typical Nitrogen Adsorption Isotherm for Mesoporous Sulfated Zirconia made by the Neutral Templating Method

(below ca. 0.05) is significantly less sharp than that which is observed in zeolites under the same conditions, suggesting that in the mesoporous SZ few (if any) micropores are present. The small rise seen at low relative pressures is likely due to adsorption of the first monolayer of nitrogen and the knee of the isotherm generally occurs near the completion of this first monolayer.[43] The thicker pore walls that occur when using the neutral templating method help improve the thermal stability of sulfated zirconia, enabling it to keep its mesoporous structure at 650°C. Therefore, these materials are thermally stable up to 650°C, the temperature needed to form the tetragonal phase (catalytically active phase) of sulfated zirconia. The pore diameters of these materials ranged from about 2.0_0 nm to 4.0_0 nm depending on the synthetic parameters. The width of the pore size distribution varied also depending on synthetic parameters and ranged from narrow (0.5_0 nm) to very broad (1.9_0 nm). The surface area of the materials also varied, ranging from 46 m^2/g to 110 m^2/g. The pore sizes and surface areas of these materials and how they varied with synthetic parameters will be discussed in detail in the next chapter.

3.1.5 Summary

Seven different methods of synthesis were used, in an attempt to see which was most successful at preparing thermally stable, mesoporous zirconia with a relatively narrow pore size distribution. Of the various methods tested only the neutral templating method gave mesopores exclusively. The cationic methods gave materials that collapsed upon calcination, so any pore structure that was present was lost, or it gave materials with no long range order present even before calcination. One of the cationic/acidic methods gave a material that had almost no surface area after calcination at 500°C, while the other method yielded mesoporous material with such a broad pore size distributions that no tailoring of the pore sizes could be done and no shape-selective catalysis would be exhibited. The first cationic/basic method (ambient temperature synthesis) did not even produce mesoporous material prior to calcination. The second cationic/basic method gave high surface areas (when calcined at 500°C), but the shape of the nitrogen adsorption isotherms indicated that some of the material synthesized was microporous. Calcination of these materials at 650°C yielded material with very large pores and very broad pore size distributions. Since only the neutral templating method was successful in synthesizing a mesoporous material with a fairly narrow pore size distribution, the parameters that affect the size of the pores formed by this method were investigated further.

Chapter 4

Tailoring the Pore Size of Mesoporous Sulfated Zirconia

4.1 Introduction

In the synthesis of mesoporous sulfated zirconia many variables may affect the final internal structure of the material. Factors such as concentration, alkyl chain length of the surfactant and nature of the cosolvent are known to affect the porosity of silicate materials and therefore, these factors may have a similar affect on mesoporous sulfated zirconia. Other factors such as pH, temperature and aging time may also have an effect on the final outcome. In this chapter, the factors studied, the expected change and the actual change in pore size will be discussed. Some of the material will also be compared to MCM (silicate) material made using the same parameters. Tailoring the pores of mesoporous sulfated zirconia to a desired size is the key to shape - selective catalysis, so a comprehensive study of all the factors that may affect the porosity of the material is vital.

4.2 Alkyl Chain Length of Surfactant

4.2.1 Silicate Based Materials

It has been found with silicate materials (made via the cationic route) that the pore diameter is related to the alkyl chain length of the surfactant used in the synthesis (Table 4.1).[18] When the alkyl chain was varied from eight to sixteen carbons (in two carbon increments), pore diameters of 1.3 to 2.2 nm were obtained. The pore diameter did not increase by the same amount with each additional two carbons in the alkyl chain, but both the porosity measurements and the d - spacing in the XRD patterns did indicate that MCM-41 pore diameter generally increased with surfactant chain length when the synthesis was carried out under comparable conditions.

Table 4.1: Pore Sizes of Mesoporous Silicate (MCM) Material[18]

Surfactant Chain Length	XRD d-spacing (nm)	Pore Diameter (nm)[a]
8	2.7	1.3
10	2.9	1.4
12	2.9	1.5
14	3.3	1.9
16	3.5	2.2

a. Calculated using BJH theory[42] and pore diameters given in reference (which were calculated by H - K theory) [44]

4.2.2 Zirconia Based Materials

The relationship between pore diameter and alkyl chain length in zirconia - based materials has been studied by other researchers. Hudson and Knowles used cationic surfactants with alkyl chain lengths that ranged from eight to eighteen carbons (in two carbon increments) to synthesize mesoporous zirconia and found that the d-spacings were independent of the chain length of the incorporated surfactant.[27] Their calculated BJH pore size distributions also did not show a consistent variation in pore size with chain length of incorporated surfactant. It has been reported that the pores in mesoporous zirconia formed by the cationic method are not related to the chain length of the incorporated surfactant.[27] Since we used a different method (neutral templating method) to synthesis mesoporous zirconia, the relationship between pore size and alkyl chain length was investigated first in order to determine whether a proportionality existed or not. Once it was discovered that a proportionality did not exist (see later) our next effort was to try to identify the factors that did influence the pore diameter.

Using the neutral templating method, mesoporous zirconia was made using surfactants with different alkyl chain lengths. In the first attempt, 10 wt% of surfactant was used in all the syntheses as this concentration is known to yield mesoporous zirconia.[37] Surfactants with chain lengths ranging from 10 to 16 carbons were used. All of these materials were sulfated before extraction of the template and calcined at 650°C. The results from these syntheses are shown in Table 4.2.

Table 4.2:Surface Areas and Porosities of Mesoporous Sulfated Zirconia made with Various Alkyl Chain Lengths (using 10 wt% of surfactant)

Alkyl Chain Length	Surface Area (m^2/g)	Pore Diameter (nm)	WHH (nm)
10	59.9	2.2_4	0.5_8
12	50.6	2.6_5	0.5_8
14	68.7	2.2_2	0.5_4
16	105	2.5_5	0.6_4

The pore diameter of the final material varied very little with an increase in alkyl chain length, so this confirmed that the pore diameters of mesoporous zirconia - based materials are not related to the alkyl chain length of the incorporated surfactant. The pore diameters of these zirconia - based materials are generally larger than those of the silicate - based materials (when using the same pore model). Since no trend relating pore diameter to chain length was observed at this concentration of surfactant, the amount of surfactant was lowered to see if simply changing the surfactant concentration would improve the results. When the surfactant concentration of hexadecylamine was lowered to 3.5 wt% a pore diameter of 3.28 nm was obtained and the pore size distribution was fairly narrow. This pore diameter compared favourably to that expected when using an alkyl chain length of sixteen carbons, so a second group of syntheses was attempted, keeping the mole ratio of surfactant/Zr^{IV} equal to 0.10 and changing the alkyl chain length of the surfactant.

Using the same amount of surfactant (0.010 mol), surfactants with chain lengths that ranged from eight carbons to eighteen carbons were used in the synthesis of sulfated zirconia. All of these materials were sulfated before and after extraction of the organic template. The results of these syntheses can be seen in Table 4.3.

Table 4.3: Surface Areas and Porosities of Mesoporous Sulfated Zirconia made with Various Alkyl Chain Lengths (at constant surfactant: Zr^{IV} mole ratio of 0.10)

Alkyl Chain Length	Surface Area (m^2/g)	Pore Diameter (nm)	WHH (nm)
8	45.9	3.6_9	1.8_6
10	72.5	3.0_1	1.2_5
12	59.5	2.9_7	0.7_9
14	56.6	3.1_4	0.8_0
16	75.8	3.2_8	1.0_9
18	47.3	3.0_9	0.8_0

As can be seen in the table, no obvious relationship was found between the chain length and the pore diameter. The smallest chain length of eight carbons actually gave the largest pore size (3.69 nm diameter and WHH = 1.86 nm). The broadness of the pore size distributions also varied, with some very broad distributions (eight carbons, WHH = 1.86 nm) and some narrower distributions (with twelve carbons, WHH = 0.79 nm). It can also be seen in Table 4.3 that all of these pore diameters are larger than the pore diameters presented in Table 4.2; the concentration of surfactant must also have an effect on the pore diameter. This lack of a proportionality between pore diameter and alkyl chain length showed that varying the alkyl chain length does not produce the same relationship that existed with the silicate materials.[18] The reasons for these different results are not known. It is clear that the different types of interactions between the surfactant and the inorganic species that exist must be involved. It is known from mechanistic studies that the choice of surfactant and the inorganic anion mediate the ordering process and determine the internal structure and porosity of silicates.[49] The ordering depends on the silicate-surfactant affinity relative to the halide (counter ion on surfactant) - surfactant affinity. Both the cationic route and the neutral templating route have been used to systematically change the pore size of silicate - based materials.[18, 35] Neither of these routes have been successful in obtaining the same systematic change for zirconia - based materials. The interactions between the zirconium species and the surfactant must be different than the interactions between the silicate species and the surfactant. It is known with the silicate species (made via the neutral templating route) that partial collapse of the mesoporous framework occurred upon calcination.[35] This contraction may also take place with sulfated zirconia. Comparing samples of sulfated zirconia before and after calcination gives pore diameters of 3.34 nm and 3.12 nm respectively. The amount of contraction that takes place will also affect the final pore size. Since the pore sizes in zirconia - based materials can not be changed systematically by altering the alkyl chain length of the incorporated surfactant and the relationship between pore size and alkyl chain length clearly is affected by other synthesis parameters (such as concentration), an investigation of the other factors which affect pore size was undertaken. The remainder of the work discussed in this chapter was all done using an alkyl chain length of sixteen carbons, unless otherwise stated.

4.3 Concentration of Surfactant

In the previous section it was seen that the concentration of surfactant affected the pore diameter of zirconia- based materials. Therefore, a more thorough study of this effect was undertaken. To test this theory, various concentrations of surfactant, such as 10, 7, 3.5 and 1 wt %, were used. The materials formed were all sulfated before extracting the template. It was

Table 4.4: Effect of Surfactant Concentration on Pore Diameter

Weight % of Surfactant	Surface Area (m^2/g)	Pore Diameter (nm)	WHH (nm)
10.0	105	2.5_5	0.6_4
7.0	65.7	3.1_3	0.7_4
3.5	80.8	3.0_6	0.9_0
1.0	53.8	3.6_5	1.3_4

found (Table 4.4) that as the concentration of the surfactant decreased, the pore diameter increased and the pore size distribution became broader. At 10 wt%, the pore diameter is 2.55 nm and the WHH is 0.64 nm. However, if the surfactant concentration is decreased to 1 wt%, the pore diameter is 3.65 nm and the WHH is 1.34 nm. The pore diameters for the 7 wt% and 3.5 wt% materials were very similar, however, the width at half height for the 3.5 wt% material was larger and this pore size distribution also had a tail on the large radius side (i.e. the pore size distribution was very lopsided). The distribution for the 1 wt% material also had a tail on the large radius side. It was thought that the increase in pore diameter (and the broadness of the pore size distribution) may be due to the shape and density of the micelle since the concentration of surfactant is known to affect the micellar structure. As the concentration of the surfactant decreases, the micelle may become more loosely packed and therefore become larger, influencing the pore size. There is probably an optimum concentration for each surfactant where the micelle is tightly packed and no more molecules can be added to it. Since this concentration will change depending on the alkyl chain length of the surfactant this factor may cause the lack of 'trend' seen with the alkyl chain length of surfactants when the same concentration of surfactant is used for the various chain lengths. Two other concentrations of surfactant were also tested to see how a high concentration of surfactant would influence the pore size. When the concentration of surfactant was increased to 20 wt% (with hexadecylamine) or 25 wt% (with dodecylamine) the established trend continued and so increasing the concentration consistently gives a narrower pore size distribution with a smaller diameter. This trend is expected to continue until the surfactant concentration becomes high enough that a phase transition from a hexagonal to a lamellar or cubic liquid crystal occurs. It was interesting to note that even at very low concentrations of surfactant (0.1 wt%), mesoporous material could be synthesized (3.48 nm, WHH = 1.2 nm). The pore diameter of this material can not be compared to the 1 wt% material presented in Table 4.4 as these two materials were sulfated and extracted in different orders which influences the pore size (Section 4.5).

4.4 Cosolvents

Various cosolvents have been tested in the synthesis of surfactant-templated silica mesophases and were found to influence the internal structure.[50] It was found that aprotic polar solvents would lead to an expanded ordered hexagonal structure (i.e. the pore size would increase) while protic polar solvents would lead to a shrunken ordered hexagonal structure. If the concentration of the polar cosolvent was increased, it would lead to a disordered hexagonal structure. The use of nonpolar cosolvents led to a cubic structure at low concentrations and a lamellar structure at higher concentrations. The use of different cosolvents has not previously been tested with sulfated zirconia, and therefore their effect was examined to see if they could be used to produce pores of different sizes.

Two different cosolvents were tested: ethanol and acetonitrile, a protic polar and an aprotic polar solvent, respectively. Non-polar cosolvents were not tested, as the hexagonal phase was desired. The pore size distributions obtained with these cosolvents were compared to material made without any cosolvent added during the synthesis. Some of the results are presented in Figure 4.1 which compares material made with no cosolvent to materials made

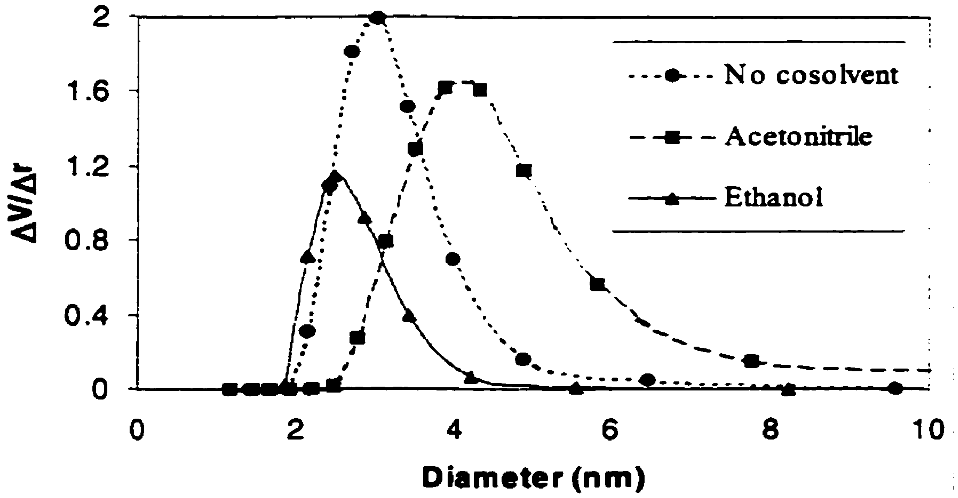

Figure 4.1: Influence of Cosolvent on the Pore Size Distribution of Mesoporous Sulfated Zirconia

with 35 mL ethanol or 35 mL acetonitrile added to the zirconium (IV) mixture (See Section 2.1.6).

The material made without cosolvent has a pore diameter of 3.00 nm and a WHH of 0.69 nm. When ethanol was added to the synthesis mixture the pore diameter decreased to 2.46 nm and the pore size distribution became slightly narrower (WHH = 0.57 nm). These observations match what was observed with the silicate materials. It is known that increasing the alcohol to water ratio decreases the average aggregate diameter and increases the area per headgroup for the surfactant. Polar molecules will generally reside in the continuous phase or be adsorbed at the micelle-water interface. Therefore, the pore diameter was expected to decrease which is what was observed. When acetonitrile was used the pore diameter increased to 3.86 nm and the pore size distribution became broader (WHH = 1.16 nm). For aprotic polar solvents in low concentrations, it is convenient to view them as additives that can be solubilized in the micellar structure owing to their hydrophobicity. The less polar and more branched the solvent, the deeper it is solubilized in the micelle. Molecules solubilized deep within the micelle can be expected to swell the micelle, and therefore the increase in pore diameter when using acetonitrile is expected. It can be seen from these results that the type of the cosolvent, both aprotic and protic, influences the size and shape of the template, and ultimately will affect the pore diameter of the mesoporous zirconia.

4.5 Order of Sulfation and Extraction

Another parameter that was changed during the synthesis was the order of the sulfation and extraction steps. In Figure 4.2 material that was sulfated before the template was extracted (SE), material that was sulfated after removal of the template (ES) and material that was sulfated both before and after removal of the template (SES) are compared.

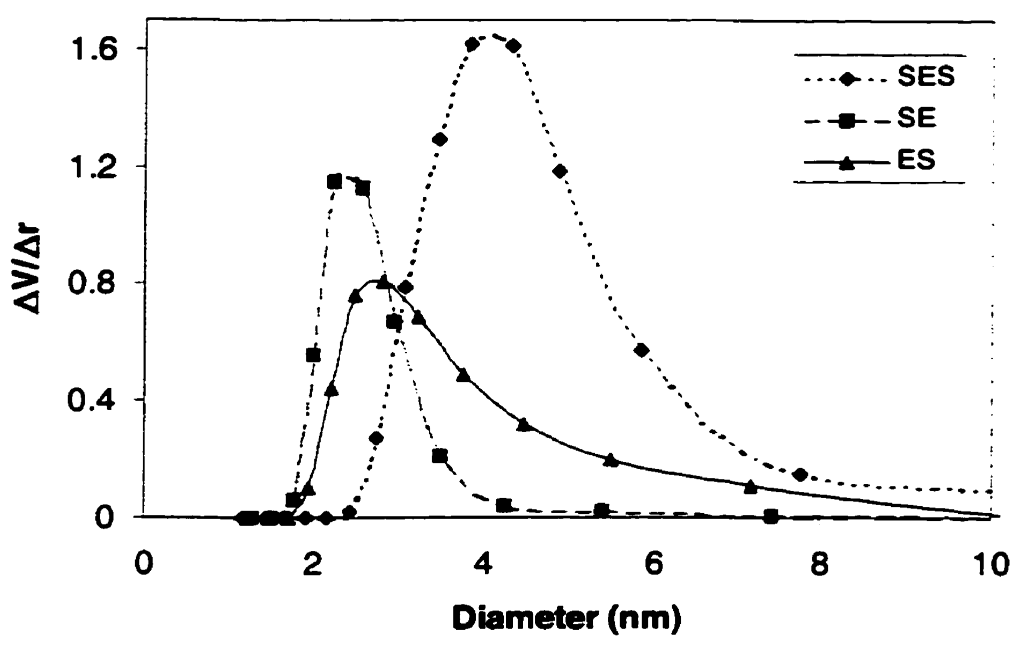

Figure 4.2: Influence of the Order of Sulfation and Extraction on the Pore Size Distribution of Mesoporous Sulfated Zirconia

When the material was sulfated first, the pore size is small (2.26 nm) and narrow (WHH = 0.51 nm). When the material was extracted and then sulfated, the pore size becomes larger (2.82 nm) and much broader (WHH = 0.93 nm). If the material is sulfated before and after extraction, the pore size once again becomes larger (3.86 nm) and even more broad (WHH = 1.16 nm). These results suggest that the sulfuric acid may be dissolving the pore walls of the material. When the material is sulfated first, the template is still present which prevents the sulfuric acid from destroying some of the wall structure. When the material is extracted first, the sulfuric acid has easier access to the pore walls. Other samples of catalyst were also sulfated in different orders and the resulting pore size distributions measured. The results for the catalyst pairs are given in Table 4.5. From the data given, catalysts that are sulfated before extraction always have a smaller pore diameter and a narrower pore size distribution.

Table 4.5: Influence of the Order of Sulfation and Extraction on the Pore Structure

Catalyst[a]	Surface Area (m^2/g)	Pore Diameter (nm)	WHH (nm)
SE1	73.6	2.2_7	0.5_1
ES1	77.4	2.8_3	0.9_3
SE2	101	2.4_1	0.5_4
ES2	62.6	3.4_0	1.5_9
SE3	102	2.3_4	0.5_0
ES3	78.1	2.5_0(tail)	0.6_9
SE4	93.6	2.4_4	0.5_0
ES4	78.2	2.5_1(tail)	0.7_6

a. SE = sulfated, extracted; ES = extracted, sulfated

In section 3.1.4, the infrared spectra of these materials were compared and it was conjectured that the material that was sulfated before extraction had bridging bisulfate groups as well as monodentate sulfate groups present, while the material that was extracted and then sulfated had only bridging bisulfate groups present. From the infrared spectra and the pore size distributions of the material, it was thought the location of the active sites might be different in both materials. In the material that was sulfated and then extracted the active sites may mainly be on the external surface of the catalyst since the sulfuric acid could not get inside the pores. In the material that was sulfated after extraction, the active sites may be inside the pores of the material. The question of the location of the active sites will be looked at further in Chapter 5.

4.5.1 Time for Sulfation

As pointed out in the previous section, it was thought that the sulfuric acid might be destroying some of the wall structure of the material. To test this theory samples of the same material were stirred in dilute sulfuric acid (0.5 M) for various amounts of time (Figure 4.3).

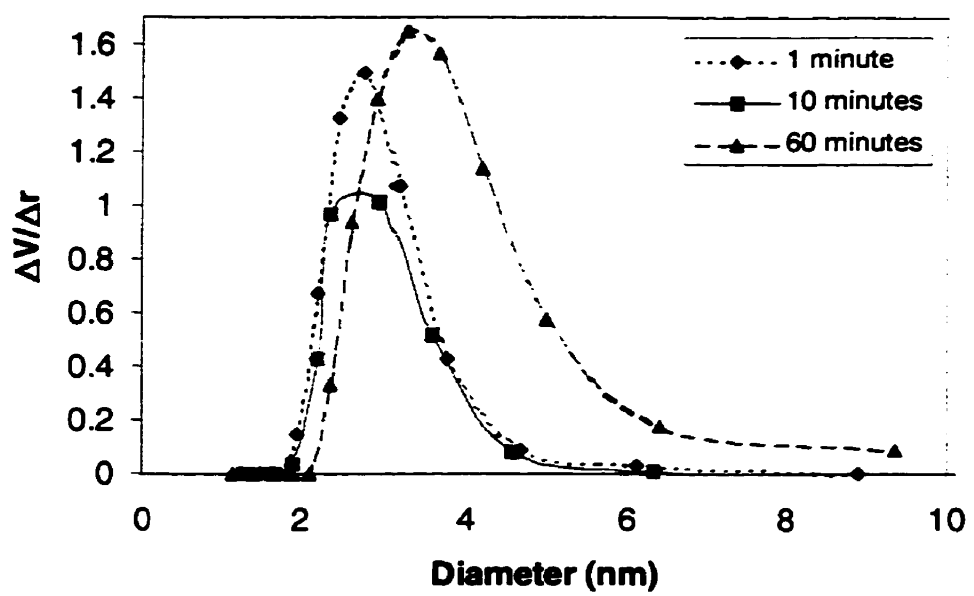

Figure 4.3: Influence of Sulfation Time on the Pore Size Distribution of Mesoporous Sulfated Zirconia

When the material was stirred in sulfuric acid for one minute the pore size distribution was quite narrow (WHH = 0.63 nm) and had a maximum at 2.82 nm. When the sulfation time was increased to ten minutes the maximum of the pore size distribution increased only slightly (maximum at 2.99 nm) and the pores were slightly broader (WHH = 0.64 nm). If the material was left in sulfuric acid for one hour, the pore size distribution changed dramatically. The pore diameter was now 3.31 nm and pore size distribution was very broad (WHH =1.01 nm). This simple test showed that the sulfuric acid did dissolve the pore walls of the material during sulfation of the catalyst. The amount of time the material was stirred in sulfuric acid also affected the surface area of the material. The surface area increased from 72.2 to 86.8 to 102 m^2/g as the time was increased from 1 to 10 to 60 minutes. Therefore, as the sulfuric acid dissolves some of the wall structure more surface is created.

4.5.2 Acid Concentration

Since the sulfation time (length of contact between the acid and the structure) affected the pore structure, it was thought that the concentration of acid used to sulfate the material might also have an effect. It is known that a higher sulfate loadings favours Bronsted acidity[12] and so the pore size distributions (Figure 4.4) and the infrared spectra (Figure 3.12) of the materials sulfated with different concentrations of acid were measured. As noted in Section 3.1.4, the infrared spectra showed that a concentration of 0.5 M H_2SO_4 was needed to create bridging bisulfate groups on the surface of the catalyst. The pore size distributions of these materials showed that, as expected, more dilute sulfuric acid did not destroy the wall structure as much as did the stronger (0.5 M) sulfuric acid. The pore size distributions (Figure 4.4) for the material sulfated with 0.25 M and 0.375 M sulfuric acid are very similar; both have a maximum at approximately 2.27 nm and a WHH of approximately 0.48 nm. The material that was sulfated with 0.5 M H_2SO_4 had a pore size distribution with a larger maximum (2.65 nm) and it was much broader (0.67 nm). Since 0.5 M sulfuric acid was necessary to create the needed bridging bisulfate groups, this concentration of sulfuric acid was used to sulfate all of the materials discussed in chapter 5 and all materials discussed in the preceding chapters unless otherwise stated.

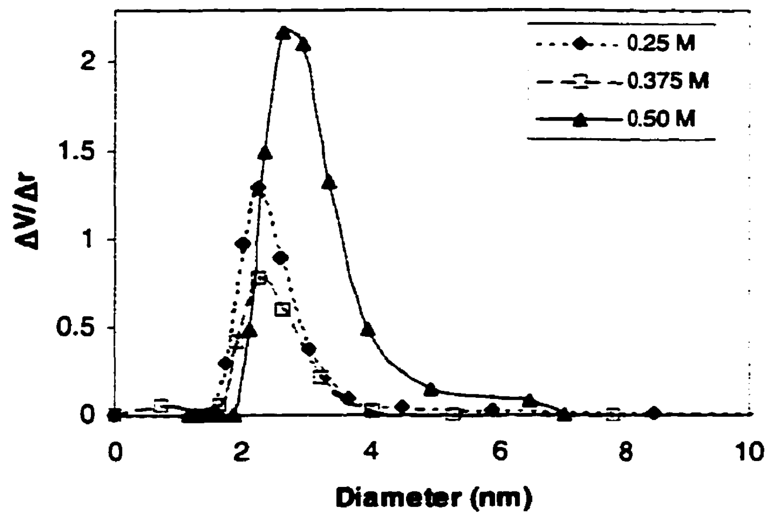

Figure 4.4: Influence of Acid Strength on the Pore Size Distribution of Mesoporous Sulfated Zirconia

4.6 Sulfation by Gaseous SO_2

Since the sulfuric acid increased the width of the pore size distributions, it was thought that an alternative approach could be used to sulfate the material. Sulfation by gaseous SO_2 may not increase the width of the pore size distribution while still giving the bridging bisulfate groups necessary for catalytic activity. Two types of material were sulfated by this method, one that had previously had the template extracted and one that still had the template intact. The results are given in Table 4.6 and can be compared to the same material that was sulfated by the standard method (with sulfuric acid).

Table 4.6: Comparison of Two Methods of Sulfation: Aqueous H_2SO_4 or SO_2 (g)

Catalyst Treatment[a]	Surface Area (m^2/g)	Pore Diameter (nm)	WHH (nm)
SO_2	60.8	2.4_2	0.5_8
extracted, SO_2	49.4	2.3_9	0.6_9
0.5 M H_2SO_4	101	2.4_1	0.5_4
extracted, 0.5 M H_2SO_4	62.6	3.4_0	1.5_9

a. All samples were made with 10 wt% of dodecylamine and calcined at 650°C

The materials that were sulfated and not extracted had very similar pore size distributions, yet their surface areas differ substantially. The pore size distributions for the materials that were extracted and then sulfated were quite different. The sample sulfated by SO_2 had a pore size distribution with a smaller maximum and it was much narrower. Therefore, sulfation by SO_2 does not appear to attack the inorganic framework and broaden the pore size distribution. However, the surface areas are always lower for material sulfated by this method, which may be an indication of lower thermal stability; during the calcination step, less stable materials would collapse more easily.

The infrared spectra of the materials sulfated by SO_2 was also compared to infrared spectra of materials sulfated by H_2SO_4 (Figure 3.11). The same sulfate stretches are seen for both materials and the pattern is very similar to that seen for zirconia that was sulfated by H_2SO_4 and then extracted (Figure 3.11, sulfated, extracted spectrum). The middle stretch at 1142 cm^{-1} is weak and this pattern was thought to indicate the presence of monodentate sulfate groups. Some bridging bisulfate groups may be present, but much less of them than that

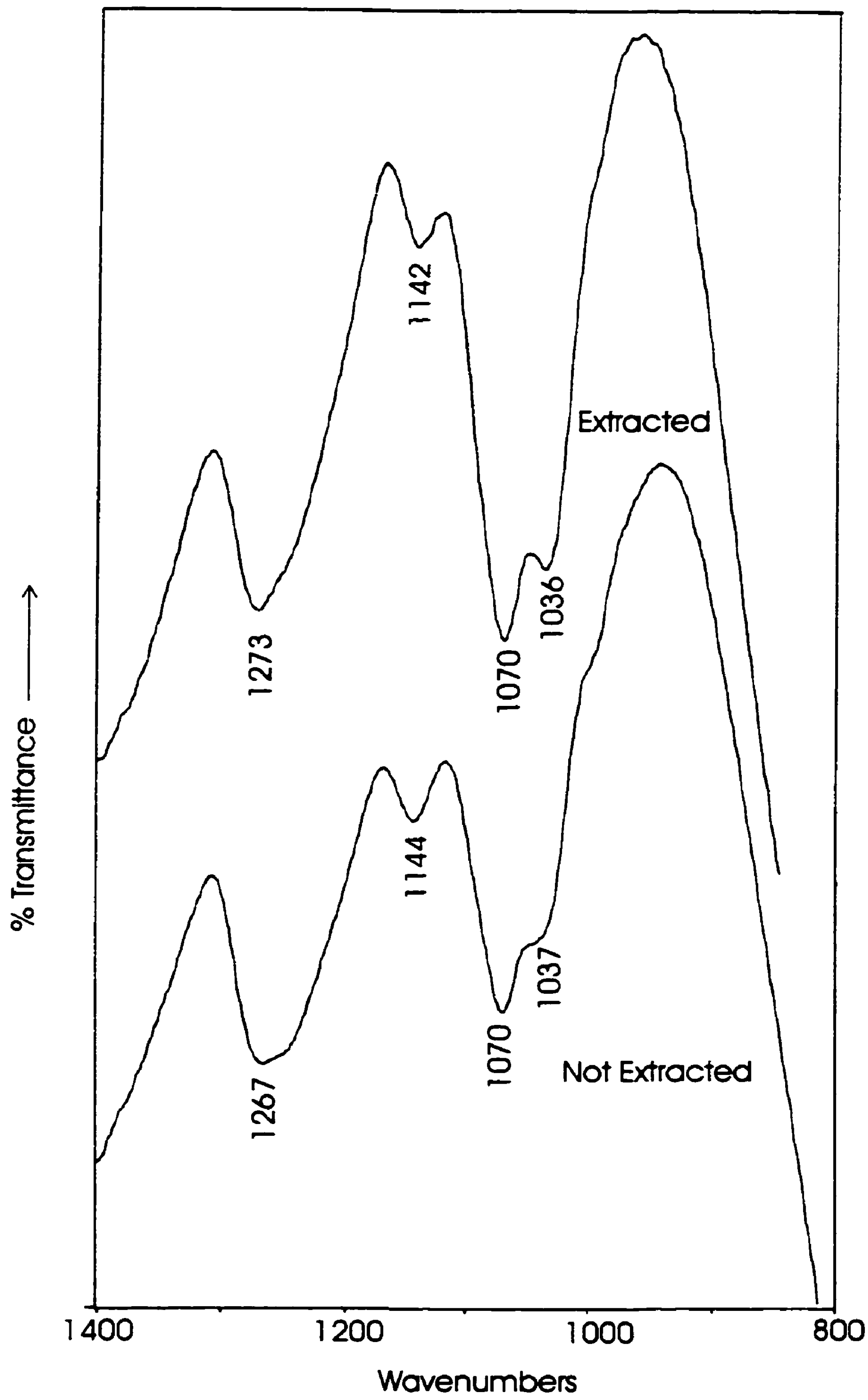

Figure 4.5: Infrared Spectra of Mesoporous Sulfated Zirconia Sulfated by Gaseous SO_2

of the monodentate sulfate groups. It was suspected that these materials may be less catalytically active due to their lower surface areas and the type of sulfate groups present. The catalytic activity of these materials will be discussed in Chapter 5.

4.7 Aging Process

When untreated mesoporous zirconia that previously had been filtered and dried at ambient temperature was treated and then calcined after being stored for approximately three months an unexpected result was found. The material that had been stored had substantially smaller pore diameters and narrower pore size distributions than the original material. Four different samples were then treated (sulfated before and after extraction) and calcined (at 650°C) and their pore size distributions measured (Table 4.7). The catalyst description lists the chain length of the surfactant and the concentration of surfactant used (as wt %).

Table 4.7: The Effect of Storage on the Porosities of Dried Untreated Mesoporous Zirconia

Catalyst Description	Surface Area (m^2/g)	Pore Diameter (nm)	WHH (nm)
C10, 2.28%	72.5	3.0_1	1.2_5
C10, 2.28%, stored[a]	81.1	2.7_2	0.6_7
C8, 1.87%	45.9	3.6_9	1.8_9
C8, 1.87%, stored	40.8	2.9_5	2.6_4
C16, 1.0%	85.2	3.9_6	1.3_9
C16, 1.0%, stored	72.0	3.2_0	0.8_1
C16, 3.5%	75.8	3.2_8	1.0_9
C16, 3.5%, stored	73.5	2.7_2	0.6_8

a. Stored as powders for approximately 3 months

These results show that the pores become smaller and generally have a narrower range of sizes after long - term storage, although the samples were all dried at ambient temperature prior to storing. Clearly, during storage some change occurred in the internal structure of the material. It could be that the aging process is continuing slowly even after the material has been filtered. Aging includes chemical reactions that produce strengthening, stiffening and shrinkage of the network.[37] From the results in Table 4.7, it appears that the gel network is shrinking. This process is called syneresis and results in the expulsion of liquid from the pores. This process is believed to be caused by the same condensation reactions that produce gelation. The increased number of condensation reactions builds a more stable gel network which stabilize the material, so the pore sizes are not broadened as much upon calcination.

It was thought that the shrinkage that occurred upon storage might occur faster if the untreated solids were heated. A sample of untreated solids was heated at 50°C for a number of days. In Figure 4.6, the results are shown for solid samples that were heated for various amounts of time (ranging from 0 to 16 days). As the solid samples were heated the maxima in the pore size distribution decreased and the pore size distribution became narrower, suggesting that syneresis is taking place and that heating increases that rate at which syneresis occurs. The maximum in the pore size distribution of the material was originally 3.11 nm and upon heating for 6 days it decreased to 2.76 nm. After heating for another 10 days, the maximum had only decreased slightly to 2.71 nm. This insignificant decrease in the maxima when heating for sixteen days instead of six days, shows there is likely a limit to the decrease in pore diameter that will occur just by heating the sample. The amount of shrinkage that occurred upon heating (for 16 days) is generally smaller than the amount of shrinkage that occurred when the powders were stored for 3 months.

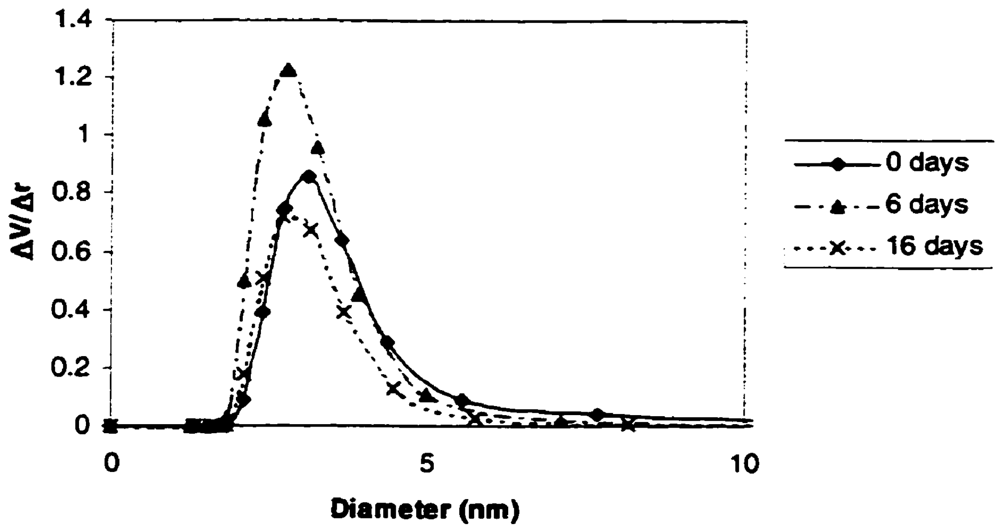

Figure 4.6: The Effect of Heating on the Porosities of Untreated Solids

Another factor that influences the internal structure of the material is the temperature during the aging of the reaction mixture. The majority of the gels were aged at ambient temperature during the synthesis, but heating was done with a few samples to study its effect on the pore size distribution. When the gel mixture was heated at temperatures of 50°C or 60°C during the aging time of 5 days, the pore diameter decreased (Table 4.8). Once again, syneresis is probably occurring and causing the gel network to shrink and therefore, the gel is more stable upon calcination at 650°C.

Table 4.8: Influence of Aging Temperature on the Pore Size Distribution

Catalyst Description	Surface Area (m^2/g)	Pore Diameter (nm)	WHH (nm)
C16, 10%	73.9	3.0_4	0.7_9
C16, 10%, aged at 50°C	101	2.6_8	0.8_0
C16, 3.5%	75.8	3.2_8	1.0_9
C16, 3.5%, aged at 60°C	70.8	2.5_4	0.6_4

4.8 Summary

It was found that the synthesis of mesoporous sulfated zirconia is influenced by many parameters. These parameters can be used to adjust the pore sizes of the materials and include the following:

i) concentration of surfactant

ii) presence of a cosolvent

iii) sulfation procedure (time and strength of acid)

iv) order of sulfation and extraction

v) aging procedure

Unlike the MCM-41 silicates, it was not possible to adjust the pore diameter simply by changing the surfactant chain length. Many other factors had to be taken into account, especially the concentration, when attempting to synthesize mesoporous zirconia with different pore sizes. Decreasing the concentration of the surfactant resulted in a material with a larger pore diameter and a broader pore size distribution. The cosolvent could be changed to increase (acetonitrile) or decrease (ethanol) the pore diameter. Sulfuric acid will attack the pore walls, resulting in a broader pore size distribution if the template is not there to protect the pore walls and therefore, the order of the sulfation and extraction steps has a large effect on the final pore size. Increasing the amount of aging that take place either by increasing the storage time (for solid powders) or by heating the gel resulted in a narrower pore size distribution. Whenever the pore diameter was increased by any of the above methods, the pore size distribution also became broader. Tailoring the pore size of mesoporous sulfated zirconia to a desired size was not simple as a very slight change in parameters caused a drastic change in the pore size distribution

When the parameters were kept the same, the results were quite reproducible, i.e. the material synthesized had the same properties. For example, material made with 10 wt% of hexadecylamine and 35 mL of ethanol, aged for 5 days under ambient conditions, sulfated with 0.5 M H_2SO_4 and then extracted was found to have the following pore diameters: 2.46, 2.53, 2.55 and 2.56 nm when made on four separate occasions (average = 2.52 nm and standard deviation = 0.05 nm). The width at half-height of the pore size distributions was also similar, 0.57, 0.57, 0.63 and 0.57 nm respectively.

The synthesis of mesoporous sulfated zirconia with different pore sizes was successful. A range of pore sizes from 2.0_0 nm to 4.0_0 nm was obtained, although the pore size distributions overlapped to some degree. This is the first time that thermally stable mesoporous sulfated zirconia of different pore sizes has been synthesized. However, the pore size distributions obtained were not as narrow as desired. Nonetheless, the pore size distributions vary enough so that reactions that occur inside the pores should occur at different rates. The catalytic activity of these materials will be the focus of the next chapter.

Chapter 5

Catalytic Testing of Mesoporous Sulfated Zirconia

5.1 Introduction

There are many different types of acid - catalysed reactions, including polymerization, isomerization, cracking and alkylation.[51] All of these reactions are used industrially in the production of petroleum products and acid catalysts are particularly useful for the catalytic cracking of heavy oils and for catalytic reforming to give fuels of high octane number. During the reaction process, carbocations are formed by the various mechanisms mentioned in Section 1.2. These carbocations can attack other reactants that are present, such as aromatics or olefins to produce more highly branched species.

Hydroisomerization and hydrocracking of straight chain hydrocarbons to produce branched ones are among the most promising catalytic applications for sulfated zirconia. The isomerization of n-butane is typically used as a test reaction for conventional sulfated zirconia. In early studies, although extremely high activities were obtained, rapid deactivation of SZ catalysts took place, presumably due to coking.[9] The rate of coking can be controlled by the addition of metals, such as platinum, to the catalyst and by using this catalyst (Pt/SZ) in a hydrogen atmosphere. The majority of the reactions tested with conventional sulfated zirconia have been gas phase reactions suitable to its microporous structure. Since the sulfated zirconia produced in this work has mesopores it is suited for liquid phase reactions of larger molecules.

5.2 Alkylation of p-Xylene with Cyclohexene

The use of solid acid catalysts in place of homogeneous catalysts such as H_2SO_4 is generally desirable for liquid -phase reactions.[46] The catalytic performance of various solid acid catalysts has been tested in the alkylation of m-xylene and trimethylbenzene with cyclohexene.[46] In that study, conventional sulfated zirconia was tested and found to be virtually inactive. Although the authors did not report a pore size distribution, it was implied that the low activity of the conventional sulfated zirconia was likely due to its microporous nature. It was also found in that study that the same sulfated zirconia was very active for the skeletal isomerization of pentane to 2-methylbutane in the gas phase. Some zeolites, HY and H-ZSM-5, which are microporous, also showed very low activities for the alkylation of m-xylene with cyclohexene despite the large amounts of acid sites possessed by these catalysts. Take et al. have reported that only small amounts of acid sites are present on the external surface of these zeolites.[52] By analogy, therefore slow diffusion into the pores of the conventional, microporous, sulfated zirconia may be the main reason for its low activity. Since conventional sulfated zirconia had such low activity for this reaction, it was wondered if the larger pores of mesoporous sulfated zirconia would increase the activity. Therefore, the alkylation of p-xylene with cyclohexene was chosen as a model reaction. P-xylene was chosen, in place of m-xylene, so that only one product would be formed instead of a mixture of isomers. Complete shape - selectivity can not be expected for materials with such large pores, as most molecules will have enough flexibility to enter them. However, if pores with different sizes are used differences in reaction rates may be observed.

Since the product of the reaction could not be purchased, the identity of the product was confirmed by GC -MS analysis of a typical reaction mixture. Two peaks were present on the GC trace with molecular weights of 106 and 188. These molecular weights correspond to unreacted p-xylene and 1-cyclohexyl-2,5-methyl benzene, respectively. This molecular weight confirmed that the expected product had been formed. A blank reaction carried out without any catalyst produced no product after three hours, even when the reaction was done at 100°C. Pairs of samples, where one sample had been sulfated and then extracted and the other had been extracted and then sulfated, were tested with the reaction above as described in Section 2.3. Due to the different results from the different types of catalysts, the data is divided into two groups: sulfated, extracted catalysts (SE) and extracted, sulfated catalysts (ES).The results of these trials are given in Table 5.1 and 5.2.

Table 5.1: Catalytic Results for Sulfated, Extracted (SE) Catalysts

Catalyst	Surface Area (m^2/g)	Pore Diameter (nm)	WHH (nm)[a]	Specific Activity (mmol/ min·m^2)[b]	Extent of Reaction between 1 and 180 min
SE1	86.3	2.2_5	0.4_5	0.0092	77.1
SE2	102	2.3_4	0.5_0	0.0097	89.9
SE3	71.8	2.3_1	0.6_4	0.0084	68.4
SE4	82.8	2.8_1	0.5_9	0.0138	94.1
SE5	71.9	3.0_5	0.7_5	0.0143	75.5

a. WHH = width at half height
b. Measured between 1 and 10 minutes

Table 5.2: Catalytic Results for Extracted, Sulfated (ES) Catalyts

Catalyst	Surface Area (m^2/g)	Pore Diameter (nm)	WHH (nm)	Specific Activity (mmol/ $min \cdot m^2$)[a]	Extent of reaction between 1 and 180 min
ES1	76.2	2.5_3	0.8_4	0.0132	70.0
ES2	78.1	2.5_0	0.6_9[b]	0.0122	72.5
ES3	80.4	2.5_4	0.6_2	0.0131	100
ES4	73.4	2.8_9	0.7_5	0.0149	78.9
ES5	47.8	3.1_2	1.1_8	0.0174	73.2

a. Measured between 1 and 10 minutes
b. pore size distribution has large tail on high diameter side

From the results shown in Table 5.1and in Table 5.2, it can be seen that the activity of the catalyst increases with pore diameter, as expected. As the pore size increases the reactants can travel to the active sites easier and therefore the reaction proceeds faster. The two different types of catalysts can also be compared by plotting the specific activity against the pore diameter of the catalyst (Figure 5.1). This plot allows the trend of increasing pore diameter and increasing activity to be seen easily.

From this figure, it is observed that the relationship between pore size and activity is almost linear, and that activity does increase as the pore diameter increases. It is also found that for the same pore diameter, the catalysts that are extracted and then sulfated are more active than the ones that are sulfated and then extracted. The extracted, sulfated catalysts are thought to have bridging bidentate sulfate groups, which are also present in catalytically active conventional sulfated zirconia, while the sulfated, extracted catalysts may have a mixture of sulfate groups. From the infrared spectra of these materials (Figure 3.11, Section 3.1.6) it

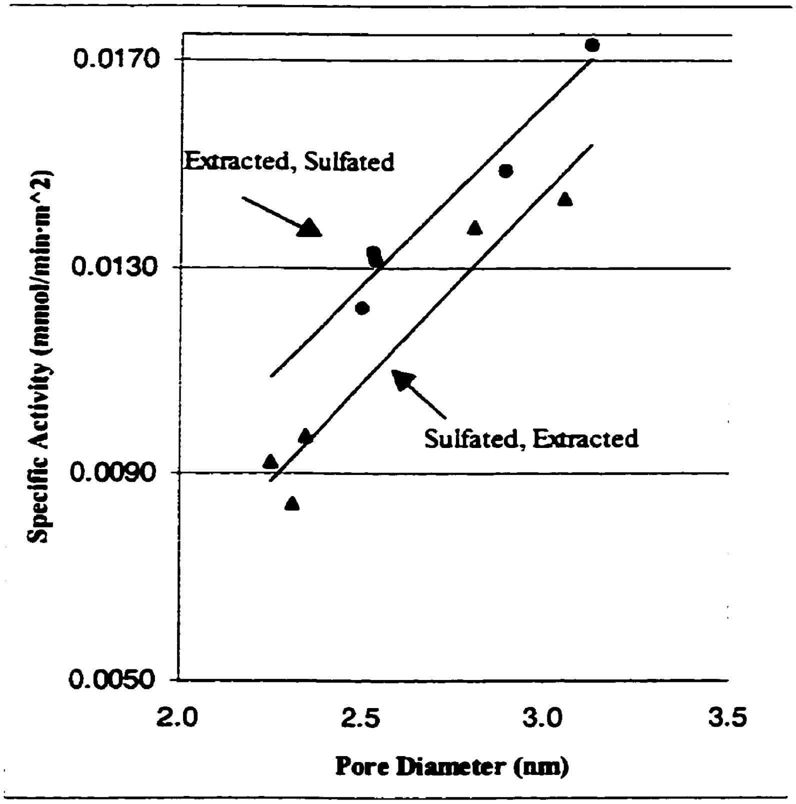

Figure 5.1: The Effect of Pore Size on the Specific Activity of Mesoporous Sulfated Zirconia

was thought that the material that was sulfated and then extracted had monodentate sulfate groups present along with a small number of bridging bidentate groups. The difference seen in activity for the two types of catalysts may partially be due to the different types of sulfate groups. The activity of the monodentate active sites may not be as high as the activity of the bidentate active sites, since both types of catalysts are thought to have approximately equal number of sulfate groups (approximately equal band strengths in the infrared spectra). In Section 3.1.6, it was suggested that the catalysts in which sulfation precedes extraction may have active sites (sulfate groups) only externally, but not in the pores, since the pores are still occupied by surfactant micelles during sulfation. It appears from these results that this is not the case; at least some of the active sites in the sulfated, extracted catalysts must be located inside the pores or no correlation would have been observed between pore diameter and activity. It is known that surface species can diffuse across the catalyst surface during crystalization and sintering[38] (which occur during calcination) and a case of sulfate migration during the crystalization of sulfated zirconia has also been reported.[53] It is also known that sulfate concentration decreases during calcination and therefore, since sulfate groups are mobile, they may possibly migrate across the catalyst surface. If the sulfated, extracted catalysts had external sulfate groups prior to calcination, some of them appear to have migrated to internal sites during calcination.

In order to determine whether the external surface would contribute to the catalytic activity, the area of the external surface of the catalyst was approximated by measuring the particle size of the catalyst by scanning electron microscopy (SEM) and converting the particle size to surface area. Random sampling of the SEM images yielded an average particle size of 104.1 μm. Assuming that the particles are spheres, with a density of 1.46 g/cm^3, the specific surface area can be calculated by $4.11\times10^{-6}/d$, where d is the sphere diameter in metres and the surface area is in m^2/g. Thus the external surface area of the material was approximated to be 0.039 m^2/g. Therefore, the external surface area is insignificant when compared to the surface area inside the pores and its contribution to the catalytic activity will be minimal.

In order to confirm that the activity of these catalysts is due to the sulfate groups and also due to the presence of mesopores, both microporous conventional sulfated zirconia and unsulfated zirconia were tested. When material that had not been sulfated was tested, no product was formed, even after running the reaction for sixty minutes, which showed that sulfate groups are necessary for catalytic activity. The conventional sulfated zirconia that was tested had a surface area of 176 m^2/g and a pore size distribution centered around 1.50 nm with a tail that extended slightly into the mesopore range. The activity of this catalyst (measured between 1 and 10 minutes) was only 0.0007 $mmol/m^2 \cdot min$, which is one hundred times smaller than the activity for any of the mesoporous catalysts. Between 1 minute and 180 minutes only another 27 % of the cyclohexene was converted to product when using the microporous catalyst, while over 70 % of the cyclohexene was converted to product in this time period for the mesoporous catalysts. The low activity this high surface area, microporous catalyst has must be due to the small number of mesopores present. These results show that the mesopores are needed for higher catalytic activity for the reactions of larger molecules.

In order to determine why the extracted, sulfated catalysts were more active than the sulfated, extracted catalysts, an attempt was made to remove the sulfate groups by NaOH extraction and infrared spectra of the NaOH extracted samples were taken (Figure 5.2). These spectra show that some sulfate groups remain in both catalysts. The sulfate groups that are bonded more strongly to the surface will remain behind, while the groups that are weakly bonded will be removed. From the spectrum for the sulfated, extracted catalyst it appears as if all of the monodentate sulfate groups have been removed and only bidentate sulfate groups have been left behind after the NaOH extraction. In contrast, for the extracted, sulfated catalyst the pattern of peaks present in the sulfate stretching region of the spectrum after NaOH extraction is similar to that obtained prior to the NaOH treatment. The spectra indicate that these are bridging bidentate groups, which are apparently harder to extract due to the higher number of bonds to the catalyst surface. The extracted, sulfated catalyst also had stronger in-

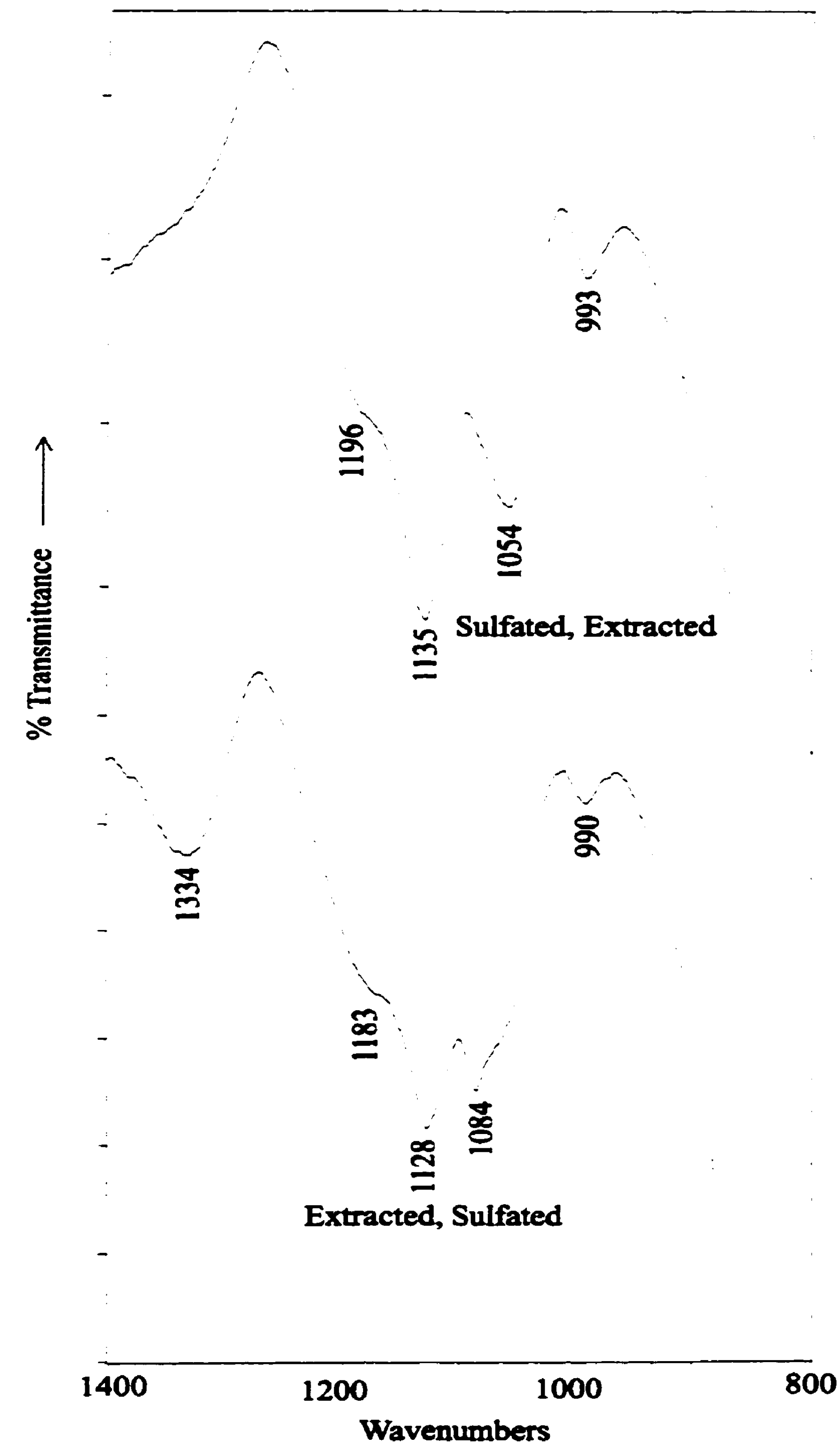

Figure 5.2: Infrared Spectra of Catalysts after 0.1 M NaOH Extraction

frared bands, indicating that more sulfate groups were left on the catalyst surface.

A typical plot of the data collected during the reaction for the above catalytic trials in Table 5.1 and 5.2, is shown in Figure 5.3. It can be seen that the rate of cyclohexene disappearing equals the rate of 1 - cyclohexyl - 2, 5 - methyl benzene forming which indicates that no other products are forming. This rate is fastest at the beginning of the reaction and decreases due to the cyclohexene being used up as the reaction progresses.

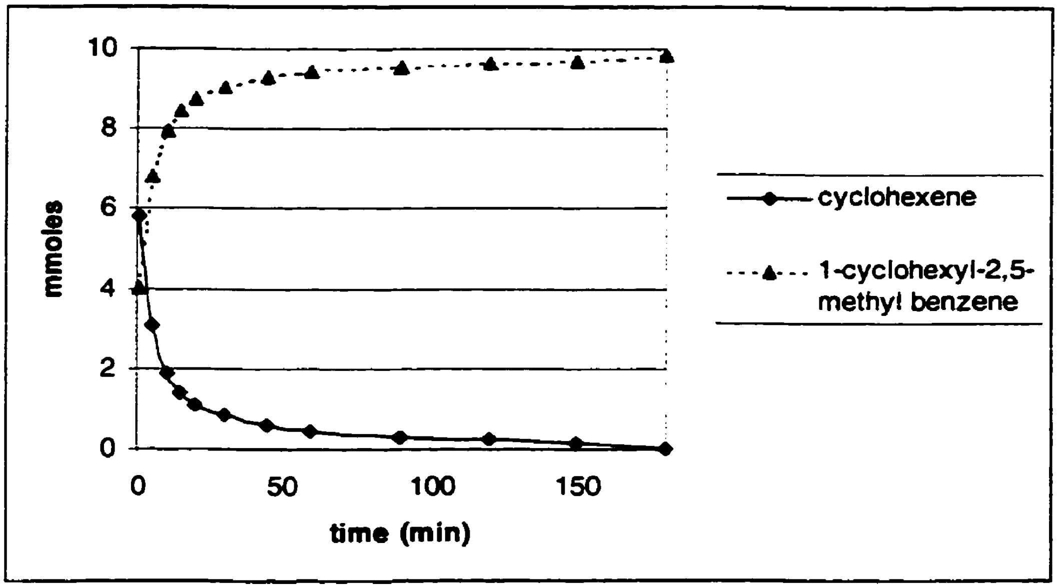

Figure 5.3: Plot of Reaction Data for the Alkylation of p-Xylene with Cyclohexene

At the end of the reaction the dried catalysts would all be grey or grey - brown in colour, indicating carbon has been deposited on the surface and that some deactivation of the catalyst has occurred. The amount of carbon deposited on the surface of the catalysts was measured after treating the used catalysts under vacuum to remove any adsorbed unreacted p-xylene or cyclohexene. The results of these measurements are presented in Table 5.3.

Table 5.3: Amount of Carbon Deposited on Used Catalysts

Catalyst	Surface Area (m^2/g)	Pore Diameter (nm)	WHH (nm)	wt % C
SE1	86.3	2.2_5	0.4_5	3.54
SE2	102	2.3_4	0.5_0	4.77
SE3	71.8	2.3_1	0.6_4	3.14
SE4	82.8	2.8_1	0.5_9	4.12
SE5	71.9	3.0_5	0.7_5	2.55
ES1	76.2	2.5_3	0.8_4	1.00
ES2	78.1	2.5_0	0.6_9 (tail)	2.56
ES3	80.4	2.5_4	0.6_2	3.51
ES4	59.9	2.6_9	1.1_0	2.58
ES5	47.8	3.1_2	1.1_8	2.44

The acidic properties of the catalyst are extremely important in determining the degree to which deactivation occurs. In addition, the pore sizes also serve to control the extent to which polymerization (the formation of heavy carbonaceous deposits) can occur. Overall, the SE catalysts have more carbon deposited on them than the ES catalysts. Comparing the extent of reaction in Table 5.1 and Table 5.2, the reactions with the SE catalysts also progressed further. Among the ES catalysts, ES3, which had the highest extent of reaction, also had the largest amount of carbon deposited on its surface. When the reaction progresses further, more cyclohexene is converted to product, but more deactivation reactions also occur which results in more carbon being deposited on the catalyst surface. The catalysts with larger pores have less carbon deposited on their surfaces and lower extents of reactions, which may indicate that the active sites are being blocked by carbon deposits (or access to the pores is blocked) in the initial stages of the reactions. This rapid deactivation would explain why these catalysts have higher specific activities measured over the first 10 minutes, but a lower extent of reaction (i.e. less of the cyclohexene is converted to product after three hours).

The pore sizes and surface areas of some of the used catalysts were also measured (Table 5.4). The surface area always decreased after the reaction, presumably due to the carbon

Table 5.4: Comparison of Surface Area and Porosities of Used and Unused Catalysts[a]

Catalyst Type	Surface Area (m^2/g)	Pore Diameter (nm)	WHH (nm)
SE	73.6 (63.5)	2.40 (2.32)	0.51 (0.54)
ES	77.4 (66.4)	2.83 (2.69)	0.93 (1.11)
SES	95.7 (86.9)	2.65 (2.56)	0.67 (0.58)
SE	101 (69.1)	2.41 (2.30)	0.54 (0.51)
ES[b]	62.6 (53.1)	3.40 (3.60)	1.59 (1.59)
SE	86.3 (72.2)	2.25 (2.04)	0.45 (0.39)
ES	73.4 (69.3)	2.90 (2.68)	0.75 (0.90)
SE	82.8 (70.5)	2.80 (2.55)	0.59 (0.67)

a. The number in parenthesis is the value for the used catalyst
b. The tail on the used catalyst is smaller

deposited on the surface of the catalyst. The majority of the pore diameters also became slightly smaller or the width of the pore size distribution decreased slightly from their original value. This data indicated that carbon had been deposited on the inside of the pores. However some of the pore size distributions actually became wider, which may indicate that some of the wall structure was destroyed during the catalytic reaction. Virtually no difference existed between the used SE catalysts and the used ES catalysts so no information about the difference in the location of the active sites (external or internal) of these two catalysts could be determined from these measurements. The infrared spectra of the used catalysts showed that the sulfate groups remained intact as the spectra are identical to those seen in Section 3.1.6 (Figure 3.13). If the active sites (sulfate groups) had been covered with coke, one would expect the infrared spectra to be affected. The fact that they are not suggests that the main cause of deactivation is pore blocking, rather than coke deposition on the active sites.

5.3 Catalytic Reactions with Platinum Loaded Catalysts

Sulfated zirconia, like other solid acid catalysts, deactivates quickly, presumably due to coke formation during catalytic reactions.[9] To overcome this problem, SZ catalysts containing small amounts of noble metals were developed.[9] In studies done with conventional SZ, it was found that the stability of the catalytic activity was greatly improved when Pt was added to the catalyst.[9, 54-56] Other transition metals (Pd, Rh, Ru, Fe, Co, Ni, W and Mo) have also been investigated, but comparison of the catalytic performance of the transition metal loaded SZ catalysts in n-pentane isomerization has shown that Pt is the most effective metal.[9]

When platinum is supported on a solid acid, the combination usually gives a bifunctional catalyst. In the presence of bifunctional catalysts, skeletal isomerization of paraffins proceeds in three successive steps: paraffin dehydrogenation, olefin skeletal isomerization and olefin hydrogenation. The first step is unfavourable in the presence of hydrogen. In contrast, Pt/SZ shows a positive effect of hydrogen partial pressure for the skeletal isomerizations of paraffins and it has low hydrogenation activity.[57] The exact reaction mechanism that occurs when using Pt/SZ and the state of Pt on Pt/SZ is still being studied. It is thought that after calcination at temperatures above 600°C the Pt is in the metallic state.[9, 54, 57] Many theories have been proposed for how Pt, in conjunction with hydrogen, stops the catalyst from deactivating. In one theory, the Pt reacts with the hydrogen gas and causes it to dissociate into two hydrogen atoms.[9, 58] The hydrogen atom spills over the catalyst surface and migrates to the Lewis acid site, where it releases an electron to convert to a proton, which then is bonded to an oxygen ion near the Lewis acid site. The formation of this bond generates a Bronsted acid site, which increases the activity of the catalyst.[9, 58] The Lewis sites become weaker when the electron is accepted and this weakening of the Lewis acidity is thought to decrease coke deposition.[9, 58] In another theory, the electron released to form a proton reacts with the another hydrogen atom to form a hydride ion.[9, 59] This resultant hydride ion adds to a carbocation on the catalyst surface and forces its desorption as a hydrocarbon molecule.[9, 59] The supply of hydride ions decreases the residence time of the reaction intermediates and prevents them from undergoing further reactions, such as cracking, isomerization and oligo/polymerization, thus preventing the formation of carbonaceous residue on the catalyst surface.[9]

To investigate whether Pt loaded onto mesoporous sulfated zirconia would have the same effect (i.e. it would decrease deactivation of the catalyst), five different samples had platinum loaded onto them (as outlined in Section 2.3.4) and the catalysts were then calcined at 650°C. After calcination, the catalysts that had been extracted and then sulfated before loading on the platinum were light beige, while catalysts that had been sulfated and then extracted before loading on the platinum were much darker, presumably due to the higher amount of metallic platinum present on these catalysts. The surface areas and pore size distributions of the Pt - loaded catalysts were measured and compared to the samples made without any platinum. For the extracted, sulfated samples the surface area did not change when Pt was loaded onto the catalysts while the maxima in the pore size distribution decreased slightly for one (from 2.89 nm to 2.56 nm) and increased for the other (from 2.53 nm to 2.76 nm). For the sulfated, extracted samples the surface area always increased while the maxima in the pore size distribution always decreased. It is thought that the surface area increased due to attack on the pore walls by the acidic solution (hexachloro platinic acid) that was used to load the platinum onto the catalyst surface. In Section 4.5.1 the pore size distribution and surface areas of samples stirred in sulfuric acid for various amounts of time was studied and it was found that as the residence time in the acid was increased from 1 to 10 to 60 minutes the surface area of the material also increased from 72.2 to 86.8 to 102 m^2/g which indicates that the acid affects the surface area of the catalyst as well as the pore size. The observed increase in surface area is presumably due to the hexachloroplatinic acid dissolving some of the catalytic surface. This acid had a greater effect on the sulfated, extracted catalysts as their pore walls had not been exposed to acid during the sulfation procedure as the template was still present.

These catalysts were also tested using the same model reaction. The results of these reactions are given in Table 5.5. The data for the corresponding catalysts without any platinum can be found in Table 5.1 or 5.2.

Table 5.5: Catalytic Reactions with Pt Loaded Catalysts

Catalyst	Surface Area (m^2/g)	Pore Diameter (nm)	WHH (nm)	Specific Activity (mmol%/ min·m^2)	Extent of Reaction between 1 and 180 min
Pt/SE1	92.3	2.1_8	0.4_3	0.0118	92.9
Pt/SE4	112	2.6_0	0.5_4	0.0104	94.0
Pt/SE5	96.8	2.6_9	0.6_9	0.0202	98.4
Pt/ES1	72.7	2.7_6	1.0_2	0.0172	93.8
Pt/ES4	73.4	2.5_6	0.7_5	0.0173	100

The specific activity increased when Pt was loaded on the catalysts for all of the samples, except Pt/SE4. If the activities (prior to dividing by surface area) are compared Pt/SE4 has a higher activity than SE4, but the higher surface area of Pt/SE4 (112 m^2/g compared to 82.8 m^2/g) results in a lower specific activity. Therefore, loading platinum onto the catalysts does increase their activities, possibly due to the formation of more Bronsted acid sites or by delaying deactivation of the catalyst. The higher extent of reaction between 1 and 180 minutes shows that more cyclohexene is reacting with these catalysts and therefore, the amount of deactivation is being decreased. A plot of the reaction data for reactions using Pt/ES1, Pt/ES4 or Pt/SE5 catalysts generated a plot similar to the one seen in Figure 5.3. However, a plot of the reaction data for the reactions using the other Pt/SE catalysts was quite different (Figure 5.4.).

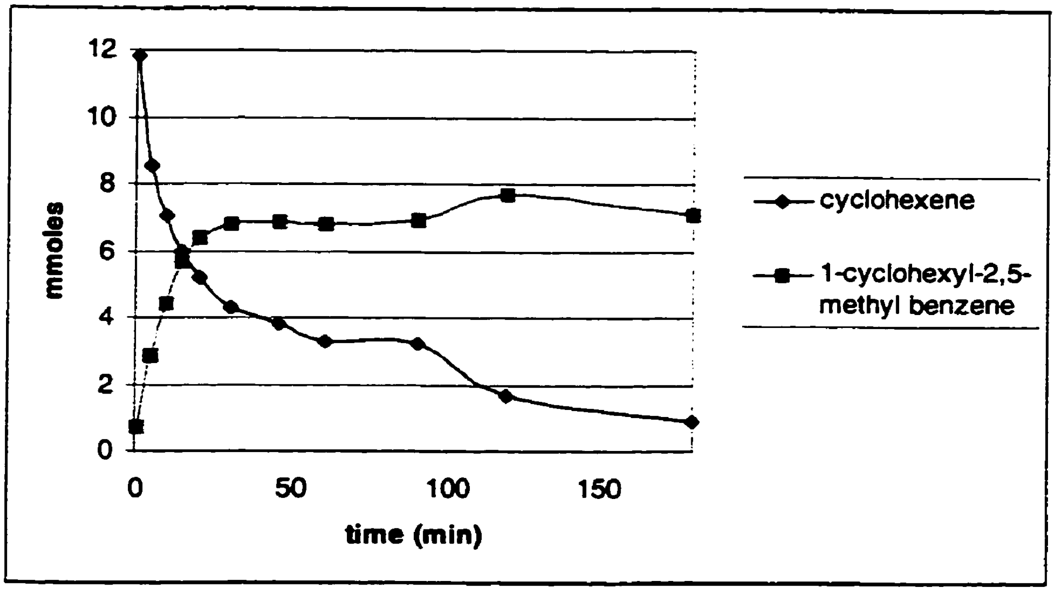

Figure 5.4: Plot of Reaction Data for the Alkylation of p-Xylene with Cyclohexene when using Pt -loaded SE1 catalyst

The amount of cyclohexene disappearing does not equal the amount of 1 - cyclohexyl - 2,5 - methylbenzene being formed. It was noticed that a new peak appeared on the GC trace with a retention time of 0.37 min (between the cyclohexene and the p-xylene peaks) after running the reaction for 90 minutes. When the reaction mixture was analysed with GC - MS it was found that the molecular weight of the new peak was 112. This molecular weight corresponds to the molecular weight of 1, 4 - dimethyl cyclohexane, and therefore, the p-xylene is being hydrogenated during the reaction. It is possible that the cyclohexene is also being hydrogenated to cyclohexane, but the retention times for these two compounds are too similar to distinguish between them on the GC trace. Also the high rate of flow of hydrogen gas through the reaction mixture may cause some of the cyclohexene or cyclohexane to evaporate during the reaction as the reaction temperature was only slightly lower than their boiling points. The GC/MS results also showed a very small amount of a compound with a molecular weight of 207 being formed. This molecular weight corresponds to a dimer of p-xylene minus one methyl group. The p-xylene may react with itself as it is being hydrogenated to form a dimer, just as the cyclohexene did when it was present in higher concentrations. To ensure that the specific activities calculated were not high due to cyclohexene being hydrogenated, the specific activities were also calculated using the amount of product formed. The two calculations gave equal specific activities, showing that the hydrogenation is not taking place until later in the reaction and that the platinum is increasing the activity of the catalyst.

The amount of platinum on the calcined catalysts and the amount of carbon on the used catalysts were measured and the results are given in Table 5.6.

Table 5.6: Amount of carbon and platinum on Pt - Loaded Catalysts

Catalyst	Surface Area (m^2/g)	Pore Diameter (nm)	WHH (nm)	wt % C	wt % Pt
Pt/SE1	92.3	2.1_8	0.4_3	2.02	0.360
Pt/SE4	112	2.6_0	0.5_4	2.62	0.389
Pt/SE5	96.8	2.6_9	0.6_9	4.35	0.105
Pt/ES1	72.7	2.9_4	1.0_2	4.27	0.080
Pt/ES4	73.4	2.5_6	0.7_5	3.30	0.100

The amount of carbon on the used Pt - loaded catalysts is not substantially lower than the samples without platinum. For three of the samples, the amount of carbon is actually higher when the sample has platinum present. These results are contrary to what was expected, since the normalized activity was higher and the amount of cyclohexene converted between 1 minute and 180 minutes was also higher. These results show that even though platinum may delay deactivation at the beginning of the reaction, deactivation still occurs and another method may be needed to stop its occurrence. The amount of platinum loaded onto the catalyst is also very important. From Table 5.6 it can be seen that the amount of platinum is much higher in the two catalysts (Pt/SE1 and Pt/SE4) that yielded different reaction profiles. All of the Pt/SE catalysts gave some hydrogenation products, but Pt/SE1 and Pt/SE4 gave substantially more 1,4 - dimethyl cyclohexane than Pt/SE5. If the Pt loading is too high, hydrogenation products dominate and the desired catalytic reaction does not occur exclusively. However, when hydrogenation products occur, the amount of carbon is also decreased showing that the H atoms produced do decrease deactivation as desired, but they also react with certain other components present in the reaction mixture. It has been found that the pressure of hydrogen in the reaction vessel will affect the rate at which hydrogenation occurs.[60] Different rates of hydrogen gas flow were not tested, but these rates could affect which reaction dominates (hydrogenation or alkylation). The results show that if the Pt loading is low the desired catalytic reaction will occur and it will occur at a faster rate when compared to the catalysts without platinum, but the amount of carbon formed on the catalyst surface is not lower. The location of the platinum and the size of the platinum particles (i.e. how well dispersed the platinum is) on the catalyst surface may also play a role.[61] XRD powder patterns were taken of the Pt-loaded catalysts; no peaks of metallic platinum were seen, confirming that the high temperature used during calcination did not cause platinum migration and crystalization, at least to a level which could be seen in the X-ray powder pattern. The amount of sulfate is known to affect the dispersal of platinum on the catalyst surface; the presence of sulfate ions causes an increase in the platinum particle size.[62]

Infrared spectra of Pt loaded catalysts, before and after the reaction, were also taken (Figure 5.5). The infrared spectra of the Pt - loaded catalysts was the same as the spectra for

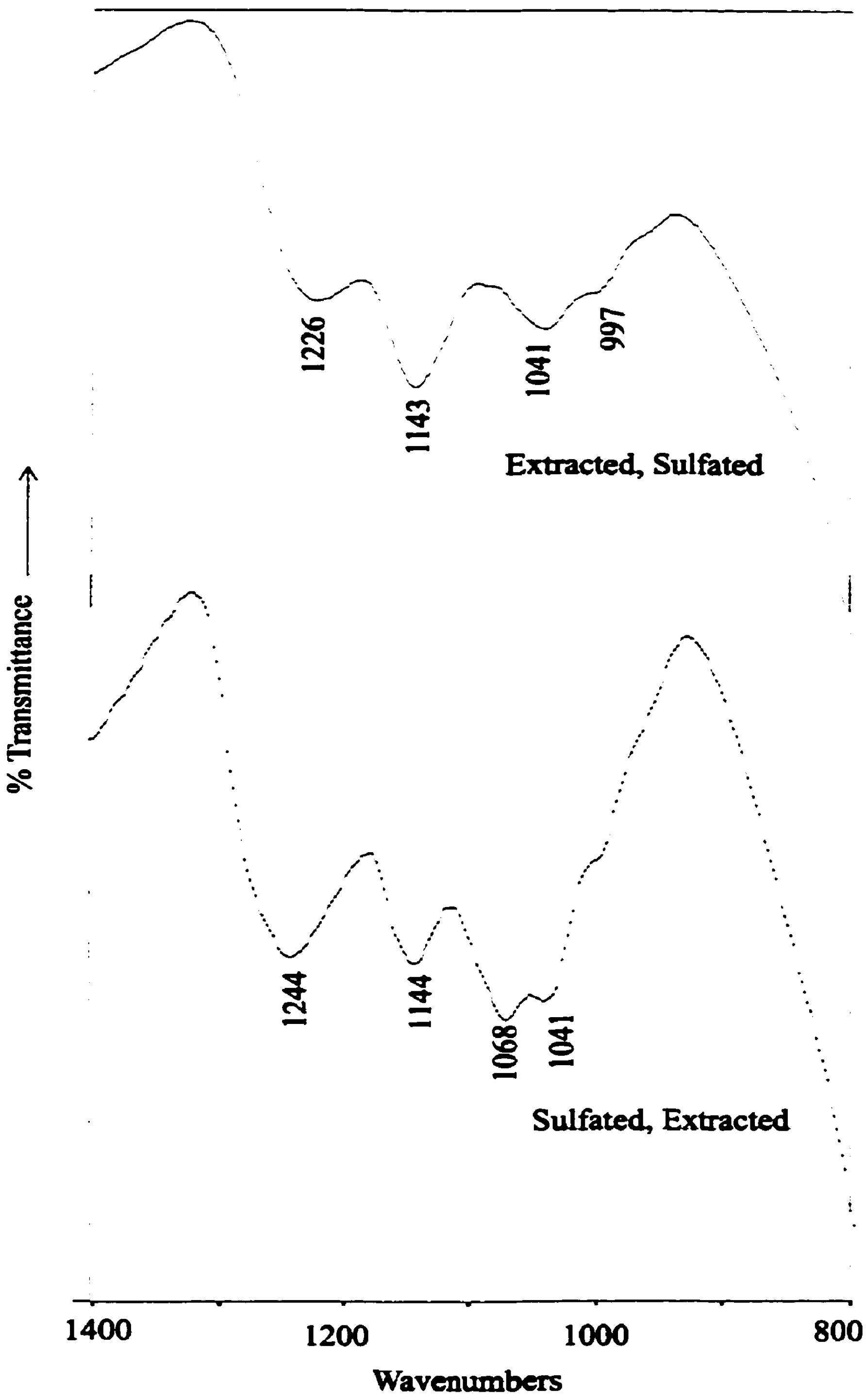

Figure 5.5: Infrared Spectra of Calcined Pt - Loaded Catalysts

the samples without any platinum. These spectra did not change after the catalyst had been used in the reaction.

5.4 Catalysts Sulfated by Gaseous SO_2

In Section 4.6 it was mentioned that sulfation by gaseous SO_2 resulted in catalysts with narrower pore size distributions. To determine whether these were still catalytically active, materials, sulfated in this manner, were tested using the same reaction and the results are presented below (Table 5.7).

Table 5.7: Catalytic Results for Catalysts Sulfated by SO_2

Catalyst	Surface Area (m^2/g)	Pore Diameter (nm)	WHH (nm)	Specific Activity (mmol/ min·m^2)	Extent of Reaction between 1 and 180 min
SO_2	60.8	2.4_2	0.5_8	0.0063	63.2
extracted, SO_2	49.4	2.3_9	0.6_9	0.0090	42.9

These catalysts are less active than those sulfated by sulfuric acid, which had activities much higher than those reported here for catalysts of similar pore diameter (Table 5.1 and 5.2). The sample that is extracted before sulfation is slightly more active than the one that is sulfated before extraction. The infrared spectra of these materials showed that they both have similar sulfate groups to the SE catalysts (sulfated by sulfuric acid), presumably a mixture of monodentate and bidentate sulfate groups, although the extracted sample had stronger bidentate bands, indicating more bidentate sulfate groups. The sulfate contents of these catalysts were measured before and after calcination. Before calcination, the sulfate content of the samples was 2.39% for the unextracted sample and 2.70 % for the extracted sample. Both of the catalysts lost some sulfate during calcination to end up with a final sulfate content of 2.36 wt % and 1.97% for the unextracted and extracted samples, respectively. Infrared spectra of these catalysts after extraction with 0.1 M NaOH to remove the sulfate groups showed that no sulfate groups remained on the catalyst surface after extraction. The types of sulfate groups on these catalysts are not bound as tightly to the surface of the catalysts and therefore are easily removed. The higher activity of the extracted sample may be due to type of sulfate groups present as this is what is thought to cause (at least in part) the higher activity for the extracted, sulfated catalysts which were sulfated by sulfuric acid.

The sulfate content of these catalysts is much lower than the sulfate content of the samples sulfated by sulfuric acid and this low sulfate concentration could be the cause of the lower activity observed. Another reason for the lower activity may be the lack of Bronsted acid sites. A Bronsted acid site requires the presence of a hydroxyl group, which can be obtained from the water present when sulfating by sulfuric acid. During sulfation by gaseous SO_2, no water is present making it difficult for Bronsted acid sites to form. The amount of carbon present on these catalysts after the reaction is quite low, 1.50% for the unextracted sample and 0.97 % for the extracted sample. These low values reflect the fact that fewer reactions are taking place on the surface of these catalysts, due to their lower acidity.

5.5 Summary

It was found that mesoporous sulfated zirconia is an active catalyst for the alkylation of p-xylene with cyclohexene. Moreover, the catalytic activity depended on the pore size of the material: the larger the pore, the more active the catalyst. Since both types of catalysts (ES and SE) displayed this dependence of catalytic activity on pore diameter, it was thought that the active sites for both catalysts are located inside the pores. If sulfate groups were present only on the external surface prior to calcination (due to the template blocking the pores), some of them apparently migrated during the high temperature calcination. It was also shown that microporous sulfated zirconia is only slightly active for the same reactions, confirming that the mesopores of this catalyst are vital for obtaining catalytic activity.

It was found that material that had been extracted and then sulfated was more active than material that had been sulfated and then extracted. The reason for the difference in activity is likely due to the amount and type of sulfate groups present. The different types of sulfate groups present in each catalyst (presumably, bidentate and monodentate) are possibly both catalytically active sites, although they may not have the same activity. When the pores are larger, the internal active sites in the extracted, sulfated catalysts and the sulfated, extracted catalysts are more accessible and therefore, their activities are higher. All of the catalysts tested had carbon deposited on their surfaces indicating that some deactivation occurred. The used catalysts with larger pores had less carbon on their surfaces and high initial activities, but not as much cyclohexene was converted to product by the end of the reaction time showing that these catalysts deactivated during the initial stages of the reaction. The amount of carbon that was deposited on the catalyst surface was proportional to the amount of cyclohexene that reacted during the alkylation.

Platinum was loaded on the catalysts and hydrogen gas used in an attempt to decrease the deactivation rate. It was discovered that the amount of platinum greatly influenced the course of the reaction; if the loading of platinum is low, the specific activity (measured between 1 and 10 minutes) of the reaction will increase, although deactivation will still occur and if the loading of platinum is high, some hydrogenation of p-xylene (and presumably cyclohexene) will occur instead of the desired catalytic reaction, but less carbon will be formed. All of the reactions with the platinum - loaded catalysts did progress further (i.e. more of the cyclohexene reacted with p-xylene after three hours) indicating deactivation was at least delayed.

Sulfation by SO_2 produced less active catalysts, presumably due to the smaller amount of sulfate groups and the type of acid sites formed, which are not likely Bronsted acid sites because no water was present during the sulfation. These factors result in a lower overall activity for the material.

The p-xylene alkylation reactions revealed differences in the catalytic behaviour of these samples. The pore size influences the rate of the reaction. It also appears that the type of sulfate groups (monodentate or bidentate) forming the active sites have an influence on the activity. The amount of Pt present is a factor in determining whether alkylation or hydrogenation occurs. Overall, mesoporous sulfated zirconia is a very active catalyst and being able to alter the pore size of the material suggests that shape - selective catalysis with larger molecules may be possible.

Chapter 6

Conclusions and Future Work

6.1 Conclusions

Mesoporous sulfated zirconia can be synthesized by the surfactant templating route which was first demonstrated for silica.[18] However, the factors which determine the sizes of the pores in zirconia are many, and they interact with each other, making the synthesis of zirconia with a specific, narrow pore size distribution a complex problem. In this work, many of the factors were studied in an attempt to prepare samples with a range of non - overlapping pore sizes which could be tested for "shape - selectivity" in an alkylation reaction.

Many different approaches were tested in an attempt to synthesize mesoporous sulfated zirconia. The majority of these approaches were unsuccessful. Many of the materials synthesized turned out to be thermally unstable, so that any pore structure present was lost upon calcination. Other materials synthesized were microporous, so the pores were too small for liquid phase reactions, or mesoporous with pores so large and broad that shape - selective catalysis would be impossible. However, one method did give material with the desired internal structure: the neutral templating method. Material made by this method was thermally stable up to 650°C, the temperature needed to form the tetragonal phase (catalytically active phase) of sulfated zirconia, and mesoporosity was still retained at this temperature.

6.1.1 Tailoring the Pore Size of Mesoporous Sulfated Zirconia

Various synthesis parameters were investigated to determine which of them affected the pore size. It was found that varying the alkyl chain length of the surfactant did not change the pore size, even though this parameter had been found to be very important in the synthesis of mesoporous silicate materials. However, the pore size distribution of mesoporous sulfated zirconia could be altered by changing the concentration of surfactant. As the concentration of surfactant decreased, the maximum in the pore size distribution became larger and the distribution became broader, presumably due the change in the shape of the surfactant micelle. Other factors that could be used to adjust the pore size distribution are the addition of a co-solvent, such as ethanol or acetonitrile, to the reaction mixture, the order of extraction and sulfation and the aging process used. Cosolvents interact with the surfactant micelle and therefore affect the template which helps determine the pore size of the material. Sulfation broadens the pore size distribution since the sulfuric acid destroys some of the wall structure. If the template is present during sulfation, it protects the wall structure and the final pore size distribution is narrower. When the temperature was increased during the aging process, more syneresis occurred resulting in a narrower pore size distribution with a smaller maximum and increasing the aging time increased this effect. By adjusting all of the factors mentioned, materials with different pore diameters (from 2.0_0 to 4.0_0 nm) were obtained. This is the first time thermally stable mesoporous sulfated zirconia of different pore sizes has been synthesized. The pore size distributions did overlap to some degree, but since the degree of overlapping was small, catalytic testing was carried out to determine if the activity was related to pore size.

6.1.2 Catalytic Activity of Mesoporous Sulfated Zirconia

The pore size distribution of mesoporous sulfated zirconia did affect the activity of the catalyst. As the diameter of the pore increased, the activity of the catalyst also increased. Larger pores allow for easier access to the active sites and therefore, reactions occur faster. It was also found that material with larger pores deactivated faster presumably due to the easy access to these active sites which meant carbon was deposited onto the active sites initially. Materials that had the surfactant template extracted prior to sulfation were more active than materials that were sulfated and then extracted. The higher activity may be due to the type and amount of sulfate groups present. Infrared spectra suggest that the two kinds of material have different types of sulfate groups (monodentate and bidentate) and although both kinds appear to be catalytically active, it is thought that the bidentate groups may be more active than the monodentate groups.

Deactivation of the catalysts occurred during the alkylation reaction. In an attempt to stop or decrease deactivation platinum was loaded onto the catalysts. Although deactivation was delayed, the presence of platinum did not stop deactivation from occurring. It was also found that the amount of platinum had an influence over what reactions would occur. If the amount of platinum was high (0.360 wt% or greater), hydrogenation reactions would dominate and therefore, the reagents would continue to be consumed but less of the desired product would form.

Sulfation by SO_2 rather than by sulfuric acid produced less active catalysts due to the low concentration of sulfate groups; infrared spectra suggest that these catalysts have predominately monodentate sulfate groups which will also influence the activity. Since sulfation occurred without any water present, very few hydroxyl groups would form to produce the Bronsted acid sites required for catalytic activity.

6.2 Future Work

In order for shape selective catalysis to be effective, the pore size distribution of the catalyst must be as narrow as possible. Many factors have been found to influence the pore size distribution of mesoporous sulfated zirconia, but there are many more that can be investigated. Different types of neutral surfactants, such as polyethylene oxide surfactants, could be used instead of neutral primary amines. Branched surfactants or double - headed surfactants may have different micellar structures and therefore would yield different pore size distributions. Other factors that could be investigated are pH, the concentration of cosolvent, the addition of other cosolvents, including the addition of organic additives such as trimethylbenzene that swell the micelle, and the concentration of Zr^{IV}. The factors that affect the aging process could also be investigated, since only preliminary work had been done in this area. If the synthetic procedure could be optimized to give the desired pore diameter, with as narrow a distribution as possible, this would improve the shape - selectivity of the catalyst. If the exact type of sulfate groups formed could be determined, along with which types are the most catalytically active, this information could be used to improve the catalyst performance. The amounts of Bronsted and Lewis acid sites present are important in determining the activity and the rate of deactivation of the catalyst. Infrared studies with bases such as pyridine could be done to determine these quantities.

The results presented in Chapter 5 did not fully resolve the question of the location of the active sites, although they did strongly suggest that both materials have internal active sites. An approach to answering this question would be to perform catalytic testing with some very large reactants, so large they (or the product) would not fit inside the pores of the catalyst. If product is formed, there must be some external active sites or alternatively, if no reaction occurs, there must only be internal active sites. Another approach would be to study the effect of reaction temperature on the reaction rate. Materials with only internal active sites should show a greater variation in reaction rate than material with external active sites, since material has to diffuse into the pores of the material with internal sites and the rate of diffusion will be affected by the reaction temperature. More work also needs to be done with platinum (or other metals) to determine if deactivation can be eliminated. The amount of platinum loaded onto the catalyst and the flow of hydrogen during the reaction both need to be optimized. The effect of sulfation on the amount of platinum loaded and the dispersal of the platinum also needs to be investigated. The stability of the catalysts during regeneration is also important if this catalyst is going to be used commercially. Obviously, a great deal of research remains to be done before mesoporous sulfated zirconia could be useful as a commercial catalyst for a variety of reactions.

References

1. J.-F. LePage, J. Cosyns, P. Courty, E. Freund, J.-P. Franck, Y. Jacquin, B. Juguin, C. Marcilly, G. Martino, J. Miquel, R. Montarnal, A. Sugier and H. Van Landeghem, "Applied Heterogeneous Catalysis", Editions Technip, Paris, 1987.
2. J. M. Thomas; Scientific American, April, 112 (1992).
3. J. M. Thomas; Angew. Chem. Int. Ed. Engl., **33**, 913 (1994).
4. M. R. Weir; Ph.D. Thesis, University of Calgary, 1998.
5. P. Behrens; Angew. Chem. Int. Ed. Engl., **35**(5), 515 (1996).
6. S. M. Bradley; Ph.D. Thesis, University of Calgary, 1991.
7. V. C. F. Holm and G. C. Bailey, U.S. Patent 3032599 (1962).
8. M. Hino, S. Kobayashi and K. Arata, J. Amer. Chem. Soc., **101**, 6439 (1979).
9. X. Song and A. Sayari, Catal. Rev.-Sci. Eng., **383**(3), 329 (1996).
10. A. Clearfield, G. P. D. Serrette and A. H. Khazi-Syed, Catal. Today, **20**, 295 (1994).
11. S. Chokkaram, R. Srinivasan, D. R. Milburn and B. H. Davis, J. Coll. Inter. Sci., **165**, 160 (1994).
12. D. A. Ward and E. I. Ko, J. Catal., **150**, 18 (1994).
13. E. E. Platero, M. Penarroya, C. O. Atean and A. Zecchina, J. Catal., **162**, 268 (1996).
14. F. Babou, G. Coudurier and J. C. Vedrine, J. Catal., **152**, 341 (1995).
15. M. Bensitel, O. Saur and J. -C. Lavalley, Mater. Chem. Phys., **19**, 147 (1988).
16. P. D. L. Mercera, J. G. Van Ommen, E. B. M. Doesburg, A. J. Burggraaf and J.

R. H. Ross, Appl. Catal., **57**, 127 (1990).

17. N. K. Raman, M. T. Anderson and C. J. Brinker, Chem. Mater., **8**, 1682 (1996).
18. J. S. Beck, J. C. Vartuli, W. J. Roth, M. E. Leonowicz, C. T. Kresge, K. D. Schmitt, C. T-W. Chu, D. H. Olson, E. W. Sheppard, S. B. McCullen, J. B. Higgins and J. L. Schlenker, J. Amer. Chem. Soc., **114**, 10834 (1992).
19. P.C. Hiemenz and R. Rajagopalan, "Principles of Colloid and Surface Chemistry", Marcel Dekker, Inc., New York, 1997.
20. F. Schuth, Ber. Bunsenges. Phys. Chem., **99**(11), 1306 (1995).
21. A. Sayari, Chem. Mater. **8**, 1840 (1996).
22. E. Armengol, M. L. Cano, A. Corma, H. Garcia and M. T. Navarro, J. Chem. Soc., Chem. Commun., 519 (1995).
23. A. Corma, A. Martinez, V. Martinez-Soria and J. B. Monton, J. Catal., **153**, 25 (1995).
24. D. M. Antonelli and J. Y. Ying, Angew. Chem. Int. Ed. Engl. **35**(4), 426 (1996).
25. D. M. Antonelli and J. Y. Ying, Angew. Chem. Int. Ed. Engl. **34**(18), 2014 (1995).
26. S. A. Bagshaw and T. J. Pinnavaia, Angew. Chem. Int. Ed. Engl. **35**(10), 1102 (1996).
27. M. J. Hudson and J. A. Knowles, J. Mater. Chem., **6**(1), 89 (1996).
28. A. F. Bedilo and K. J. Klabunde, J. Catal., **176**, 448 (1998).
29. G. Larsen, E. Lotero, M. Nabity, L. Petkovic and D. S. Shobe, J. Catal., **164**, 246 (1996).

30. G. Pacneco, E. Zhao, A. Garcia, A. Sklyarov and J. J. Fripiat, Chem. Commun., 491 (1997).

31. Y. Huang and W. H. M. Sachtler, Chem. Commun., 1181 (1997).

32. U. Ciesla, S. Schacht. G. D. Stucky, K. K. Unger and F. Schuth, Angew. Chem. Int. Ed. Engl., **35**(5), 541 (1996).

33. U. Ciesla, K. Unger and F. Schuth in "Characterization of Porous Solids IV", Society of Chemical Industry, Cambridge, 1997, (B. McEnaney (Editor)), p90.

34. J. S. Reddy and A. Sayari, Catal. Letters, **38**, 219 (1996).

35. P. T. Tanev and T. J. Pinnavaia, Science, **267**, 865 (1995).

36. E. Prouzet and T. J. Pinnavaia, Angew. Chem. Int. Ed. Engl., **36**(5), 516 (1997).

37. Y. Huang, T. J. McCarthy and W. H. M. Sachtler, Appl. Catal. A: Gen., **148**, 135 (1996).

38. C. J. Brinker and G. W. Scherer, "Sol - Gel Science", Academic Press, Inc., Boston, 1990.

39. H. P. Lin, S. Cheng and C.-Y. Mou, J. Chin. Chem. Soc., **43**, 375 (1996).

40. P. Liu, J. Liu and A. Sayari, Chem. Commun., 577 (1997).

41. S. Brunauer, P. H. Emmett and E. Teller, J. Amer. Chem. Soc., **60**, 309 (1938).

42. E. P. Barrett, L. G. Joyner and P. P. Halenda, J. Amer. Chem. Soc. **73**, 373 (1951).

43. S. Lowell and J. E. Shields, "Powder Surface Area and Porosity", Chapman and Hall, London, 1991.

44. G. Horvath and K. Kawazoe, J. Chem. Eng. Jpn., **16**(6), 470 (1983).

45. U. Ciesla, M. Grun, T. Isajeva, A. A. Kurganov, A. V. Neimark, P. Ravilovitch,

S. Schacht, F. Schuth and K. K. Unger *in* "Access in Nanoporous Materials", Plenum Press, New York, 1995, (T. J. Pinnavaia and M. F. Thorpe (Editors)), p231.

46. T. Okuhara, T. Nishimura, H. Watanabe and M. Misono, J. Mol. Catal., **74**, 247 (1992).

47. D. Myers, "Surfactant Science and Technology", VCH Publishers, Inc., New York, 1988.

48. K. Nakamoto, "Infrared and Raman Spectra of Inorganic and Coordination Compounds", Wiley-Interscience Publication, New York, 1978.

49. S. B. McCullen, J. C. Vartuli, C. T. Kresge, W. J. Roth, J. S. Beck, K. D. Schmitt, M. E. Leonowicz, J. L. Schlenker, S. S. Shih and J. D. Lutner *in* "Access in Nanoporous Materials", Plenum Press, New York, 1995, (T. J. Pinnavaia and M. F. Thorpe (Editors)), p7.

50. M. T. Anderson, J. E. Martin, J. G. Odinek and P. P. Newcomer, Chem. Mater, **10**, 311 (1998).

51. G. C. Bond, "Heterogeneous Catalysis: Principles and Applications", Clarendon Press, Oxford, 1987.

52. J. Take, H. Yoshioka and M. Misono in "Proc. 9th Int. Congr. Catal.", The Chemical Institute of Canada, Ottawa, 1988, (M. J. Philips and M. Ternan (Editors)), p372.

53. D. Farcasiu, J. Q. Li and S. Cameron, Appl. Catal. A: Gen., **154**, 173 (1997).

54. S. R. Vandagna, R. A. Comelli, S. A. Canavese and N. S. Figoli, J. Catal., **169**, 389 (1997).

55. H. Liu, V. Adeeva, G. D. Lei and W. M. H. Sachtler, J. Mol. Catal. A: Chem., **100**, 35 (1995).

56. J. C. Yori, M. A. D'Amato, G. Costa and J. M. Parera, J. Catal., **153**, 218 (1995).

57. A. Dicko, X. Song, A. Adnot and A. Sayari, J. Catal., **150**, 254 (1994).

58. H. Hattori, T. Yamada and T. Shishido, Res. Chem. Intermed., **24**(4), 439 (1998).

59. K. Ebitani, J. Konishi and H. Hattori, J. Catal., **130**, 257 (1991).

60. J. Manoli, C. Patvin, M. Muhler, U. Wild, G. Resofszki, T. Buchholz and Z. Paal, J. Catal., **178**, 338 (1998).

61. T. Kurosaka, H. Matsuhashi and K. Arata, J. Catal., **179**, 28 (1998).

62. K. Ebitani, T. Tanaka and H. Hattori, Appl. Catal. A: Gen., **102**, 79 (1993).